2010

The Pleiotropic Mutant R50 (*sym16*): A Link Between Cytokinin and Starch Metabolism May Explain Its Seed Phenotype

Chengli Long
Wilfrid Laurier University

Your file Votre référence
ISBN: 978-0-494-75384-2
Our file Notre référence
ISBN: 978-0-494-75384-2

THE PLEIOTROPIC MUTANT R50 (*SYM16*): A LINK BETWEEN CYTOKININ AND STARCH METABOLISM MAY EXPLAIN ITS SEED PHENOTYPE

by

Chengli Long

A

thesis

submitted to the

Department of Biology,

Faculty of Science

in partial fulfillment of the
requirements for the degree of

Master of Science

in

Integrative Biology

at

Wilfrid Laurier University

Waterloo, Ontario, Canada, 2010

I hereby declare that I am the sole author of this thesis

I authorize the Wilfrid Laurier University to lend this thesis to other institution or individual for the purpose of scholarly research

I further authorized the Wilfrid Laurier University to reproduce this thesis by photocopying or by other means, in total or in part, at the request of other institutions or individuals for the purpose of scholarly research

Abstract

The pleiotropic mutant R50 (*sym16*): A link between cytokinin and starch metabolism may explain its seed phenotype

Chengli Long
Wilfrid Laurier University, 2010

Supervisor:
Dr. Frédérique C. Guinel

Cytokinins are a class of adenine-based plant hormones that stimulate cell divisions and are therefore essential for organ growth and development. The role that cytokinin plays in nodulation and that of R50 (*sym16*) in particular is very complex. In this study, a cytokinin antagonist and a cytokinin oxidase (CKX) inhibitor were used as tools to study the effects of cytokinin perception or cytokinin degradation on nodulation in pea, the cytokinin transduction pathway, especially that induced by CRE1/AHK4, and CKX play a significant role in pea nodulation. Comparison of the full length sequences *PsCKX2* cDNAs from Sparkle and R50 indicated that *PsCKX2* is likely not *sym16* The availability of the full length *PsCKX2* cDNA facilitated the assessment of *PsCKX1* and *PsCKX2* expression profiles in seedling development using semi-quantitative RT-PCR. Along with a morphological study (dry weight of R50 cotyledons are not decreasing as fast as those of wild type) and microscopic studies (R50 starch grains within the cotyledons are not digested as fast as those of wild type) of seedling development, a working model which integrates cytokinin and starch metabolism is proposed to explain the seedling phenotype of R50.

Acknowledgements

I am extremely grateful to my supervisor Dr Frédérique Guinel (Biology, Wilfrid Laurier University) for her support, guidance, and encouragement. Without her expertise and insight, the completion of this project would not have been possible. Her personality also has profoundly influenced me in my life I would also like to thank the members of my committee Dr. Barbara Moffatt (Biology, University of waterloo) and Dr Matthew Smith (Biology, Wilfrid Laurier University), who along with Dr F C. Guinel, have contributed greatly to the success of this project

I would like to give special thanks to Dr.Moffatt and her technician Yong Li for all their help for my molecular study I also would like to thank Dr. Smith for his critical-thinking skills They were always supportive, humble and easily approachable when needed

I thank Dr. Lucas Spíchal for generously providing the PI-55 and INCYDE for my research. I am grateful for his help and guidance.

I extend my gratitude to my fellow lab-mates Emily Macdonald, Scott Clemow, Jaroslav Nisler, Mark Welsh, Jessica Morrison, Ishari Chamika, Katja Engel, Andre Masella and Christian Huynh for their accompaniment and help during the long days and nights in the lab.

Special thanks go out to my friends Xue Bai and Hongyan Wang. They have been there for me through all the hard times in my life and for that I am forever grateful

Last but most importantly, I would like to thank my parents and my family Their unconditional love and constant encouragement have given me the support to complete my degree

This thesis is dedicated to my parents and Grandpa for their unending love and support

Table of Contents

List of Figures

List of Tables

Chapter 1 Introduction

1.1 Nodulation

1.1.1 Biological and agriculture importance

Legumes are important crops for humans, their family includes 670-750 genera and 18,000 to 19,000 species (Polhill *et al.* 1981) They are considered as old crops dating back to 6,000 BC, appearing early in Asia, the Americas (the common Phaseolus bean in several varieties), and Europe (broad beans), and have been domesticated for more than 3,000 years in the Americas and Asia (Hymowitz and Singh 1987; Kaplan and Lynch 1999). Many of them, including *Glycine max* (soybean) and *Pisum sativum* L. (pea) became a staple, essential for supplementing proteins in the human diet

Manure, cinder, and ironmaking slag had been used as fertilizers to improve crop yields for centuries Between the 17th century and the end of the 19th century, inorganic artificial fertilizers replaced these early growth promoters, they were one innovation of the Agricultural Revolution. Fertilizers released innumerable workforce, helped drive the Industrial Revolution, and therefore created unprecedented development. However, they also contributed to tremendous population growth and to environmental pollution. They are responsible for most arable impoverished soils (Specht *et al.* 1977), the eutrophication of water (Bijay-Singh *et al.* 1995), and the emission of methane into the atmosphere (Bodelier *et al* 2000). Most importantly, it has been found that the application of fertilizer inhibits the mutualistic symbiosis between rhizobia and legumes, and thereby significantly reduces nodulation (Wahab *et al.* 1996). Legumes play a critical role in biological nitrogen fixation. Every year, some 40 to 60 million metric tons of nitrogen are fixed biologically by agriculturally

important legumes, and another 3 to 5 million metric tons are fixed by legumes in their natural ecosystems (Smil 1999).

1.1.2 Symbiosis and nodule organogenesis

Legumes are notable for their ability to fix nitrogen in symbiosis with rhizobia. The mutualistic relationship between the two symbionts induces the formation of a biological nitrogen-fixing organ, the nodule. Within the nodule, bacteria fix atmospheric nitrogen and convert it into the plant-usable form, ammonium, while the plants provide the bacteria with carbohydrates. The interaction is initialized generally by a molecular dialogue between the two organisms (Brelles-Mariño and Ané 2008). Legume roots exude compounds such as flavonoids that induce the expression of rhizobial nod genes, these genes are responsible for the production of Nod factors which are required for nodule development (Brelles-Mariño and Ané 2008) Different legumes produce different nodule structures. Soybean and *Lotus japonicus* (Lotus) bear determinate nodules, which lose meristem activity shortly after initiation, and therefore their shapes are spherical. In contrast, pea and *Medicago truncatula* (barrel medic) exhibit indeterminate nodules that are generally cylindrical in shape and have a continually growing meristem. In indeterminate nodules, the area of initial cell division is in the inner cortex close to the root vasculature, while the first cell division of determinate nodules is located in the outer cortex (Brelles-Mariño and Ané 2008).

In the case of indeterminate nodule organogenesis, rhizobia bind to the root hair and secrete Nod factor which activates cell division in the pericycle. Cell activation progresses in the inner cortex where cells divide to form the initial nodule primordium. The root hairs then

get primed; they curl and trap the bacteria within the curl. Soon an infection thread appears in the root hair. Simultaneously, the outer cortical cells get ready to receive the infection thread; they organize their cytoplasm and form pre-infection threads which make a path for the infection thread to take. As the cells of the nodule primordium continue to divide, a nodule meristem differentiates The nodule grows outward whereas the infection thread with the bacteria extend inward The infection threads penetrate cells behind the meristem; soon after the nodule emerges from the root surface (Timmers *et al.* 1999, Fig. 1.1). Indeterminate nodules, maintaining an active apical meristem over their life, exhibit five zones (Zone I meristematic zone, Zone II: early symbiotic zone or infection zone; Zone III· late symbiotic zone or fixation zone; Zone IV· senescent zone, Zone V saprophytic zone, Fig 1 1) corresponding to different stages of cell development (Guinel 2009) Zone II-III is the interzone where bacteria are released and differentiate into bacteroids (Guinel 2009). Bacteroids are the form of bacteria which express nitrogenase; this enzyme is responsible for the fixation of atmospheric nitrogen For this reaction to occur, oxygen levels in the nodule must be very low, this is achieved partially by an oxygen diffusion barrier located in the cortex of the nodule (Guinel 2009).

1.1.2.1 Nodulation and phytohormones

As any developmental process, nodule organogenesis is highly regulated by phytohormones. Ferguson and Mathesius (2003) proposed a model to demonstrate that nodule development is regulated by hormone interaction For example, ethylene, a gaseous organic compound, which can be produced from essentially all parts of higher plants, has an inhibitory effect on nodule formation (Grobbelaar *et al.* 1971); furthermore, it decreases nitrogenase activity

(Goodlass and Smith 1979) The negative effect of ethylene in nodulation has been demonstrated in pea mutants. A proper nodulation phenotype can be partially restored in the low nodulation mutant lines E2 (Guinel and LaRue 1991) and E107 (Guinel and LaRue 1992) by treating their roots exogenously with either the ethylene inhibitor aminoethoxyvinylglycine (AVG) or the antagonist (Ag^{+}). Lee and LaRue (1992a) demonstrated the inhibitory effect of ethylene on nodulation when they mimicked the E107 nodulation phenotype (infection thread blocked in the basal epidermal cell) by treating wild type with ethylene.

Another example of an hormone playing a role in nodulation is that of auxin which is a phytohormone primarily produced in the shoot apex and transported throughout the plant by polar transport In 1973, Libbenga *et al.* (1973) illustrated that the ratio of auxin to cytokinin is essential for nodule formation. By determining the auxin content, Ridge *et al.* (1992) found that auxin levels in legume nodules increased by treating plants with synthetic auxin (2,4-dichlorophenoxyacetic acid) By treating plants with auxin transport inhibitor NPA [N-(1-naphthyl) phthalamic acid] and TIBA (2, 3, 5-triiodobenzoic acid), Hirsch *et al.* (1989) demonstrated that expression of the early nodulin genes *ENOD2* and *Nms-30* can be induced Fusing the auxin responsive promoter *GH3* to the *GUS* reporter gene, Mathesius *et al.* (1998) found auxin levels increased after rhizobial inoculation, indicating that auxin inhibits nodule primordia initiation and thus controls nodule number during the early stages of nodule formation A study by de Billy *et al.* (2001) demonstrated that the auxin import carrier *MtLAX* genes are initially expressed in the early nodule primordium, indicating that auxin plays a role in early nodule development.

Along with ethylene and auxin, another important family of phytohormones are the

cytokinins (comprehensively introduced later). There is much evidence indicating that cytokinin is linked to nodulation Such a relationship has been demonstrated by many authors. In 1959, Arora *et al* (1959) reported that pseudo-nodule structures can be induced by treating tobacco roots with kinetins. An exogenous treatment of cytokinin was also conducted by Lorteau *et al.* (2001), who demonstrated that BAP (benzyladenine) induced a dose-dependent effect on nodules in pea. High levels of BAP results in few, flat, pale nodules, and abnormal infection threads in wild type (Lorteau *et al.* 2001). ENOD*2*, an early nodulin gene expressed in nodules and nodule primordial, can be induced by the exogenous application of cytokinin to alfalfa (Cooper and Long *et al* 1994) The exogenous application of BAP on legume root induces cortical cell divisions and expression of the early nodulin ENOD40 (one of the nodulation marker genes) in alfalfa (Fang and Hirsch 1998) Cytokinin application stimulated early nodulation responses such as cortical cell division and amyloplast deposition (Bauer *et al* 1996)

Recent research further illustrates a direct connection between cytokinin and nodulation Cytokinin receptors appear to play a significant role in nodule organogenesis (Gonzalez-Rizzo *et al.* 2006, Murray *et al* 2007, Tirichine *et al* 2007, Frugier *et al.* 2008) A gain-of-function mutant (*snf2*) of the *Lotus japonicus* cytokinin-receptor gene (*LHK1*) can form spontaneous nodules, i.e., without rhizobial infection, indicating that cytokinin signaling is indispensable for cell division and initiating nodule development (Tirichine *et al* 2007) The loss-of-function mutant (*hit1*) of *Lotus japonicus* LHK1 displays abundant infection threads but fails to trigger cortical cell divisions (Murray *et al.* 2007) Furthermore, RNA interference of CRE1 (an ortholog to LHK1) in *Medicago truncatula* leads to strongly

reduced nodulation; both infection progress and nodule primordia formation are affected (Gonzalez-Rizzo *et al* 2006) Much remains unknown about how the cytokinin signaling pathway is involved, its relationship with Nod factor signaling, and how it relates to each precise nodulation step. In a review, Frugier *et al.* (2008) constructed a model in which cytokinins play many roles, including influencing bacterial infection, controlling the expression of many nodulin genes such as *NIN* (Nodule Inception), and regulating other transcriptional regulators (Fig. 1.2, Frugier *et al.* 2008). They proposed that cytokinin may be the most important differentiation signal for cortical cell division and nodule organogenesis (Frugier *et al.* 2008)

1.2 Cytokinin

1.2.1 General background

Cytokinins were originally defined as substances which with proper nutrients and the phytohormone auxin would promote cell division and differentiation In a review by Das *et al.* (1956), it was reported that Wiesner (1892) first brought the idea that exogenous growth factors initiate cell division in plants, and that Haberlandt (1913) provided the first experimental evidence for cell divisions controlled by endogenous factors In 1948, Caplin and Steward (1948) demonstrated that the liquid endosperm of coconut could promote cultured cell growth although they failed to purify any biologically active compound from the endosperm In 1955, Miller *et al* found that autoclaved herring sperm could stimulate mitosis and cell division in tobacco callus tissues in vitro The compound responsible was named kinetin and later identified as 6-(furfurylamino) purine (Miller *et al.* 1956) This was the first cytokinin compound discovered. Kinetin was shown to have biological activity in stimulating cell division in the tobacco callus bioassay; for some time, it was thought not to occur naturally in plant tissues (Skoog *et al* 1967). It is now known in plants (Barciszewski *et al.* 1996) The first natural cytokinin was discovered in immature kernels of *Zea mays* in 1963 by Letham, who termed the compound zeatin

1.2.2 Structure

Generally, cytokinins are considered to be a class of adenine-based plant hormones (Fig. 1.3). They consist of an adenine ring possessing a side chain at the N^6 position; the side chains are

primarily isoprene-derivatives (Fig. 1 3, iP: N_6-isopentenyladenine and tZ *trans*-zeatin), but they can be aromatic derivatives (Fig 1 3, BAP) Cytokinins have three forms, free base form (adenine with side-chain, i e. iP), nucleoside form (with an attached ribose sugar, i.e iPR: iP riboside), and nucleotide form (with an attached ribose sugar and phosphate group, i.e. iPRMP. iP riboside 5'-monophosphate) (Hirose *et al* 2008; Fig. 1.4). When free base cytokinins are exogenously applied to plant tissues, they quickly interconvert to their corresponding nucleoside and nucleotide forms (Sakakibara *et al* 2006). Although isoprenoid cytokinins were considered to be the only biologically active form of cytokinins in plant tissues, Strnad (1997) demonstrated that aromatic cytokinins exhibit biological activities in plant tissues as well The free base form is considered the most active form because it can bind to cytokinin receptor and stimulate downstream effects (Sakakibara *et al* 2004) Since the nucleoside form is mainly present in the xylem and phloem saps, it is considered as a translocation form (Sakakibara *et al* 2004), whereby it would act as a systemic signal The biological activities of that form apparently depend on the structure of its side chain (Hirose *et al.* 2008). Furthermore, the nucleoside may be involved in a selective transport system (Hirose *et al.* 2008). Less is known about the function of the nucleotide form (Sakakibara *et al* 2004).

1.2.3 Activity

As already mentioned, these hormones were first reported as compounds that promoted cell proliferation and stimulated growth in cultured plant cells (Miller *et al* 1955) Since then, they have been found to play many roles in plant growth and development, including in the

process of seed germination, vascular development, apical dominance and leaf senescence (Mok and Mok 1994). The biological function of cytokinin is regulated by other phyto-hormones, such as abscisic acid (ABA) and auxin, and by environmental cues, such as water stress or drought (Sakakibara *et al.* 2006)

1.2.4 Biosynthesis and metabolism

Cytokinins are synthesized via two pathways. The first biosynthetic pathway is initiated by tRNA-IPTs that catalyze the prenylation of tRNA using DMAPP and tRNA (Fig. 1.4). The major initial product is cZ nucleotide (Sakakibara *et al.* 2004), apparently, this pathway is mainly responsible for the synthesis of the cis-form of the cytokinins The second pathway is much more complex Its initial step is catalysed by adenosine phosphate-isopentenyltransferase (IPT) using dimethylallyl diphosphate (DMAPP) and ATP or ADP or AMP (Fig. 1.4). In higher plants, the major initial product is an iP nucleotide, such as iP riboside 5'-triphosphate (iPRTP) or iP riboside 5'-diphosphate (iPRDP) (Kakimoto 2001) In *Arabidopsis*, iP nucleotides are hydroxylated into tZ nucleotides by cytochrome P450 mono-oxygenases CYP735A1 and CYP735A2 (Takei *et al.* 2004; Fig 1 4).

The first IPT gene identified, *tmr*, was found in *Agrobacterium tumefaciens*, a crown gall-forming bacterium (Akiyoshi *et al.* 1984; Barry *et al* 1984) *A tumefaciens* has two IPT genes one is *tmr* which is located in the T-DNA region of the Ti-plasmid; the other is *tzs* which is located on the virulent region After infection, *tmr* is integrated into the genome of host plants, whereas *tzs* functions within the bacterial cells themselves The IPT activity of the recombinant *tmr* was identified in vitro, and it was revealed that *tmr* exclusively utilizes AMP

as the acceptor (Sakakibara 2004) In Arabidopsis, seven IPT genes (*AtIPT1* and *AtIPT3* to *AtIPT8*) are involved in cytokinin biosynthesis (Kakimoto 2001) and many of them (*AtIPT1*, *AtIPT3*, *AtIPT5*, and *AtIPT8*) are located in plastids (Kasahara *et al.* 2004), indicating that these organelles are likely the major subcellular compartment for iP-type CK biosynthesis (Sakakibara 2006)

In higher plants, the naturally-occurring cytokinins *trans*-zeatin (tZ), N_6-isopentenyladenine (iP), cis-zeatin (cZ), and dihydrozeatin (DZ) widely exist (Mok and Mok 2001, Fig. 1.4). These cytokinins are diverse, they differ in their side chain structure (hydroxylation at their side chain terminus, saturation of the isoprenoid side chain, and in the stereo-isomeric position) They are the result of diverse chemical reactions. For example, iP can be irreversibly converted into tZ by hydroxylase and tZ can be catalyzed irreversibly to DZ by zeatin reductase The conversion of cZ to tZ may be conducted by zeatin isomerase (Sakakibara *et al* 2004, Fig 1 4)

Conversion of iP-, tZ-, DZ-, and cZ- riboside 5'-monophosphate to their more active free base forms occurs by dephosphorylation and deribosylation (Fig. 1.4) The nucleotides are dephosphorylated to the ribosides and subsequently converted to free-base cytokinins (Chen and Kristopeit 1981a and 1981b), but the corresponding genes encoding the nucleoribotidase (Chen and Kristopeit 1981a) and nucleosidase (Chen and Kristopeit 1981b) have not yet been identified However, another pathway exists whereby the cytokinin nucleotide forms are directly converted to free-base forms by LOG, a cytokinin nucleoside 5'-monophosphate phosphoribohydrolase (Kurakawa *et al.* 2007; Fig. 1.4).

Inactivation of cytokinins is carried out by conjugation or degradation Glu-

cose-conjugation to cytokinins occurs at the N_3, N_7 and N_9 positions of the purine ring, or in the hydroxyl group of the prenyl side chain (Kudo *et al.* 2010). The degradation of cytokinin is less complicated. Cytokinin oxidase (CKX) catalyzes the irreversible degradation of the cytokinin iP and Z, and their nucleosides, by oxidative side-chain cleavage to produce adenine and 3-methyl-2-butenal (Werner *et al.* 2006; Fig 1.5). CKX, because it is the only enzyme to degrade cytokinins, plays a significant role in plant development and physiology Its activity is known to vary during the different developmental stages in maize (Jones *et al.* 1992), tobacco (Singh *et al.* 1992), pea (Held *et al.* 2008), and *Arabidopsis* (Werner *et al* 2006) In Chapter 4, more background information will be provided on CKX.

1.2.5 Perception

For almost 30 years, scientists have been searching for a cytokinin-binding protein to function as a cytokinin receptor. Some proteins with binding activity were found but their K_d values were too low for them to be qualified as receptors (Mok and Mok 2001) Finally in 2001, the first cytokinin receptor CRE1/AHK4 was identified in *Arabidopsis* (Inoue *et al.* 2001, Suzuki *et al* 2001; Ueguchi *et al.* 2001), this discovery has allowed a better understanding of the cytokinin signal transduction pathway

As shown in Fig 1 6 (modified from To and Kieber 2008), the cytokinin signal is perceived and transmitted through a His-Asp multi-step phosphorelay, which is comprised of the cytokinin receptor, a histidine protein-kinase, the histidine phosphotransfer protein (AHP) and many response regulators (ARRs). In this signaling system, a membrane-recognition domain sensor binds the cytokinin, triggering the autophosphorylation of a histidine (H')

within a cytoplasmic transmitter domain (Heyl and Schmulling 2003; To and Kieber 2008). The phosphoryl group (P) is further transferred to an aspartate (D) residue within the receiver domain at the receptor C terminus, and then to an AHP. The transfer of phosphorous ultimately activates either a type-A ARR or a type-B ARR; in both cases, the phosphoryl group is passed on an aspartate (D) residue (To and Kieber 2008). Upon ARR phosphorylation, many genes are transcribed and in the end cytokinin-related events are induced in the plants

1.3 The R50 (*sym16*) phenotype

1.3.1 General background

The model plants used in nodulation study are *Lotus*, *Medicago* and some other legumes, such as pea and soybean. Mutants of model plants are very useful to help understand the complex process of nodulation In Dr Guinel's lab, there are many pea mutants, including E107, E151, and R50. Early in the 1980s, wild type seeds of pea were exposed to either chemical mutagens such as ethyl methanesulfonic (EMS) or to gamma–radiation to create mutant lines Low nodulation was used as a screen for the resulting plants (Kneen and LaRue 1988; Kneen *et al* 1994) Since this thesis focuses on R50, I will discuss it further R50, a gamma radiation induced mutant (Kneen *et al* 1994), is a single recessive mutant of the symbiosis gene 16 (*sym16*), mapped on linkage 5, chromosome 3 (Ellis and Poyser 2002).

1.3.2 R50 phenotype

Compared to its wild type, R50 is a pleiotropic mutant with many traits. R50 seeds are larger than those of wild type, likely because of a larger embryo. R50 is thought to have a delayed germination, although this has never been tested For seedling root systems, R50 has a short primary root with few and short lateral roots (Guinel and Sloetjes 2000). R50 also exhibits abnormal root vasculature, the primary root has an increased number of vascular poles whereas the lateral roots have fewer (Pepper *et al* 2007). As for its shoot, R50 is reduced in stature because of short internodes, and its older internodes are thicker than those of wild type (Guinel and Sloetjes 2000). R50 leaves are thick and have a pale phenotype resulting

from decreased total chlorophyll content (Guinel and Sloetjes 2000). R50 nodules, 21 days after inoculation, are small and pale compared to those of wild type which are large and pink, suggesting that R50 nodules have a low nitrogen-fixing activity (Held *et al.* 2008) The infection threads are arrested in the inner cortex and coil within the enlarged cortical cells instead of growing directly towards the nodule primordia, R50 nodule primordia are flatter than those of wild type, because of a reduced number of periclinal cell divisions (Guinel and Sloetjes 2000). The R50 nodulation phenotype is root-controlled since only a low number of nodules develop when R50 is used as a stock in grafting experiments (Guinel and Sloetjes 2000). R50 also has delayed flowering and senescence.

1.3.3 R50 and phytohormones

Compared to wild type, R50 has thicker internodes and shorter stature, which are known to be symptoms of ethylene exposure (Ainscough *et al* 1992). Lee and LaRue (1992b) found that high concentrations of ethylene inhibit pea nodule development Exogenous application of an ethylene inhibitor, such as aminoethoxy vinyl glycine (AVG) or Ag^{+}, to the roots of R50, restored indeed the nodulation phenotype to the level of wild type Therefore, it was proposed that this mutant was either overproducing ethylene or oversensitive to ethylene Later investigation revealed that R50 roots did not exhibit oversensitivity to exogenous ethylene but R50 shoots appear to be less sensitive to the hormone than wild type (Ferguson *et al.* 2005).

A crosstalk between ethylene and cytokinin has been confirmed by Vogel *et al.* (1998), who demonstrated that cytokinin elevates ethylene biosynthesis primarily by a posttran-

scriptional modification of ACS5 (the first enzyme in ethylene biosynthesis in *Arabidopsis*). Lorteau *et al* (2001) demonstrated that in pea roots, treatments of the synthetic cytokinin BAP led to an increase in ethylene evolution and induced a dose-dependent effect on nodulation; furthermore, the treated wild type mimicked the R50 nodulation phenotype. Based on Lorteau's results, Ferguson *et al.* (2005) hypothesized that the low nodulation of R50 was caused by high levels of cytokinin, they demonstrated that R50 in fact accumulated active cytokinin in shoots, roots (Ferguson *et al* 2005; Fig. 1 7) and nodules (Held *et al.* 2008; Fig 1 8) High levels of a compound can be caused either by too high its production or too low its degradation Because the biosynthesis of cytokinin consists of many steps and the degradation is straightforward with a single enzyme, Held *et al* (2008) according to the principle of parsimony studied the degradation of cytokinin CKX They found that R50 displayed lower total CKX activity (Fig 1.9) but higher transcript levels of *PsCKX1* and *PsCKX2* than wild type (Fig. 1 10)

Above is the general introduction necessary for understanding my objectives For each of the next chapters (2, 3 and 4), an introduction will be provided, followed by the hypotheses or objectives specific to that chapter; the section materials and methods will lead to the results section which will be followed by a discussion . Whereas chapter 2 will focus on R50 nodulation and cytokinin homeostasis, chapter 3 will report the cloning and characterization of *PsCKX2*, and chapter 4 will concentrate on R50 early seedling development and cytokinin homeostasis. In chapter 5, conclusions, further discussion, and a working model will be provided

1.4 Objectives

The long-term objectives of this thesis are 1) to understand how cytokinin affects nodulation in pea, and 2) to investigate if improper seedling development has an effect on nodulation. To achieve these two objectives, I chose as a tool R50 which accumulates cytokinins, exhibits low nodulation and abnormal seedling development My short-term objectives were to 1) study the effects of cytokinin level alteration on the wild type, 2) clone *PsCKX2*, an isoform of the CKX gene family in pea, and 3) follow the transcript levels of the two isoforms *PsCKX1* and *PsCKX2* during the early development of the seedling. Each of these objectives is addressed in subsequent chapters.

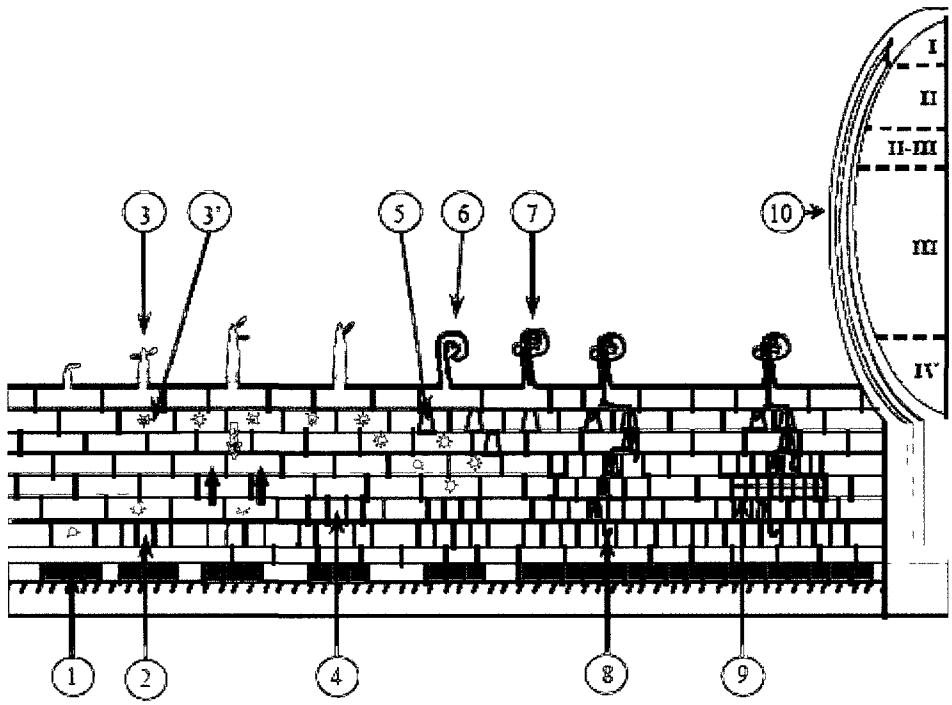

Figure 1.1 Nodule organogenesis in Medicago. ① NF have been released and pericycle cells have divided, the cortical cells are primed (red asterisks) ② Cortical cells divide anticlinally initiating nodule primordium formation ③ Root hair gets activated and prepares for bacterial entry while outer cortical cells are primed with reorganization of the cytoskeleton. ④ Outward gradient of cell differentiation whereby inner cortical cell gets ready for division; the result will be the growth of the nodule primordium (shown with black arrow) ⑤ Inward gradient of cell differentiation (shown with red arrow) whereby the outer cortical cells rearrange their cytoplasm; the result will be the formation of the pre-infection threads (PIT; shown in pink). ⑥ Simultaneously to the PIT formation, the root hair curls because of an asymmetric growth of the wall, it entraps ultimately bacteria which divide continuously to form a colony. Chemical degradation and physical pressure allow the entry of the bacteria within the hair. ⑦ The bacteria are progressing within an infection thread (IT), which is an environment where they continue to divide and to release NFs. ⑧The IT, growing centripetally because of the continuous division of the rhizobia, will follow the path paved by the PIT. ⑨ Cells of the middle cortex which have been traversed by the IT will dedifferentiate to form the nodule meristem ⑩The meristem is now capable of taking over and ends up to be responsible for the growth of the mature nodule. There are 6 zones within a mature nodule: the meristematic zone (I), the infection zone (II), the interzone where plant cells and rhizobial cells get ready for nitrogen fixation zone (II-III), the nitrogen fixation zone (III), the senescence zone (IV), and the saprophytic zone (not shown here) (Timmers *et al* 1999)

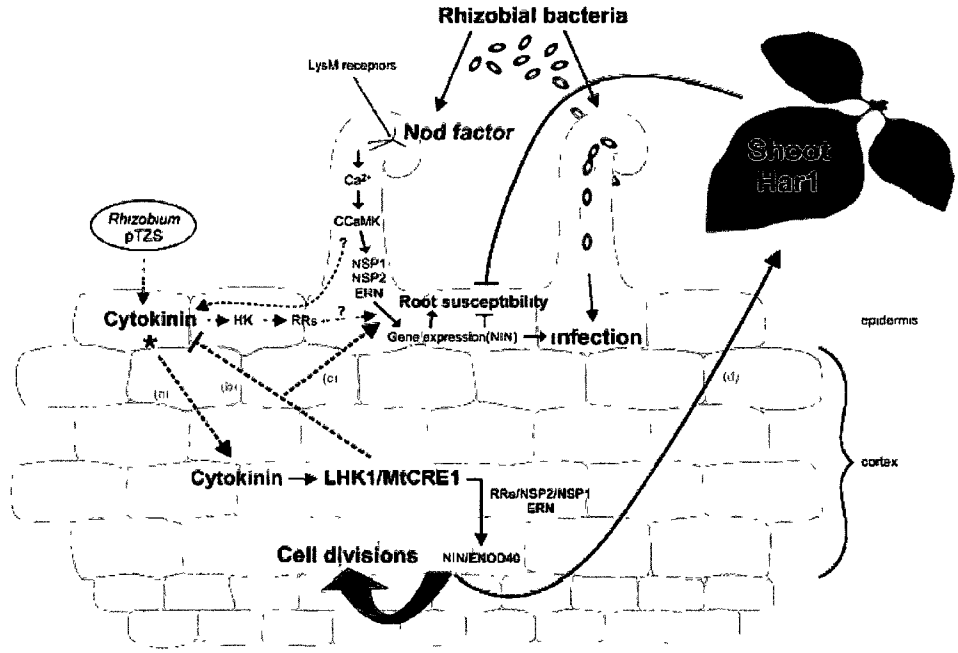

Figure 1.2 A constructed model of cytokinin functions in nodulation and infection events. Epidermally-produced cytokinin might be translocated to the cortex (a) These cytokinins are perceived by LHK1 or MtCRE1, and signaling through cytokinin response regulators (ARRs) leads to initiation of nodule organogenesis (cell division) This requires transcription factors, such as NSP2, NSP1 and ERN, as well as downstream functions, such as NIN and ENOD40. In *Lotus*, LHK1 participates in negative regulation of root susceptibility to infection (b). In *Medicago truncatula*, both nodule inception and infection thread progression, but not initiation, are linked to MtCRE1 function (c). Cytokinin might also participate in autoregulatory feedback mechanisms, possibly involving HAR1, to restrict nodule number (d) (Frugier *et al.* 2008).

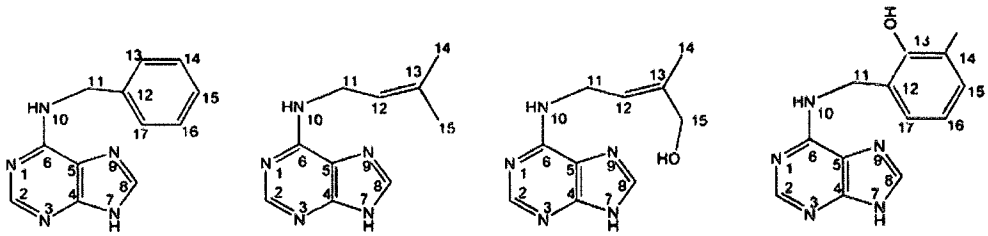

Figure 1.3 Cytokinin structures. Whereas N^6-Benzyladenine (BAP) is an aromatic-derivative cytokinin, N^6-isopentenyladenine (IP) and trans-zeatin (Z) are isoprene-derivative cytokinins; they are free-base cytokinins. IP and Z are substrates of cytokinin oxidase The last structure is that of PI-55, which has a structure similar to that of BAP. It differs at a specific position (13) of the aromatic side chain, and has cytokinin antagonistic properties (figures adapted from Malito *et al.* 2004 and Spíchal *et al.* 2009a).

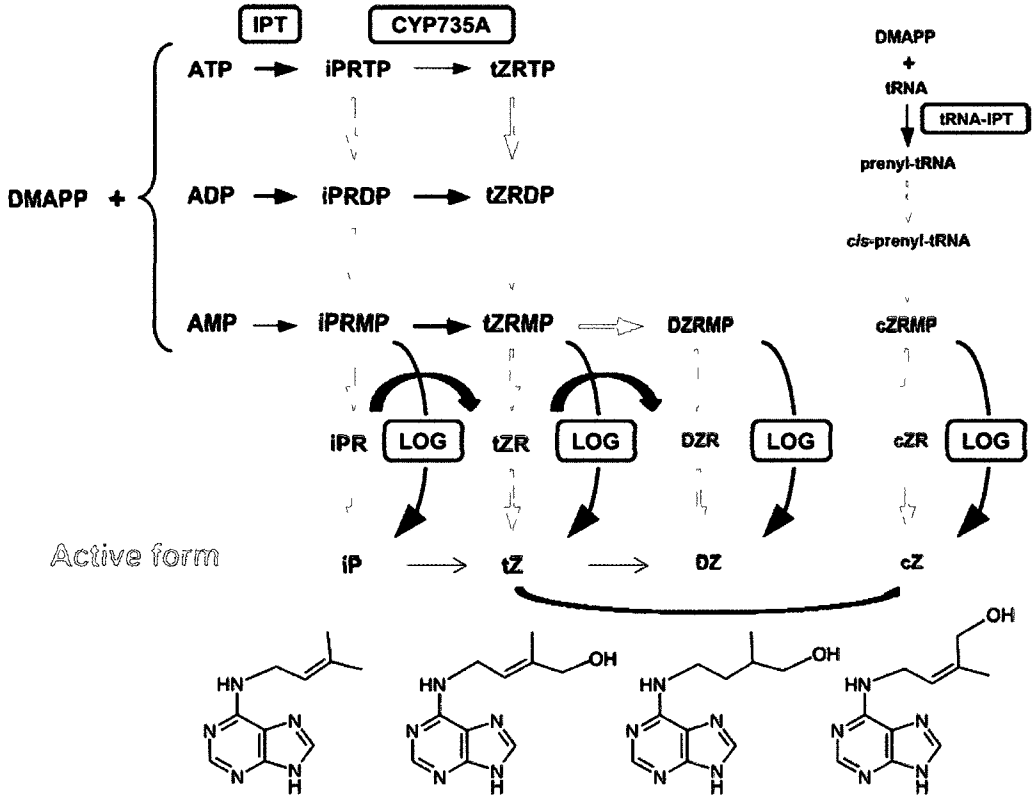

Figure 1.4 A model of cytokinin biosynthesis pathways and metabolism. Dimethylallyl diphosphate (DMAPP), adenosine phosphate-isopentenyltransferase (IPT); iP riboside 5'-triphosphate (iPRTP); iP riboside 5'-diphosphate (iPRDP); iP riboside 5'-monophosphate(iPRMP); tZ riboside 5'-triphosphate(tZRTP), tZ riboside 5'-diphosphate (tZRDP); tZ riboside 5'-monophosphate (tZRMP), DZ riboside 5'-monophosphate (DZRMP); cZ riboside 5'-monophosphate (cZRMP); (iPR) iP riboside, (tZR) tZ riboside, (DZR) DZ riboside; cZ riboside (cZR); N_6-isopentenyladenine (iP), *trans*-zeatin (tZ); (DZ) dihydrozeatin; (tZ), *cis*-zeatin (cZ). CYP735A is a cytochrome P450 mono-oxygenase. LOG is a cytokinin nucleoside 5'-monophosphate phosphoribohydrolase. Blue arrows indicate reactions with known genes encoding the enzyme, and grey arrows indicate that the genes have yet to be identified (Figure from Hirose *et al.* 2008). The chemical structure of each cytokinin active form is illustrated at the bottom of the figure.

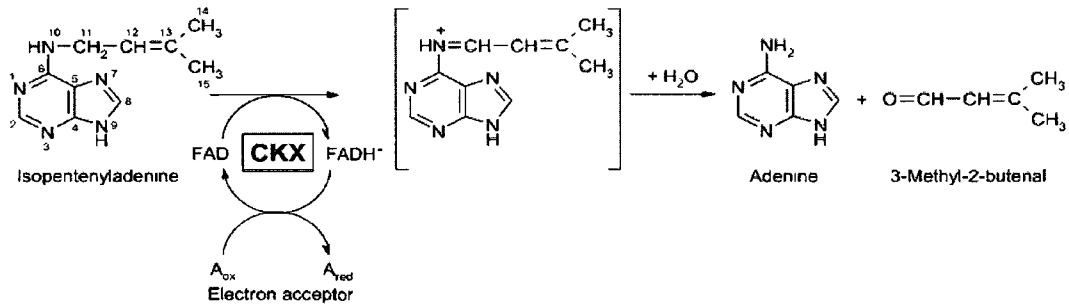

Figure 1.5 Cytokinin degradation. The reaction catalyzed by CKX with isopentenyladenine (IP) as a substrate is a two-step reaction, however, the end-product of the first step (in brackets) is very unstable and quickly converted to adenine and 3-methyl-2-butenal (figure from Werner *et al.* 2006). Nucleoside cytokinins can also be degraded by CKX; they are converted to adenosine and 3-methyl-2-butenal (not shown)

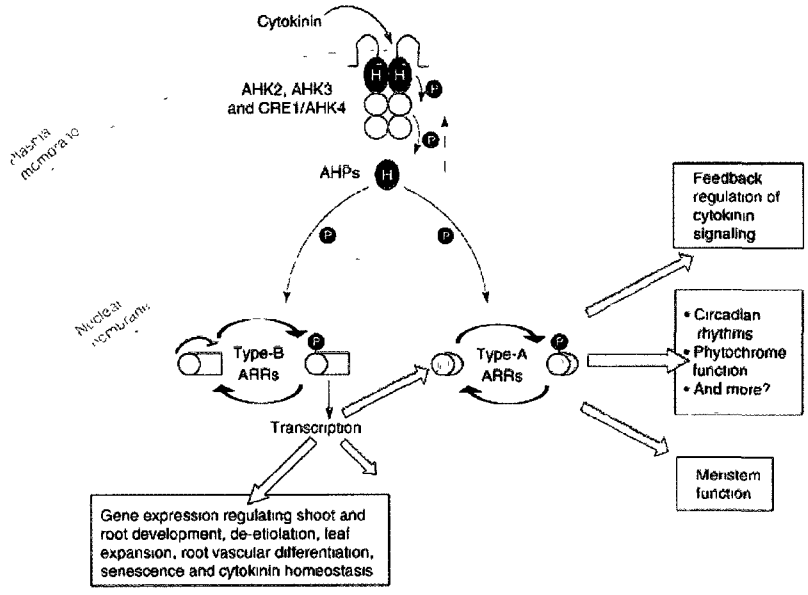

Figure 1.6 Cytokinin signal transduction pathway and downstream action. Cytokinin receptors consist of an extracellular cytokinin-binding CHASE domain, cytoplasmic His-Kinase domain (darkest green with H'), receiver domain (light green), and receiver-like domain (lightest green). Phosphoryl groups (dark blue) are transferred to AHP (dark green with H) The AHPs can translocate into the nucleus to transfer P to a type-A ARR or a type-B ARR Phosphorylation of type-B ARRs induces transcription of a subset of cytokinin-regulated targets (yellow arrows), mediating downstream cytokinin-regulation processes, including shoot and root development, de-etiolation, cytokinin homeostasis, etc (in white box). Phosphorylated type-A ARRs are activated to mediate downstream processes (orange arrows), including feedback regulation of cytokinin signaling, circadian rhythms, phytochrome function, and meristem function (in yellow box) (figure modified from To and Kieber 2008).

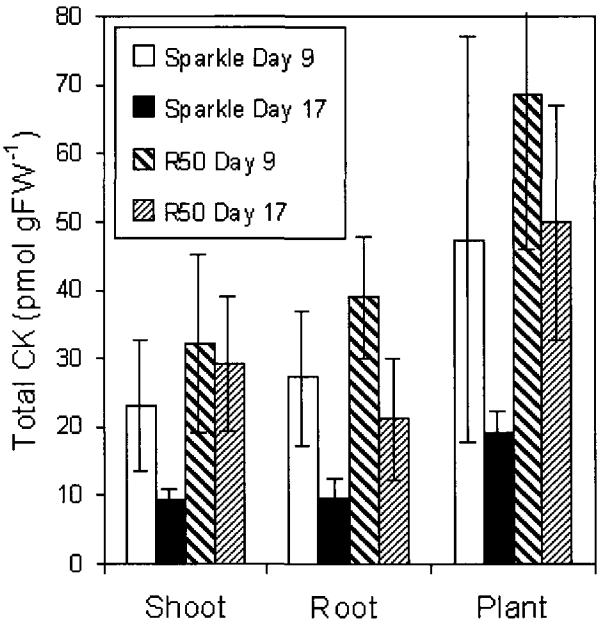

Figure 1.7 Total cytokinin concentration in shoot and roots. Total cytokinin concentration in the shoot, root, and entire plant of wild type and R50 at 9 and 17 DAP Values are means ± SE of three replicates (Figure from Ferguson *et al* 2005)

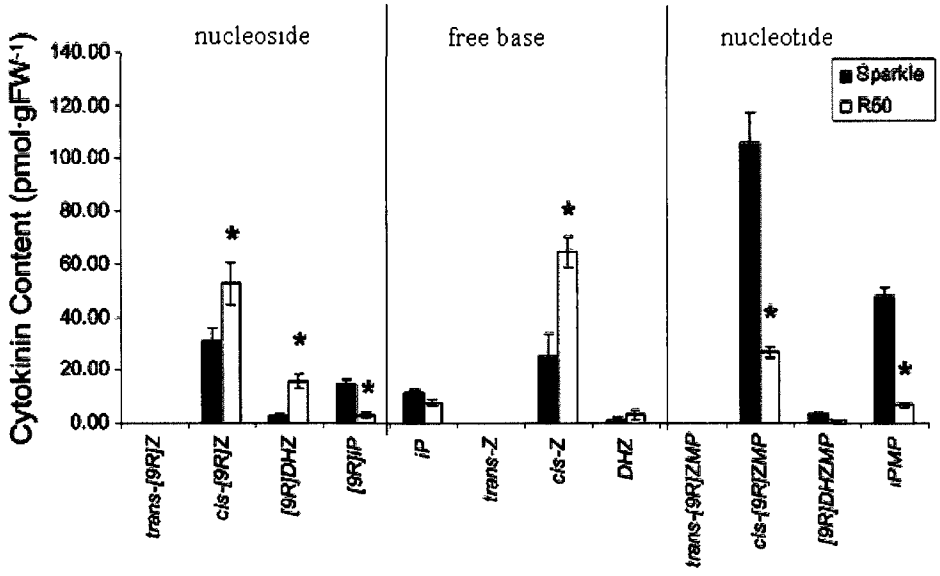

Figure 1.8 Cytokinin forms and contents in nodules. Three types of cytokinins are found in nodules of R50 (white bars) and wild type (black bars). An asterisk denotes significant line-related difference between R50 and wild type (figure from Held *et al.* 2008)

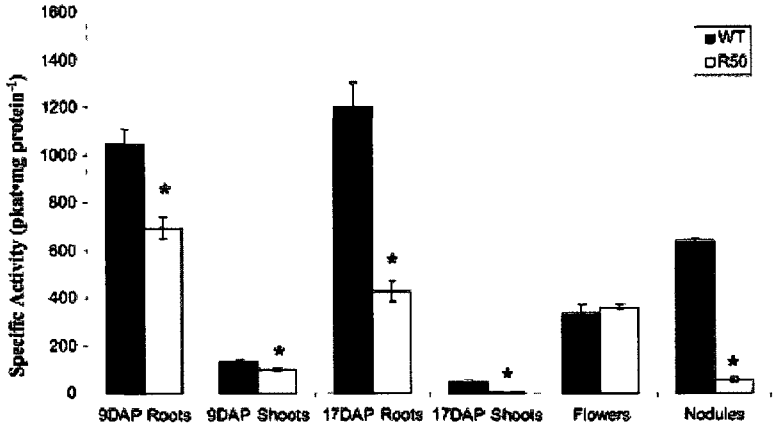

Figure 1.9 Total CKX activities in tissues. In vitro cytokinin oxidase activities are shown in young shoots (9 day), old shoots (17 day), young roots (9 day), old roots (17 day), flowers and nodules from wild type (black bar) and R50 (white bar). An asterisk denotes significant line-related differences between wild type and R50 (figure from Held *et al* 2008).

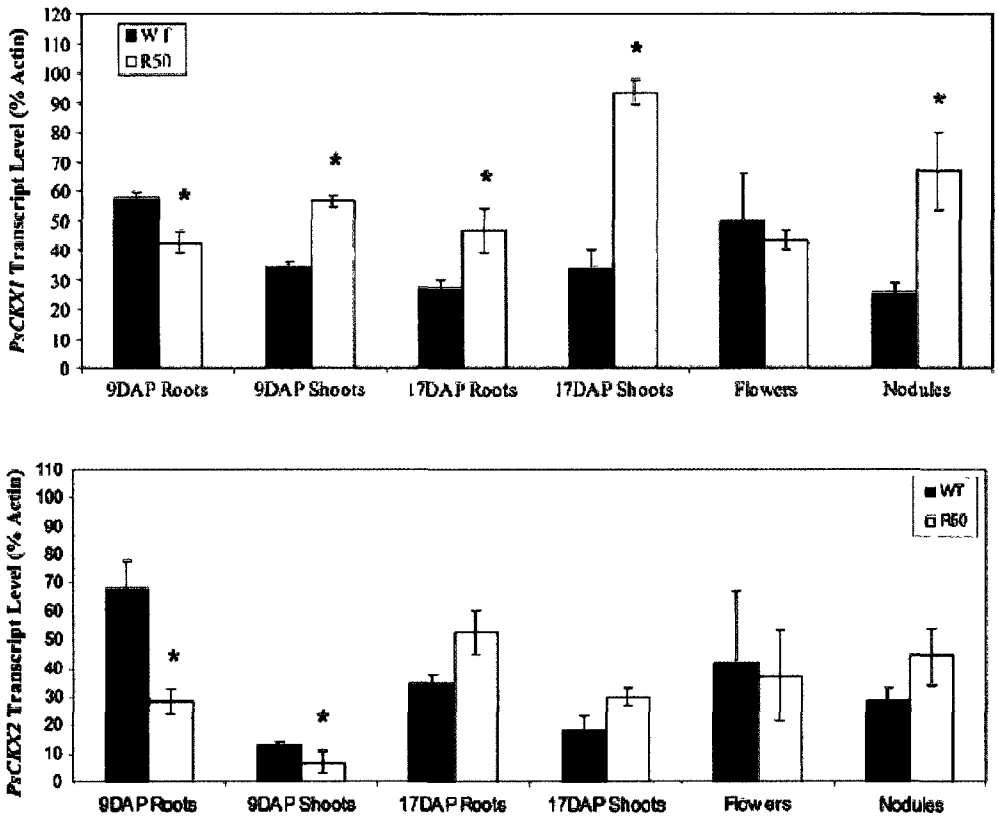

Figure 1.10 Semiquantitative RT-PCR of *PsCKX* transcripts. Semiquantitative RT-PCR of *PsCKX1* and *PsCKX2* transcripts from young shoots (9 day), old shoots (17 day), young roots (9 day), old roots (17 day), flowers and nodules from wild type (black bar) and R50 (white bar). An asterisk denotes significant line-related differences between pea lines (figure from Held *et al.* 2008).

Chapter 2 Nodulation and cytokinin homeostasis

2.1 Introduction

2.1.1 Cytokinin perception and signal transduction

As plants cannot perform any movement, they are not able to escape from stressful environmental conditions. In order to survive, they depend mainly on their abilities to react quickly and efficiently They have developed and optimized many different and sophisticated signal perception and transduction systems (Grefen *et al.* 2004). The cytokinin perception and signal transduction pathway is one of them. In 1955, Skoog, Miller, and collaborators purified the first cytokinin crystal and demonstrated its strong effect on cell division in tobacco tissue culture (Amasino *et al.* 2005). It then took some 40 years to identify the first genes involved in cytokinin signaling *CKI1*, a receptor histidine kinase gene, was identified during a large screen based on the effects of cytokinin on cultured *Arabidopsis* tissues (Kakimoto *et al* 1996) This gene, which encodes a protein similar to a two-compound regulator, can induce typical cytokinin response when over-expressed; according to Kakimoto *et al.* (1996), CKI1 may be considered as a candidate for a cytokinin receptor These results initiated numerous studies in this area. Finally in 2001, CRE1/AHK4, another histidine kinase from *Arabidopsis*, was identified as the first cytokinin receptor (Inoue *et al* 2001; Suzuki *et al.* 2001, Ueguchi *et al.* 2001)

Three cytokinin receptors, AHK2, AHK3, and CRE1/AHK4, have been identified so far. The *WOL1/CRE1/AHK4* gene (hereafter referred to as CRE1/AHK4) was originally identified in a screen for short root mutants (*wol*) in *Arabidopsis* (Mähönen *et al.* 2000). The same gene was later isolated in a genetic screen for cytokinin-response (CRE) mutants that

exhibited a reduced response to cytokinin treatment (Inoue *et al.* 2001) CRE1/AHK4 and its homologs AHK2 and AHK3 encode histidine kinases that can bind cytokinin and exhibit cytokinin-dependent kinase activity in heterologous bacterial and yeast systems (Suzuki *et al.* 2001). There might be some differences between the individual AHKs in their affinities for specific cytokinins (Yamada *et al* 2001). For example, AHK3 and CRE1/AHK4 are both sensitive to free bases, but CRE1/AHK4 is not activated by the nucleoside and nucleotide forms; furthermore, AHK4 recognizes only trans-zeatin whereas AHK3 recognizes cis-zeatin and dihydrozeatin as well (Spíchal *et al* 2004).The signal transduction pathway has been introduced in Chapter 1, Fig 1 6 (modified from To and Kieber 2008); for further information, the reader is invited to go to the excellent review paper by To and Kieber (2008)

Because of the lack of appropriate tools, the study of the cytokinin signaling transduction pathway has been relatively slow compared to that of other hormones, particularly ethylene. Often, research on cytokinins has been based on experiments where the effects of altering either exogenously or endogenously their levels in plants were studied For example, Lorteau *et al* (2001) treated plants with BAP whereas Werner *et al.* (2003) overexpressed *AtCKX* genes in *Arabidopsis* Cytokinin inhibitors have also been utilized as a tool. One popular cytokinin inhibitor is lovastatin; it indeed can inhibit nodulation and primary root growth in *Medicago truncatula* (Kevei *et al* 2007). However, its action is too far upstream in the cytoplasmic isoprenoid synthesis pathway to link it directly to cytokinins (Kevei *et al.* 2007) Another group of common cytokinin inhibitors are the synthetic cytokinin antagonists: triazolo[4,5-d]pyrimidines, pyrazolo[4,3-d]pyrimidines; pyrrolo[2,3-d] pyrimidines; pyri-

do[2,3-d]pyrimidines; urea derivatives; carbamate derivatives, and 1, 3, 5-triazine derivatives (Vaseva-Gemisheva *et al* 2005b) Although the number of cytokinin inhibitors is high, the number of studies taking into account their mode of action is low. Almost no information about the influence of anticytokinins on cytokinin mechanism is available (Vaseva-Gemisheva *et al.* 2005b).

Recently, a group of chemists in the Czech Republic has synthesized cytokinin antagonists to study the mechanisms of cytokinin perception and signal transduction. The first identified molecule to antagonize cytokinin at the receptor level is PI-55, a 6-(2-hydroxy-3-methylbenzylamino) purine (Fig 1.3), the structure of which is analogous to that of BAP (Spíchal *et al.* 2009a) PI-55 primarily inhibits the binding of the natural ligand trans-zeatin to the *Arabidopsis* cytokinin receptors CRE1/AHK4 (Spíchal *et al.* 2009a) Through cytokinin bioassays, the authors have demonstrated that PI-55 antagonizes cytokinin effects in *Nicotiana tabacum* (tobacco) and *Triticum aestivum* (wheat) PI-55 also accelerates the germination of *Arabidopsis* seeds, promotes root growth, and stimulates root branching (Spíchal *et al.* 2009a), however, the effects of PI-55 on a legume have not yet been determined.

In 2010, another cytokinin receptor antagonist named LGR-991 was identified by Jaroslav Nisler, a Czech student who came to Dr. Guinel's lab as a visiting Ph.D student (Nisler *et al* 2010). LGR-991 not only acts as a competitive inhibitor to the cytokinin receptor AHK3, but it also blocks CRE1/AHK4 in a minor way. Besides its competitive effect towards the endogenous cytokinins, LGR-991 is capable of competing in an inhibitory manner with the exogenous cytokinin BAP (Nisler *et al* 2010). It stimulates the germination

of *Arabidopsis* seeds and increases the hypocotyl length of dark-grown seedlings; both actions are symptomatic of reduced cytokinin levels Therefore, LGR-991 can compete with cytokinin receptors and induce an effect analogous to that of decreased cytokinin content. These results complement the biochemical finding that LGR-991 acts as a cytokinin receptor antagonist (Nisler *et al* 2010).

2.1.2 Cytokinin degradation

One major metabolic pathway to inactivate cytokinin biological activity in plant cells is degradation Cytokinin oxidase (CKX) is the only identified plant enzyme capable of degrading naturally-occurring cytokinins. It was discovered first in a crude extract of cultured tobacco tissue more than 30 years ago (Pačes *et al* 1971), since then this enzyme has been purified in a number of lower plants, such as mosses, ferns and horsetails, and in higher plants, such as maize, bean, poplar, and wheat (Mok and Mok 2001) CKX had been mechanistically classified for many years as a copper-containing amine oxidase (Hare and van Staden 1994), however, many recent investigations have revealed that this enzyme acts as a dehydrogenase enzyme (e g , Galuszka *et al.* 2004) This enzyme selectively and irreversibly degrades free cytokinin bases and ribosides by cleaving their isoprenoid side-chain from the adenine ring (Haberer and Kieber 2002). The cytokinin oxidase from higher plants catalyses the cleavage of the N_6-unsaturated isoprene side chain of the cytokinin molecule. In the case of N_6-isopentenyladenine, the products of the reaction were identified as adenine (McGaw and Horgan 1985) and 3-methyl-2-butenal (Brownlee *et al* 1975), which originates from the oxidation of the isoprene side-chain.

CKX is a highly substrate-specific enzyme, generally in all higher plants, CKX appears to have a preference for isopentenyladenine, zeatin, and their ribosides (Galuszka *et al.* 2004). It cannot recognize cytokinins with saturated side-chains (e.g dihydrozeatin) or with cyclic side-chains (e.g. kinetin and benzyladenine), with the exception of the wheat CKX which degrades benzyladenine, though 40-fold less effectively than isopentenyladenosine (Laloue and Fox 1989) and the CKX from the moss *Funaria hygrometrica* which prefers kinetin (Gerhauser and Bopp 1990). It is clear that the isoprene chain which bears a double bond is necessary for the binding of the cytokinin to the active site of the enzyme (Galuszka *et al* 2004). Therefore, side-chain modification such as O-glucosylation apparently confers resistance to CKX (Sakakibara *et al* 2004) It has also been discovered that the cytokinins bearing a hydrophilic group in position 2 of the purine ring are better substrates than non-substituted molecules (Frébort *et al.* 1999) The three-dimensional crystal structure of a *Zea mays* CKX determined through X-ray analysis by Malito *et al* (2004) illustrates the actual action of cytokinin degradation catalyzed by CKX. This maize enzyme consists of a FAD-binding domain and a substrate-binding domain specific for isoprenoid cytokinins (Fig. 2.1) The FAD molecule binds to a histidine residue in the internal cavity of the enzyme and a funnel-shape region on the enzyme surface serves as the catalytic site where cytokinin can bind. The substrate displays a "plug-into-socket" binding model that seals the catalytic site. The adenine ring of the cytokinin sticks out from the surface of the protein to be cleaved.

The group of chemists previously mentioned from the Czech Republic successfully synthesized substituted 6-anilinopurines, which are a group of potent CKX inhibitors; one of

which is called INCYDE. The inhibitory effects of INCYDE are displayed in vitro and in vivo (Spíchal *et al* 2009b) For example, INCYDE inhibits the degradation of exogenously-applied radiolabelled isopentenyladenosine in *Arabidopsis* seedlings. Furthermore, INCYDE application to CKX-overproducing transgenic plants leads to an increase of shoot growth (Spíchal *et al.* 2009b)

2.1.3 Cytokinin receptor and nodulation

That cytokinins are involved in nodulation is supported by numerous lines of evidence, such as exogenous application experiments (Lorteau *et al.* 2001), cytokinin induction of the expression of several early nodulin genes (Cooper and Long 1994; Fang and Hirsch 1998), cytokinin application simulating early nodulation responses such as cortical cell division and amyloplast deposition (Bauer *et al* 1996). Recent research further illustrates a direct connection between nodulation and cytokinin receptor CRE1/AHK4 (Gonzalez-Rizzo *et al* 2006, Murray *et al* 2007; Tirichine *et al* 2007, Frugier *et al.* 2008)

Figure 2.1 Overall structure of the maize CKX enzyme. It consists of a substrate-binding domain (in red) and a FAD-binding domain (in blue) The FAD molecule (in yellow) binds to the FAD-binding domain The cytokinin ligand is shown in black. The N-terminal and C-terminal residues are labeled by N and C, respectively (Malito *et al.* 2004)

2.1.4 Objectives and hypotheses

2.1.4.1 Effects of PI-55 treatment on wild type

In this section, I hypothesize that:

1) CRE1 is involved in the nodulation of pea because it has been demonstrated that cytokinin receptors were extremely important for the nodulation of *Medicago* and *Lotus*. I will test my hypothesis by treating wild type plants with the cytokinin receptor antagonist PI-55 and examine its effects on nodule number If cytokinin sensing is essential to nodulation, disturbing cytokinin perception (less cytokinin perceived may result in a less strong signal transduction) should have a negative effect on nodulation. If fewer nodules are found in PI-55-treated plants than in control plants, then CRE1/AHK4 is likely involved in pea nodulation. It may also implicate AHK3 in nodulation because PI-55 is known to bind AHK3 in a minor way

2) The traits, other than nodulation, exhibited by R50 are the result of a disruption of cytokinin perception. I will test this hypothesis by treating wild type plants with PI-55 and examine the effects of PI-55 on lateral root number, primary root length, shoot height, and third internode length and diameter. If PI-55-treated wild type plants mimic the R50 traits, such as fewer lateral roots, a shorter primary root (Guinel and Sloetjes 2000), shorter shoot height, shorter and thicker third internode (Kneen *et al.* 1994), then R50 phenotype is likely caused by a cytokinin signal disruption. It is possible that only certain traits of R50 will be mimicked; this could then mean that the R50 phenotypes is only partially caused by a disruption of a cytokinin signal.

3) PI-55 can compete with both endogenous and exogenous cytokinins because this compe-

tition character was found in *Arabidopsis*. I will test this hypothesis by treating wild type exogenously with either PI-55 alone or PI-55 together with BAP If PI-55 can compete with endogenous cytokinins, then treated wild type should have reduced nodulation (this would be equivalent to hypothesis 1) If PI-55 is capable of competing with exogenous cytokinin, then wild type treated with a combination of PI-55 and BAP should exhibit higher number of nodules than wild type treated with BAP alone because high concentrations of BAP inhibit nodulation (Lorteau *et al.* 2001).

2.1.4.2 Effects of INCYDE treatment on wild type

According to Lorteau *et al* (2001), nodule number is dependent on exogenous BAP concentrations; 1μM is optimal and lower or higher concentrations have a negative effect on nodulation [Fig. 2 2 A, figure modified from Lorteau *et al.* (2001)] Unfortunately, I cannot know how much endogenous cytokinin gets utilized by plants Therefore, I defined the optimal concentration for nodulation (1μM BAP in Fig. 2 2 A) as the optimal cytokinin concentration in use in plants (2 in the Fig 2 2 B). At that optimal concentration, both endogenous and exogenous cytokinins are utilized optimally by the plants to produce the most nodules In this section, I hypothesize that.

1) CKX plays an essential role in the nodulation of pea. I will test my hypothesis by treating wild type plants with the cytokinin inhibitor INCYDE and examine its effects on nodule number If INCYDE inhibits CKX, a plant treated with INCYDE should accumulate cytokinin, and thus should have a negative or positive effect on nodulation. If a negative effect on nodulation (i e , cytokinin in use above 2 in Fig 2 2 B) or a positive effect on nodulation (i.e., cytokinin in use below 2 in Fig. 2 2 B) is observed, then CKX is essential to pea nodulation.

If no effect on nodulation is observed, CKX is likely not important to nodulation or INCYDE is not effective on pea.

2) The traits other than that of nodulation exhibited by R50 are the result of a defect in cytokinin degradation. I will test this hypothesis by treating wild type plants with INCYDE and examine the effects of INCYDE on lateral root number, primary root length, shoot height, and third internode length and diameter If INCYDE-treated plants mimic the R50 traits mentioned above, then the R50 phenotype is likely caused by a defect in cytokinin degradation It is possible that only certain traits of R50 will be mimicked, this could then mean that the R50 phenotype is only partially caused by a defect of cytokinin degradation.

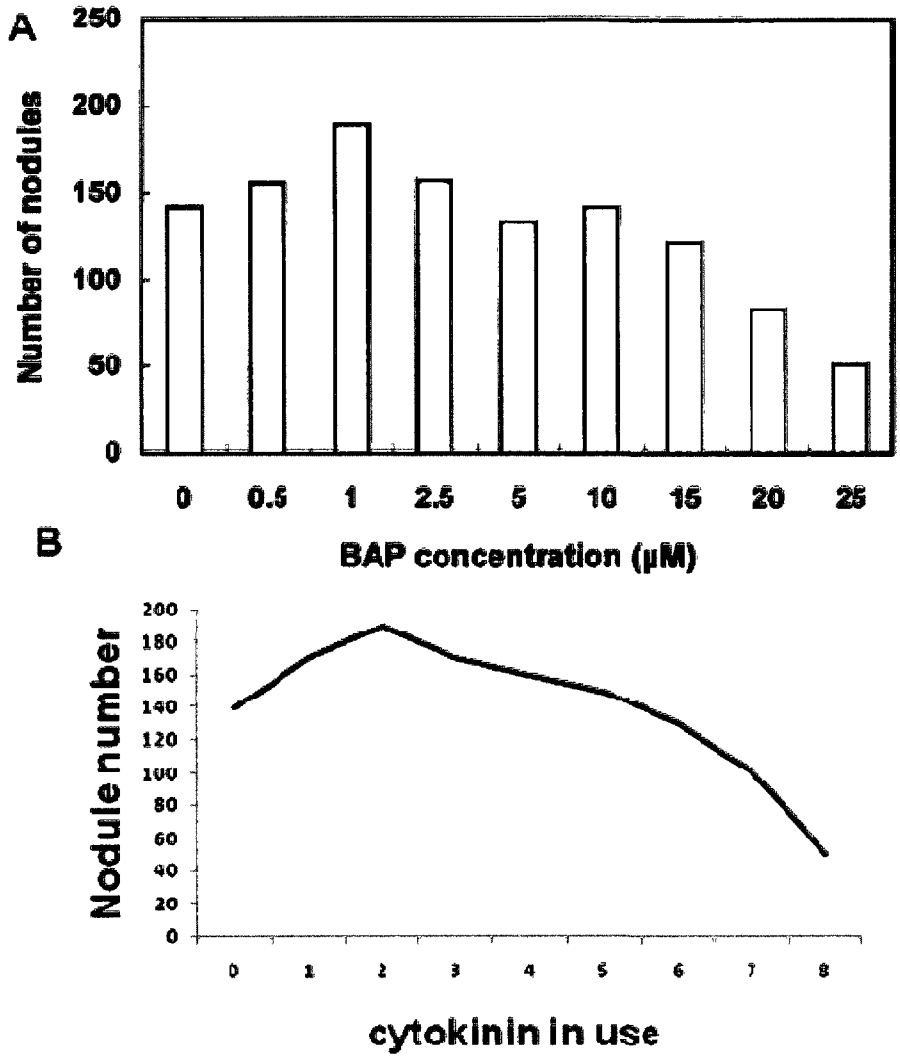

Figure 2.2 Effects on BAP and the simulated model. A) Effects of BAP on nodulation. Less than 1μM BAP stimulates nodulation, while more than 1μM BAP inhibits nodulation (figure modified from Lorteau *et al* 2001). B) The simulated model from Fig. 2.2 A. I defined the optimal concentration (relative amount) for nodulation (1μM BAP in Fig. 2 2 A) as the optimal cytokinin concentration in use in plants (2 in the Fig. 2 2 B) The control-treated plants are named zero in both Fig. 2 2 A and Fig. 2.2 B.

2.2 Materials and methods

2.2.1 Plant material and growth conditions

Randomly selected wild type seeds were surface-sterilized with an 8% bleach solution (5.25% NaOCl), washed for 5 min, and rinsed with sterile water 3 times for 30 seconds They were placed in water to imbibe in the dark for 16h Seeds were then planted individually in yellow Conetainers™ (66ml, 2.5 cm × 16 cm; Stuewe &Sons Inc., Corvallis, OR) filled with sterile vermiculite (Holiday, Vil Vermiculite Inc , Toronto, ON), six in a beaker. Plants were grown under incandescent (OGE 600 hour, 60 – 120 W, 120 Volts, General Electric) and cool white fluorescent lights (Watt-Miser GE, F96TIZ-CW-HO-WM) in a growth-room with a 16h/8h, 23°C/18°C hour, light/dark regime The total light intensity received by the plants was 280 mol $m^{-2} \cdot s^{-1}$. The seedlings were inoculated 3 days after planting (DAP) with 5ml of a 2% solution of *Rhizobium leguminosarum* bv *viciae* 128C53K (gift from Dr S. Smith, EMD Crop Bioscience, Milwaukee, WI). The bacteria had been cultured for 48 hours in yeast-mannitol broth in an orbital shaking water-bath incubator (25°C, 100rpm) until the broth appeared turbid. Water and low nitrogen nutrient solution [2 mM KH_2PO_4, 0 5 mM $Ca(NO_3)_2$, 2 mM K_2SO_4, 1 mM $MgSO_4 \cdot 5H_2O$, 0 2 mM Fe III EDTA and micronutrient (0.05 mM KCl, 0.025 mM H_3BO_3, 0.002 mM $ZnSO_4 \cdot 7H_2O$, 0.002 mM $MnSO_4 \cdot H_2O$, 0.005 mM $CuSO_4$ H_2O, and 0.005 mM $Na_2MoO_4 \cdot 2H_2O$)] were added to the beakers containing the Conetainers™ (at times indicated on Table 2.1)

2.2.2 Chemical treatment

2.2.2.1 PI-55 treatment only

PI-55 (MW=255.28), a cytokinin receptor antagonist, was received from Dr. L. Spíchal (Laboratory of Growth Regulators, Institute of Experimental Botany, AS CR & Palacký University, Olomouc, Czech Republic). PI-55 (10 mg) was dissolved in DMSO (dimethyl sulfoxide; 783 45µl) to prepare a 50 mM stock solution A range of concentrations of PI-55 (0µM, 0.5µM, 1µM, 2µM, 3.5µM, 5µM, 10µM and 25µM) was prepared, and appropriate controls (DMSO and water) were performed. Each seedling was treated three times as indicated in Table 2.1 at its crown with 10 ml of either control or PI-55 solutions. This method of application was adapted from Lorteau *et al.* (2001) Plants were harvested at 18 days (Table 2 1)

2.2.2.2 PI-55 and BAP treatment

In order to study the antagonistic effects of PI-55, a competition experiment was performed by treating plants simultaneously with different concentrations of PI-55 and BAP at 5µM, a concentration known to inhibit nodulation (Lorteau *et al.* 2001). Appropriate PI-55 concentrations (the same as above) and BAP (MW=255 3; 50 mM stock solution prepared by dissolving it in 443.85µl NaOH) were prepared, and controls (DMSO, water, NaOH, and DMSO plus NaOH) performed. At days indicated in Table 2.1, 10 ml of control solutions, BAP solution, or PI-55 and BAP solution were added to appropriate plants Plants were harvested at day 18 (Table 2 1).

2.2.2.3 INCYDE treatment

INCYDE (MW=275.7), a cytokinin oxidase inhibitor, was also received from Dr. L. Spíchal. INCYDE (10 mg) was dissolved in DMSO (846.11µl) to prepare 50 mM stock solution One

control was DMSO (concentration is the same as the DMSO concentration in 1μM INCYDE) in water. Another control was BAP at 100nM because Lorteau *et al.* (2001) found that less than 1μM BAP increased nodule number. A range of concentration of INCYDE (1μM, 100nM and 10nM) was prepared Each seedling was treated three times as indicated in Table 2.1 at its crown with 10 ml of either the control (DMSO in water), BAP or INCYDE solutions. This method of application was adapted from Lorteau *et al.* (2001) Plants were harvested at day 18 (Table 2.1).

2.2.2.4 Measurement of parameters

Plants were removed from the Conetainers™ and the vermiculite was washed off gently from their roots Various morphological measurements were assessed For the root, nodules and lateral roots were counted and the primary root length was measured All the nodules including mature nodules which are pink and young nodules which are white were counted For the shoot (Fig 2 3), height, and third internode length and diameter, were determined The lengths and diameter were measured using a ruler and a digital caliper, resectively.

2.2.2.5 Statistical analysis

For all experiments, data were analysed for statistical significance with the program Sigma-Stat® version 2 03 software (SPSS Inc., Chicago Illinois). The Student's t-test was applied to determine significant difference ($P \leq 0\ 05$) between wild type and R50, unless mentioned otherwise Each trial was composed of 6 plants for each pea line, and performed at least in triplicates

Table 2.1 Time line.

Time line (days)	PI-55 experiment	PI-55 &BAP experiment	INCYDE experiment
0	Imbibition	Imbibition	Imbibition
1	Planting	Planting	Planting
2	Water	Water	Water
3			
4	Inoculation	Inoculation	Inoculation
5	PI-55 treatment 1	PI-55 and BAP treatment 1	INCYDE treatment 1
6			
7	PI-55 treatment 2	PI-55 and BAP treatment 2	INCYDE treatment 2
8			
9	PI-55 treatment 3	PI-55 and BAP treatment 3	INCYDE treatment 3
10			
11	Water	Water	Water
12			
13	Water	Water	Water
14			
15	Low nitrogen nutrient solution	Low nitrogen nutrient solution	Low nitrogen nutrient solution
16			
17	Water	Water	Water
18	Harvest	Harvest	Harvest

This table indicates the times at which the treatments were given to different sets of wild type pea plants. I defined the day of imbibition as day zero

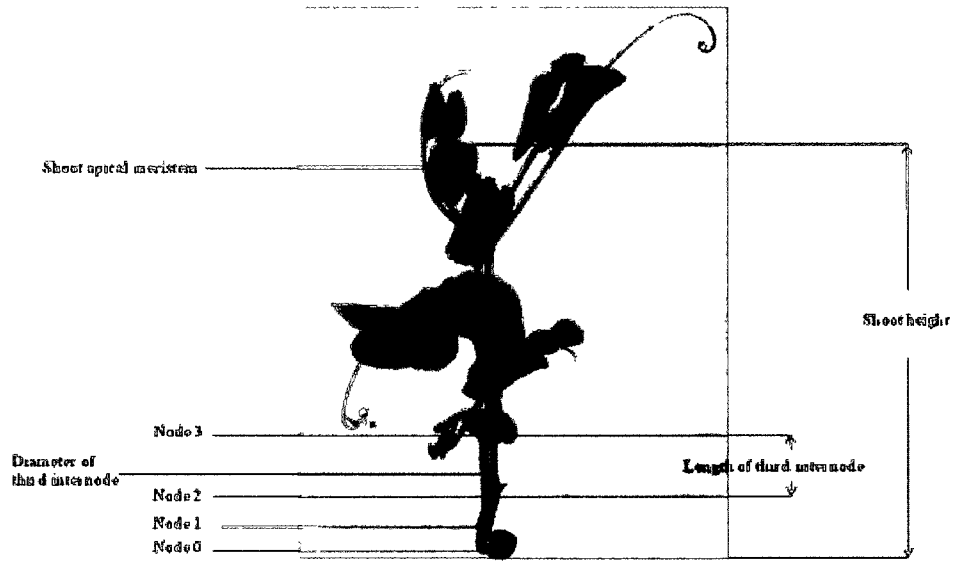

Figure 2.3 Parameters measured on shoot. Shoot of wild type pea plant illustrating the measurements which were taken at harvest time The three parameters are shoot height, and the third internode length and diameter. The shoot height is the length from the cotyledonary node to the shoot meristem. For measuring third internode length, I defined the cotyledonary node as node 0 and the first bract (from bottom to top) as node 1, the second as 2, and the third as 3. Thus, the internode between nodes 2 and 3 is the third internode. The diameter of this internode was measured at mid-point between node 2 and 3

2.3 Results

2.3.1 Effects of PI-55

The average number (69) of nodules from the control DMSO-treated plants was not different from that (60) of the water control (data not shown). Therefore, all the figures in this chapter only display results obtained with DMSO as a control. Plants treated with 25μM PI-55 were short and had very thick lateral roots and a short primary root, their appearance was not healthy. Therefore, those plants have not been taken into account As Fig. 2.4A illustrates, at low PI-55 concentrations (0 5 to 3.5μM), nodule numbers were not affected. However, at higher concentrations (5μM and 10μM), PI-55 inhibited significantly nodulation. When compared to the control treatment, the nodule number was reduced by half at 10μM (Fig 2 4A). When compared to the control DMSO treatment, lateral root numbers were not significantly affected by most of the concentrations of PI-55 (Fig. 2.4B) PI-55 at 3.5μM, however, had a significant positive impact on lateral roots This concentration was identified as the optimal concentration to promote lateral root formation, and also as a threshold concentration PI-55 at other concentrations increased, although not significantly, the lateral root number. For other parameters, primary root length (Fig 2.5A), shoot height (Fig 2 5B), third internode length (Fig. 2.6A), and third internode diameter (Fig 2 6B), no significant differences were found between PI-55-treated plants and controls However, trends may be seen: the shoots appeared to get taller as PI-55 concentration increased (Fig 2 5B) but likely not because of longer internode, furthermore, the diameter of the third internode seemed to vary in a dose-dependent manner with the PI-55 concentration (Fig. 2 6B).

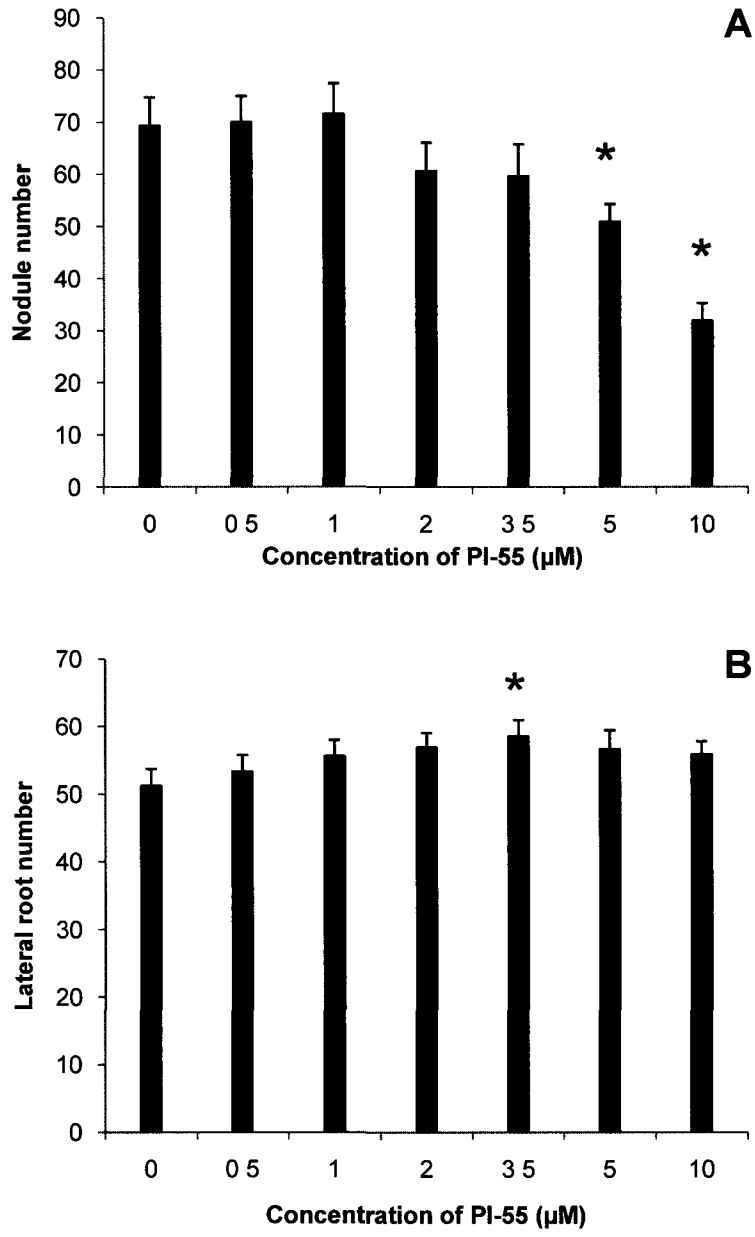

Figure 2.4 Effect of PI-55 on (A) nodule and (B) lateral root numbers. These data are those obtained when three trials were combined. Values are means ± SE, n=32 Asterisks represent statistical significance from the DMSO control at $P \leq 0.05$. Statistics were determined using Student's t-test.

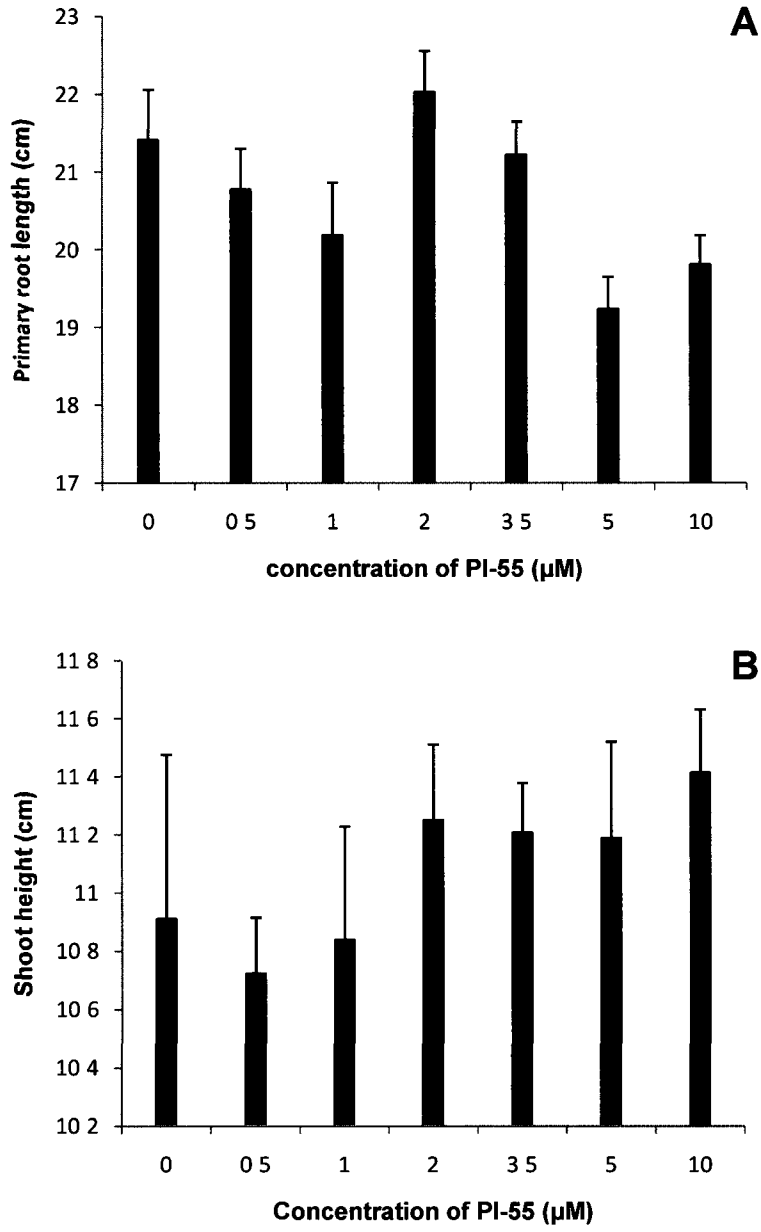

Figure 2.5 Effect of PI-55 on (A) primary root length and (B) shoot height. These data are those obtained when three trials were combined. Values are means ± SE, n=32. Asterisks represent statistical significance from the DMSO control at P≤0 05. Statistics were determined using Student's t-test

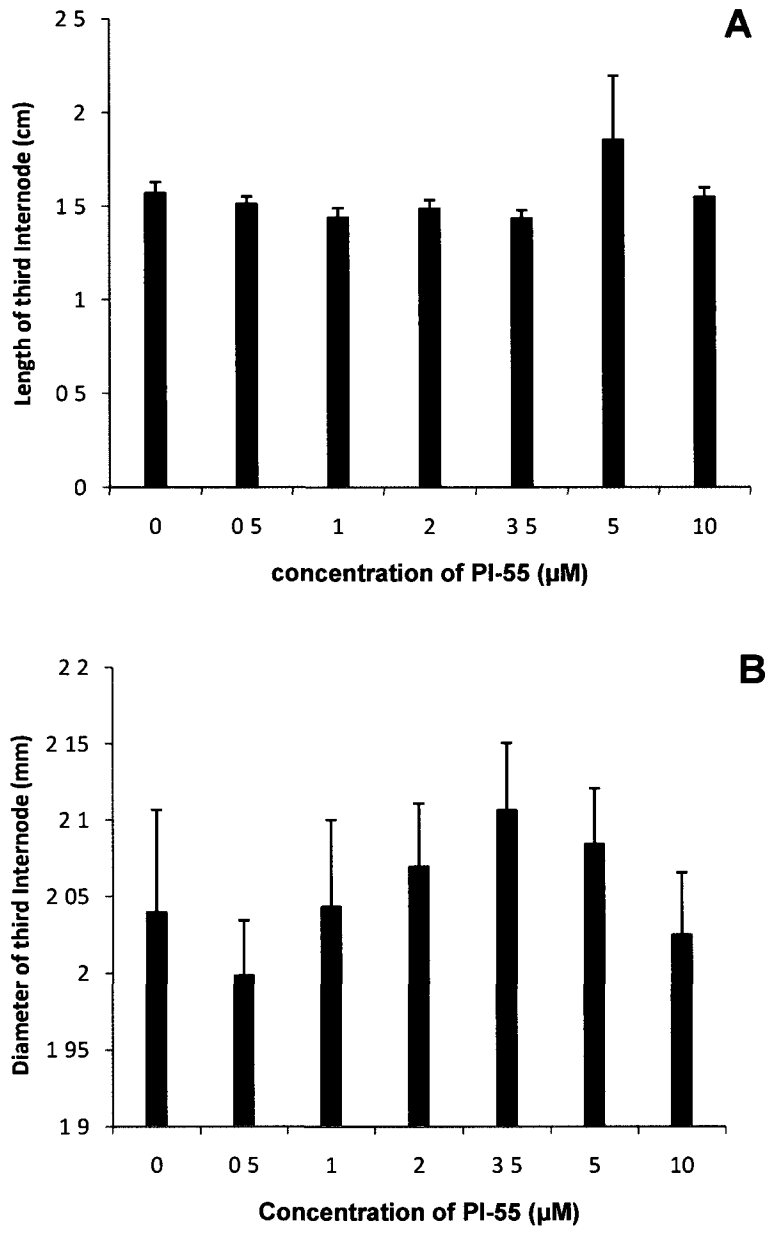

Figure 2.6 Effect of PI-55 on (A) third internode length and (B) diameter. These data are those obtained when three trials were combined. Values are means ± SE, n=32. Asterisks represent statistical significance from the DMSO control at $P \leq 0.05$ Statistics were determined using Student's t-test and one way ANOVA test

2.3.2 Effects of PI-55 in competition with BAP

As Fig 2 7A shows, compared to the DMSO control plant which produced about 90 nodules, the BAP-treated plants had less than 10 nodules. This is in agreement with the finding of Lorteau *et al.* (2001) Therefore, I used this concentration of BAP (5μM) as control for all competition experiments. While the BAP-treated plants had few nodules, the PI-55 and BAP-treated plants produced about 20 nodules Thus, when in competition with BAP, PI-55 had a stimulatory effect on nodulation at all concentrations (Fig. 2.7A)

Compared to the control DMSO plants which produced about 45 lateral roots, the BAP-treated plants had about 35 lateral roots (Fig. 2.7B). It is in agreement with the finding of Spíchal *et al* (2009a). PI-55 at low concentrations when in competition with BAP did not have a stimulatory effect on lateral root number However, at a concentration of 3.5μM and higher, PI-55 was able to compete effectively with BAP as lateral root number increased significantly. Surprisingly, when treated with PI-55 at a concentration of 10μM in competition with BAP, plants produced even more lateral roots than the control group (Fig 2.7B). Compared to the control plant the shoot height of which is about 13 cm, the BAP-treated plants had a shoot height of about 10 cm, indicating the negative effects of BAP on epicotyl growth at high concentrations. For all the competition concentrations of PI-55, only PI-55 at 5μM has a stimulatory effect on shoot height when in competition with BAP (Fig 2.8A) However, even at that concentration, the PI-55-treated plants were shorter than the control plants

BAP was shown to have a negative effect on primary root length (Fig. 2.8B) and third internode length (Fig 2.9A). Compared to the DMSO controls, primary root length (Fig 2 8B)

and third internode length (Fig 2.9A) were also significantly affected by the combined concentrations of PI-55 and BAP. However, primary root length (Fig 2.8B) and third internode length (Fig. 2 9A) were not affected significantly when compared with BAP controls. For third internode diameter (Fig 2.9B), no significant differences were found in competition experiments either compared with DMSO or BAP controls.

2.3.3 Effect of INCYDE

According to Lorteau *et al.* (2001), application of less than 1μM BAP promoted nodule number. My experiment confirmed this because 100nM BAP increased significantly nodule number (Fig 2 10A). Therefore, all the figures in this section use BAP concentration 100nM as a control When compared to the DMSO control treatment, nodule numbers were significantly increased at 100nM and 1μM INCYDE (Fig. 2.10A) When compared to the control DMSO treatment, primary root lengths were significantly affected by INCYDE from 100nM up (Fig 2 10B) INCYDE had a significant negative impact on primary root length.

For other parameters, lateral root number (Fig. 2 11A), shoot height (Fig. 2 11B), length (Fig 2.12A), and third internode diameter (Fig 2 12B), no significant differences were found between INCYDE-treated plants and DMSO controls

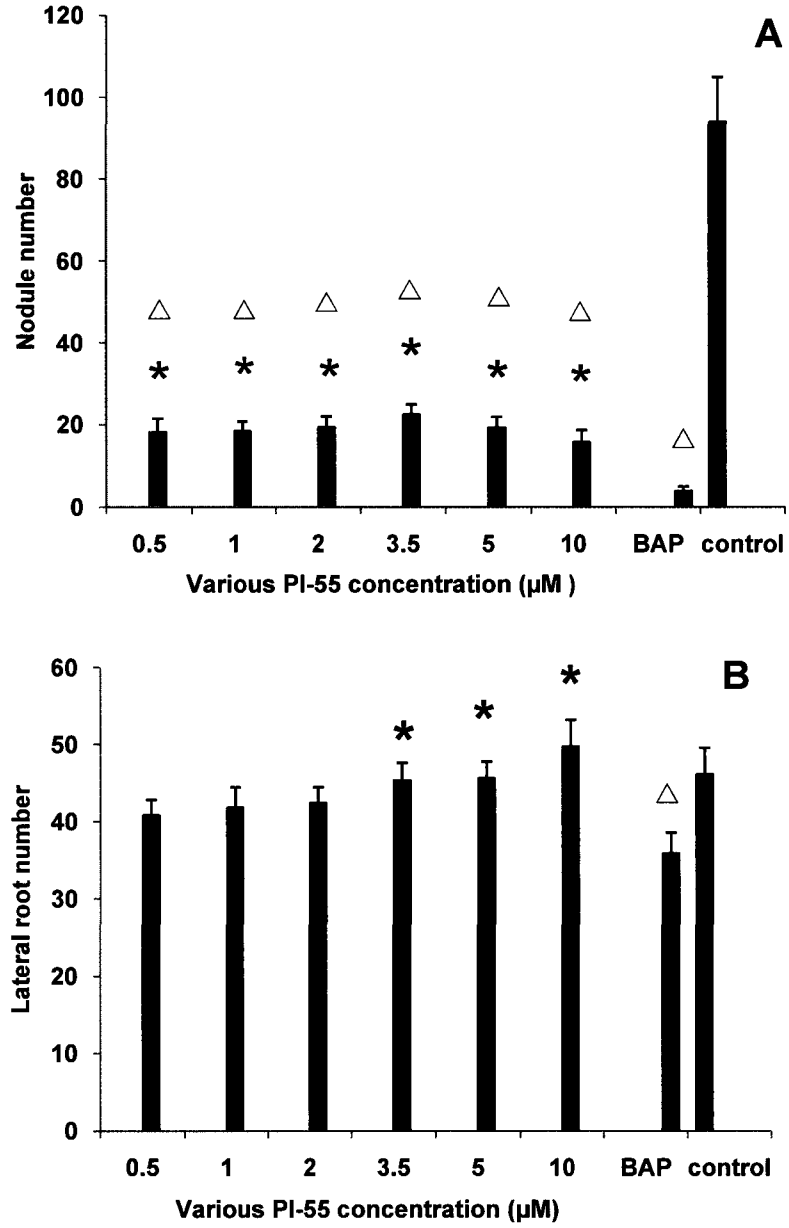

Figure 2.7 Effect of PI-55 and BAP (5µM) on (A) nodule and (B) lateral root numbers. The PI-55 concentrations represent here the various PI-55 concentrations supplemented with 5µM BAP. These data are those obtained when three trials were combined. Values are means ± SE, n=18 Triangles represent statistical significance from DMSO control at $P \leq 0.05$ and asterisks represent statistical significance from BAP control at $P \leq 0.05$. Statistics were determined using Student's t-test.

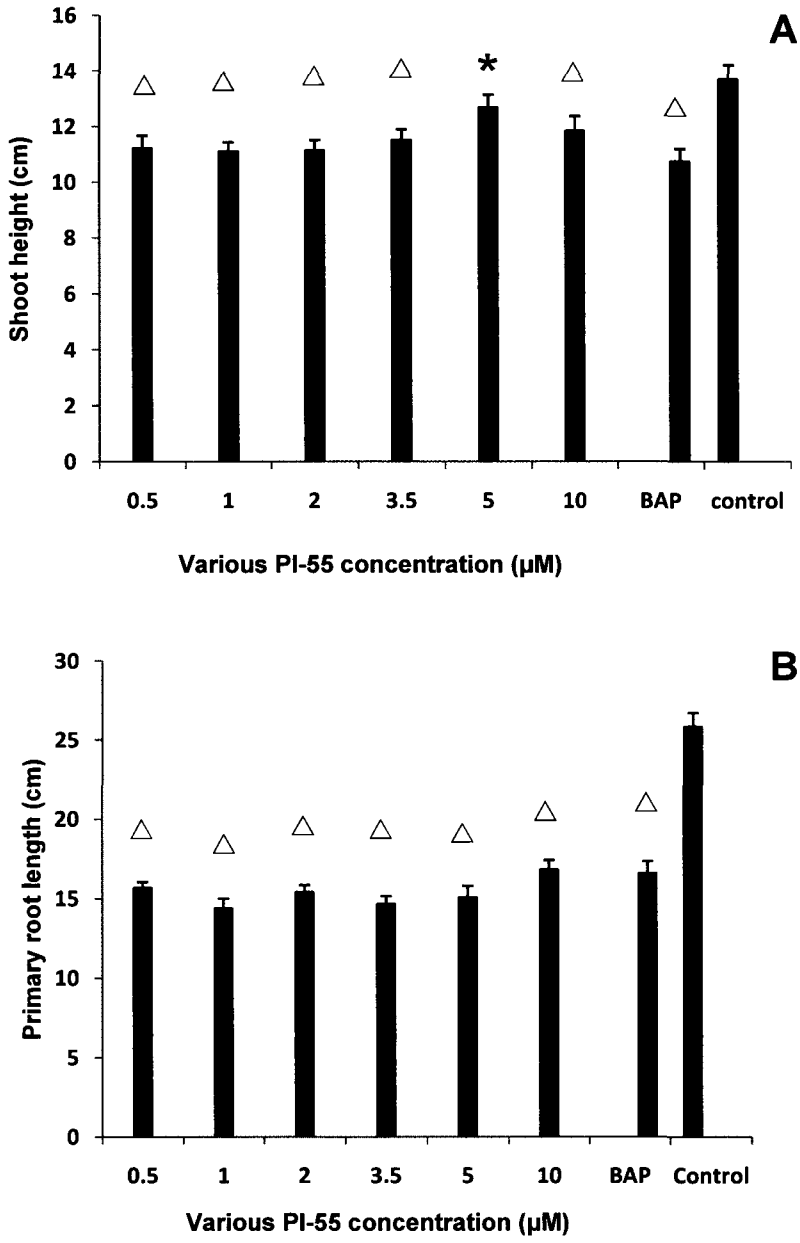

Figure 2.8 Effect of PI-55 and BAP (5µM) on (A) shoot height and (B) primary root length. The PI-55 concentrations represent here the various PI-55 concentrations supplemented with 5µM BAP These data are those obtained when three trials were combined. Values are means ± SE, n=18 Triangles represent statistical significance from DMSO control at $P \leq 0.05$ and asterisks represent statistical significance from BAP control at $P \leq 0.05$. Statistics were determined using Student's t-test.

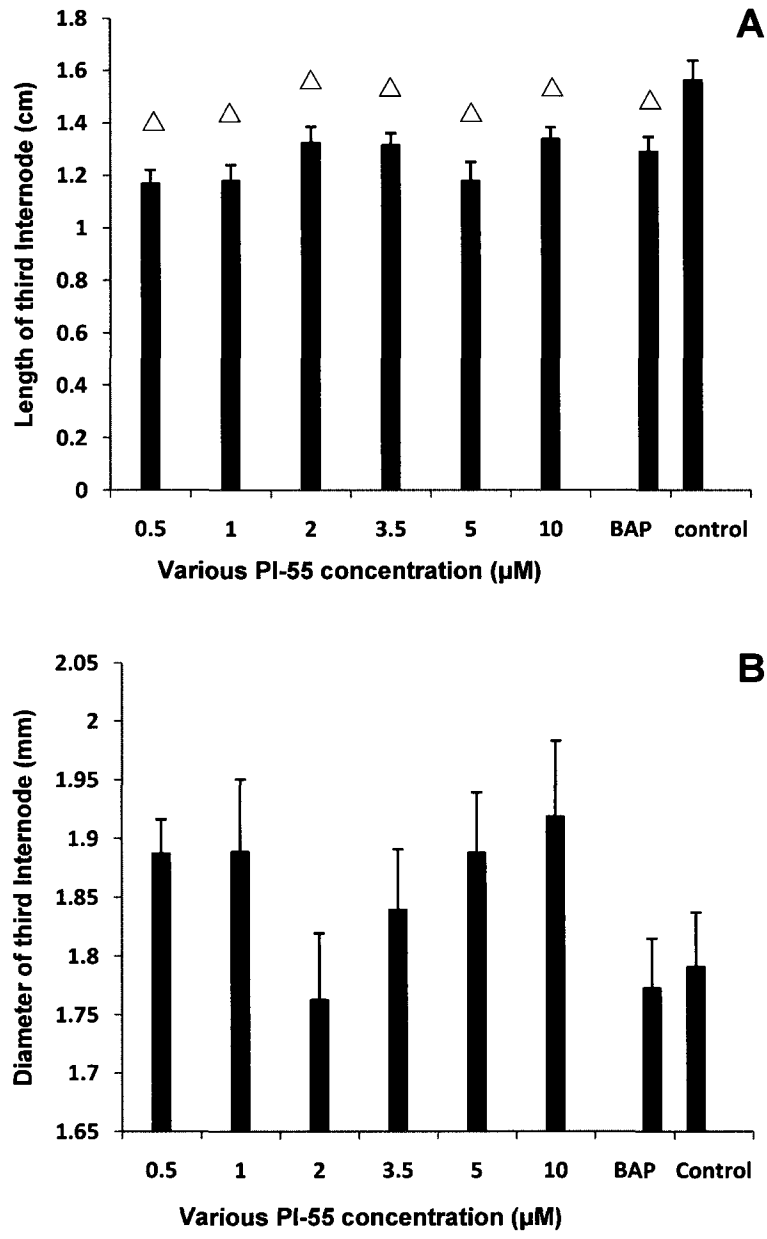

Figure 2.9 Effect of PI-55 and BAP (5µM) on (A) third internode length and (B) diameter. The PI-55 concentrations represent here the various PI-55 concentrations supplemented with 5µM BAP These data are those obtained when three trials were combined. Values are means ± SE, n=18. Triangles represent statistical significance from DMSO control at $P \leq 0.05$. Statistics were determined using Student's t-test.

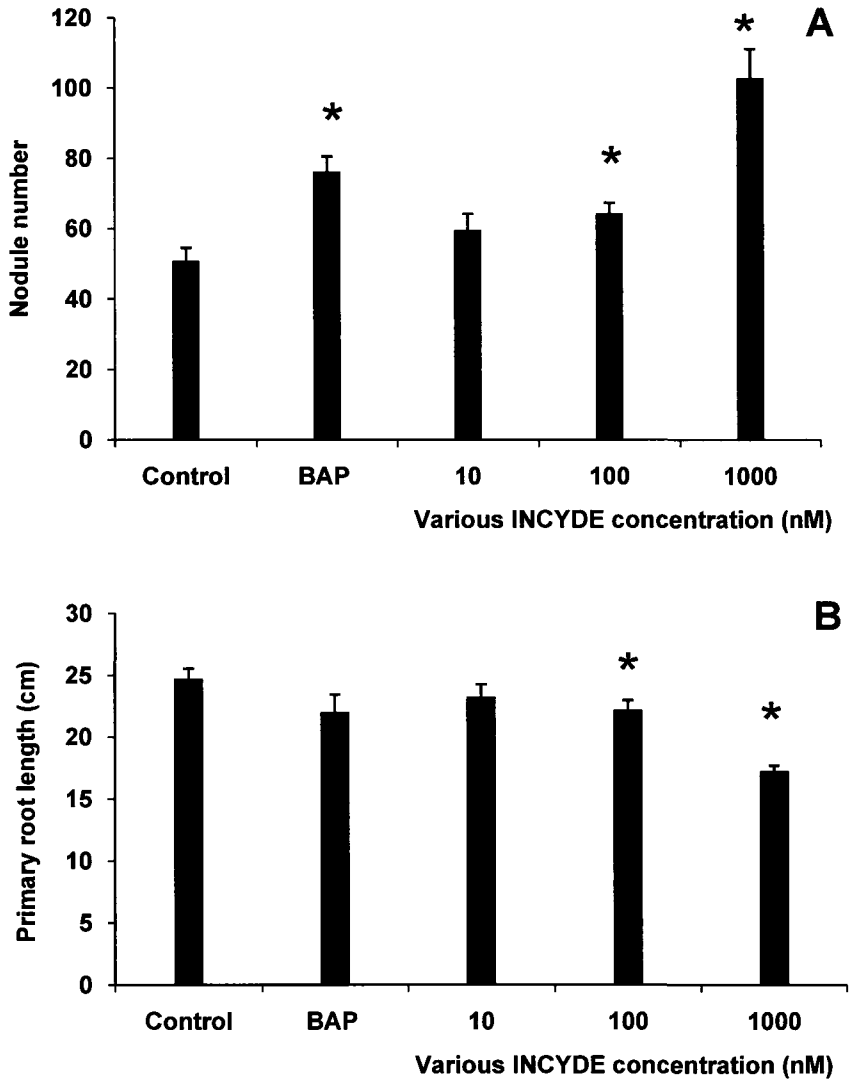

Figure 2.10 Effect of INCYDE on (A) nodule number and (B) primary root length. These data are those obtained when three trials were combined. Values are means ± SE, n=18. Asterisks represent statistical significance from the DMSO control at P≤0 05. Statistics were determined using Student's t-test The BAP concentration is 100nM.

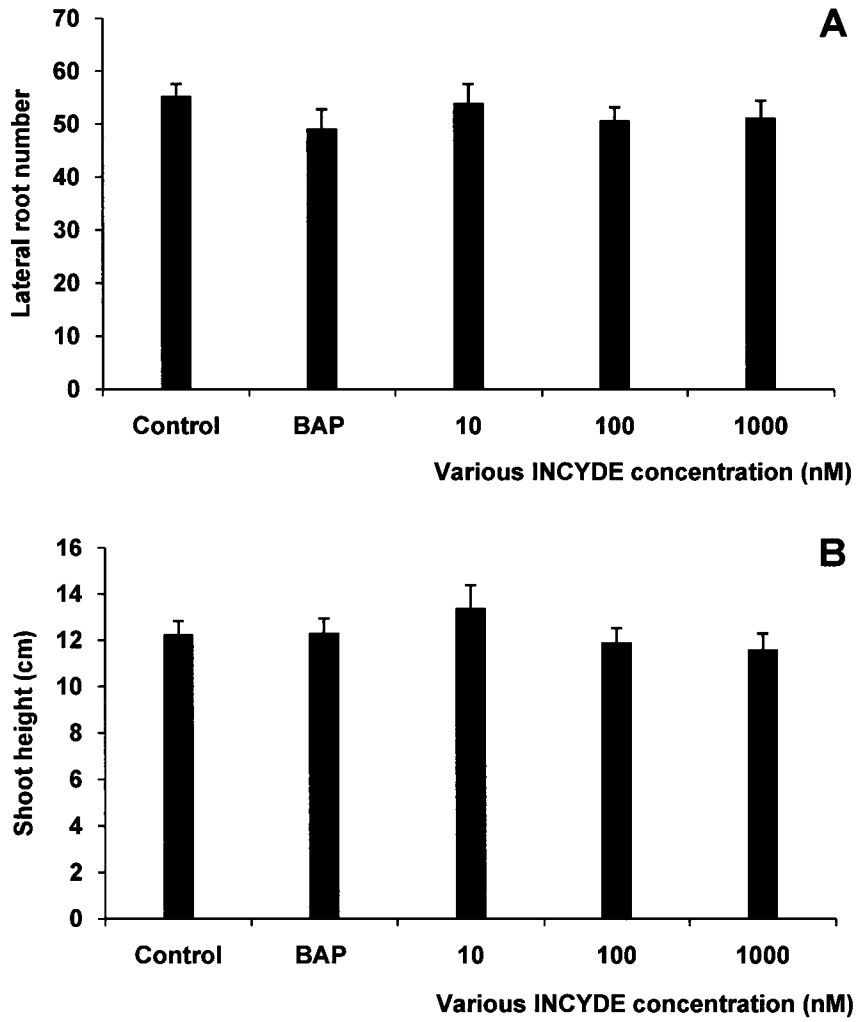

Figure 2.11 Effect of INCYDE on (A) lateral root number and (B) shoot height.
These data are those obtained when three trials were combined Values are means ± SE, n=18 Statistics were determined using Student's t-test. The BAP concentration is 100nM.

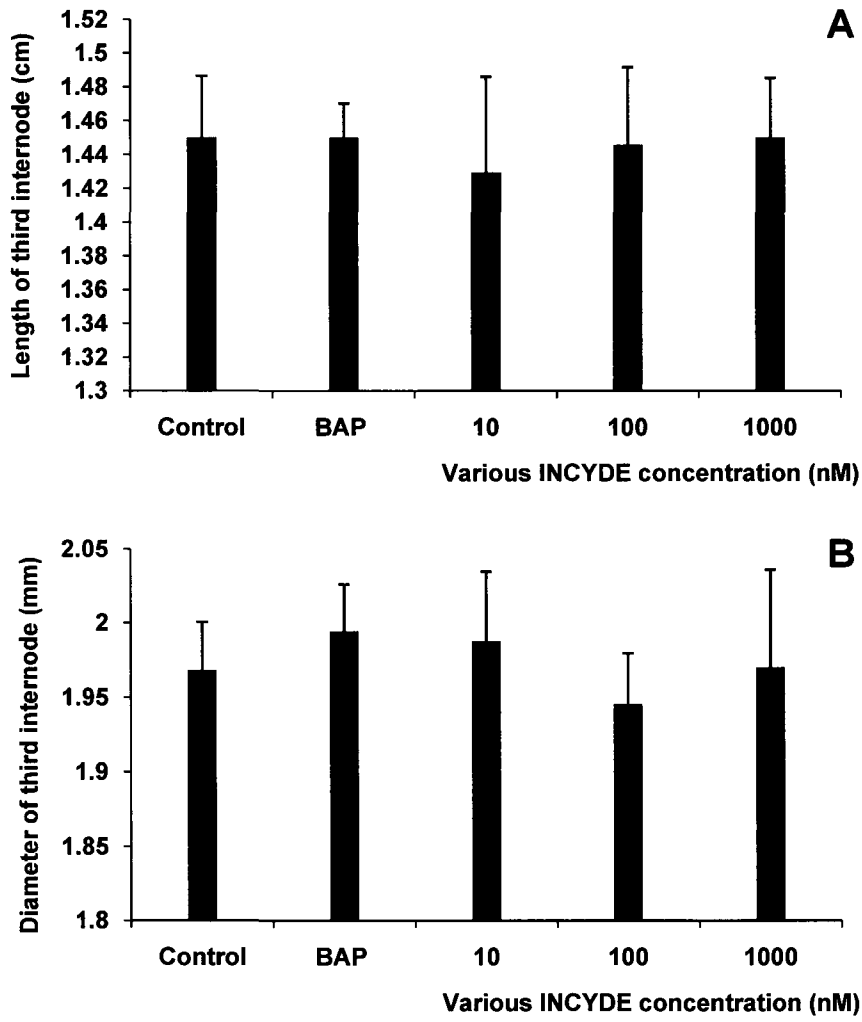

Figure 2.12 Effect of INCYDE on (A) third internode length and (B) diameter.
These data are those obtained when three trials were combined. Values are means ± SE, n=18 Statistics were determined using Student's t-test. The BAP concentration is 100nM.

2.4 Discussion

Our observation of an increase in lateral root number with the PI-55 treatment supports the finding that cytokinin is considered to be a negative regulator of the root system (Werner *et al.* 2003; Lohar *et al.* 2004; Gonzalez-Rizzo *et al* 2006, Riefler *et al.* 2006). From a cytokinin perception perspective, RNA interference of CRE1 in *Medicago truncatula* leads to an increased number of lateral roots (Gonzalez-Rizzo *et al.* 2006) Riefler *et al.* (2006) demonstrated that *ahk2ahk3* double mutant developed primary roots faster and with more lateral roots. It is assumed that full or partial disfunction of cytokinin receptor will reduce the strength of the signal transduction, thus bringing about the enhanced root system If it is the case, the explanation for cytokinin playing a negative role in the root system is reasonable. From a cytokinin degradation perspective, the CKX transgenic *Lotus japonicus* roots carrying either *AtCKX3* or *ZmCKX1* had a significant increase of lateral roots (Lohar *et al.* 2004) Overexpressing six *AtCKX*s in transgenic *Arabidopsis* induced more cytokinin breakdown, and subsequently promoted lateral root formation (Werner *et al* 2003). In both cases, overexpressing *CKX*s is thought to reduce the endogenous cytokinins, stimulating lateral root formation. Unfortunately, in either study, the authors did not determine the total CKX activity or cytokinin content of the plants

Depending on the target cells affected, the response may be different For example, I found that PI-55 at 5 μM had an inhibitory effect on nodule number but had a stimulatory effect on lateral root number at 3 5 μM (Fig 2 4A and Fig 2 4B), indicating that different tissues exhibited different sensitivity to PI-55.

The experiments described in this chapter allow me to demonstrate that pea nodulation is regulated by a cytokinin signal transduction pathway, especially that starting at the CRE1/AHK4 receptor. As found by previous researchers (e g Frugier *et al.* 2008), CRE1/AHK4 is involved in nodulation.

A reverse relationship seems to exist between nodulation and lateral root formation based on my data An interaction between nodulation and lateral root formation is also supported by physiological experiments performed bt Nutman (1984), who demonstrated that whatever the time of harvest the sum of lateral roots and nodules are approximately the same and that inoculated seedlings had fewer lateral roots than uninoculated seedlings in red clover Many mutant studies also support a relationship between nodulation and lateral root formation The *Lotus japonicus* hypernodulating mutant *har1* (hypernodulation aberrant root formation) has shorter roots (Wopereis *et al.* 2000). *Medicago truncatula* mutant *nip* (numerous infections and polyphenolics) has small nodules, short primary roots and defective lateral roots (Veereshlingam *et al.* 2004) Another *Medicago truncatula* mutant *latd* initiates nodule, primary root and lateral root formation but the development of these is not completed (Bright *et al* 2005). Lohar *et al* (2004) found a significant decrease of nodules but an increased root system by over-expressing *AtCKX3* or *ZmCKX1* in the CKX transgenic *L japonicus* root; their results indicate that a reverse relationship likely exists between nodulation and lateral root formation. In a review, Mathesius *et al* (2008) links the relationship between nodule organogenesis and lateral root formation by cytokinin; she demonstrated that cytokinin is a positive regulator for cell cycle activation in nodules, while it plays an opposite role in lateral root cell division. Gonzalez-Rizzo *et al.* (2006) proposed that reduced nodulation may correlate to a block of

cortical cell divisions, while increased lateral root formation may be caused by the activation of pericycle divisions Therefore, tissue-specific activation of the cytokinin signaling pathway may be critical for the root regulation

It is assumed that PI-55 is specific to CRE1/AHK4 (Spíchal *et al.* 2009a) Thus, apparently, CRE1/AHK4 plays a role in pea nodulation but also in its formation of lateral roots. It is aslo involved in the growth of the shoots as PI-55 promotes shoot height when in competition with BAP That cytokinin receptors are involved in multiple functions in plant growth has been shown by Riefler *et al.* (2006), who revealed that CRE1/AHK4 plays a role in many physiological events, such as germination, seed size, primary root elongation, root branching, and chlorophyll retention Riefler *et al* (2006) further demonstrated that CRE1/AHK4 exhibits redundant function in plant development. Interestingly, the redundant functions of the cytokinin receptors have been confirmed in my results Because 1) the number of nodules on plants treated with PI-55 and BAP together is never as high as that of control plants (Fig 2 7A); and 2) the highest concentration of PI-55 (10μM) does not completely inhibit nodulation, the receptors AHK2 and AHK3 may play a minor role in the physiological process (Fig 2 4A). We could use LGR-911 as a good chemical tool to test whether AHK3 is also involved in pea nodulation because LGR-911 is another cytokinin receptor antagonist which binds primarily to AHK3 (Nisler *et al.* 2010). My result of these parameter studies also show that PI-55-treated plants did not mimic all the traits of R50, such as short internode length, thick diameter and pale leaves, indicating that R50 phenotype may be only partially caused by the cytokinin signal transduction pathway.

PI-55 antagonizes endogenous cytokinins and decreases nodule number; with BAP it

enters in competition and increases the lateral root number. These results indicate that PI-55 is an antagonist of both endogenous and exogenous cytokinins The existence of such an antagonism has already been demonstrated in *Arabidopsis* (Spíchal *et al.* 2009a).

INCYDE-treated plants did not mimic R50 plants with their reduced nodule number. It is likely because even 1μM INCYDE concentration is not optimal for wild type to accumulate cytokinin, at least up to concentrations seen in R50 (between 0 and 2 in Fig 2.2 B). However, INCYDE treatment at 100nM and above promotes nodule formation (Fig 2.10A). The positive effect of INCYDE on nodulation indicates that cytokinin degradation catalyzed by CKX plays an essential role in pea nodulation

Held *et al.* (2008) found that R50, characterized by its low nodulation phenotype, has high cytokinin content. According to Lohar *et al.* (2004), over-expressed *AtCKX3* or *ZmCKX1* in the CKX transgenic *L japonicus* root led to a significant decrease of nodules. I found INCYDE at 100nM and above promoted nodule formation (Fig. 2 10A). Although my results are not similar to those of Lohar *et al* (2004) and Held *et al* (2008), it is likely that cytokinin has a dose-dependent effect on nodulation (Fig. 2 2) The cytokinin content in use in our plants (defined in the introduction in chapter 2) and their nodulation in our experiment are probably not in the same phase as theirs (Fig. 2.2) Although Lohar did not measure the cytokinin content, it is not hard to imagine that the cytokinin content after CKX over-expression is less than before. Assuming that the cytokinin content before CKX expression is 0 (Fig 2 2), it is reasonable that after CKX over-expression, it should be less than 0 (Fig 2 2) and induce fewer nodules. INCYDE-treated plants have high cytokinin content and increased nodulation (between 0 to 2 in Fig 2.2). The R50 phenotype with fewer nodules but high cytokinin content (Held *et al.* 2008)

is plausibly in the phase after 2 in Fig 2 2

Other traits of INCYDE-treated wild type did not mimic those of R50 except primary root length, indicating that the R50 phenotype is partially caused by a defect of cytokinin degradation Although INCYDE-treated plants did not show any effects on lateral root number, they display decreased primary root length. This negative effect of root caused by INCYDE is correlated well with results from other authors (Werner *et al.* 2003, Lohar *et al.* 2004; Gonzalez-Rizzo *et al.* 2006; Riefler *et al.* 2006), who demonstrated that cytokinin is considered to be a negative regulator of the root system.

Chapter 3 Cloning and characterization of *PsCKX2*

3.1 Introduction

R50 is a gamma radiation mutant of *Pisum sativum* cv Sparkle (Kneen *et al* 1994). It is a recessive mutant of the symbiosis gene 16 (*sym16*) located on linkage 5, chromosome 3 (Ellis and Poyser 2002). The mutation causes pleiotropic effects; when compared to the wild type Sparkle, R50 displays a shorter stature, a shorter primary root, fewer lateral roots, fewer and paler nodules, flattened nodule primordia, and meandering infection threads (Guinel and Sloetjes 2000). That so many morphological traits are affected by this mutation suggests the involvement of a hormone (Karlowski and Hirsch 2003) Indeed, Guinel and Sloetjes (2000) showed that ethylene is involved in the low nodulation phenotype of R50 as the phenotype can be rescued in the mutant by treating it with ethylene inhibitors Lorteau *et al* (2001) further confirmed that crosstalk occurs among ethylene, cytokinin and nodulation, they demonstrated that the synthetic cytokinin benzyladenine (BAP) stimulated ethylene production, and induced a dose-dependent effect on nodulation. The nodule number was increased at less than 1μM BAP and decreased thereafter Based on the results of Lorteau *et al.* (2001), Ferguson *et al* (2005) hypothesized that the low nodulation of R50 was caused by excessively high levels of cytokinin; they demonstrated that R50 accumulated cytokinin in its shoots and roots at 9 and 17 DAP; however, they did not determine whether these high cytokinin levels were the result of increased production or reduced degradation. This problem was tackled by Held *el at* (2008) who decided to focus on the degradation of cytokinin since this involved a single enzyme, cytokinin oxidase (*PsCKX*), whereas the biosynthesis of cytokinin requires many enzymes. They found that the elevated cytokinin content of R50 was linked to low total CKX activity However, the levels of *PsCKX* transcripts (*PsCKX1* and

PsCKX2) were higher in R50 than in wild type in young roots and shoots In this regard, it is thus possible that *sym16* corresponds to another member of the CKX family

The study of CKX is needed to better understand how cytokinin and CKX affect nodulation In higher plants, it is known that CKX is encoded by many members, usually more than five belonging to a single gene family (Schmülling *et al* 2003). The first full-length CKX gene (*ZmCKX1*) was successfully cloned in 1999 from maize (Houba-Hérin *et al.* 1999, Morris *et al.* 1999). By 2003, the full sequences of 17 putative CKX genes had been identified by BLAST searches in the NCBI database (Schmülling *et al* 2003, Fig 3 1) Seven members form the family in *Arabidopsis*, five in rice, and eight in wheat (Schmülling *et al* 2003, Galuszka *et al.* 2004) No such study has yet been done in pea It is likely that, in higher plants, the existence of multiple CKX genes is needed for the proper regulation of the many processes in which cytokinins are involved; different isoforms are expressed in different tissues and at different developmental stages (Schmülling *et al* 2003). For example, in *Arabidopsis*, *AtCKX1* is expressed in the young floral tissue and at the branching points of lateral roots, whereas *AtCKX6* is expressed in the leaf and root vasculature (Werner *et al.* 2006; Fig 3.2). Furthermore, some isoforms of CKX contain specific target sequences that are predicted to allow them to be directed to the apoplast, while others are directed to the cytoplasm (Schmülling *et al.* 2003).

In 2005, two CKX genes in pea were partially sequenced (Vaseva-Gemisheva *et al* 2005b) Based on one of these partial sequences, full-length *PsCKX1* cDNA was obtained by RACE-PCR (Held *et al* 2008). *PsCKX1* cDNA is 1560bp in length and translates into a 519-amino-acid product *PsCKX1* displays the typical FAD-binding motif shared by CKX

genes in other species, termed the GHS domain. It also contains other highly conserved sequence domains typical of CKX (Schmülling *et al* 2003) Furthermore, *PsCKX1* is predicted to encode a cytoplasmic product because the product lacks a predicted targeting sequence (Held *et al* 2008) A comparison of *PsCKX1* sequences between wild type and R50 revealed no differences (Held *et al.* 2008), suggesting that *PsCKX1* is likely not mutated in R50, however, a mutation in the 5' or 3' UTRs of the gene in R50 is still possible. Nonetheless it is interesting that the transcript levels of *PsCKX1* are abnormal in R50 as compared to those of wild type; they are increased significantly in all vegetative organs including the nodules (Held *et al.* 2008, Fig 1.10). Similarly, the transcript levels of *PsCKX2* in R50 are aberrant, their expression of is considerably lower in R50 young shoots and roots than in those of wild type (Held *et al* 2008, 10; Held) *PsCKX2* has not yet been cloned in its full length in the wild type Sparkle although another research group has obtained the full-length cDNA of *PsCKX1* and *PsCKX2* from the pea cultivar Alaska (Mori, personal communication)

In this chapter, I report on the cloning and sequencing of the full-length of *PsCKX2* cDNA from the wild type Once the full-length *PsCKX2* cDNA was cloned, further characterization was performed based on its nucleotide and amino acid sequences To test whether *sym16* is *PsCKX2*, I further cloned and sequenced the full-length of *PsCKX2* from the mutant R50, and compared it with that from wild type. The comparison shows that *PsCKX2* from R50 is not mutated

Figure 3.1. The full sequences of 17 putative CKX genes. Sequences were aligned using the CLUSTAL W program. The first two letters of the names indicate the initials of the species Zm *Zea mays*, Os *Oryza sativa*, Ds *Dendrobium* sp., Ns *Nostoc* sp., Rf *Rhodococcus fascians* Conserved amino acids are highlighted. Identical amino acids of at least 80% of the CKX proteins are indicated by white letters on a black background (figure from Schmülling *et al* 2003).

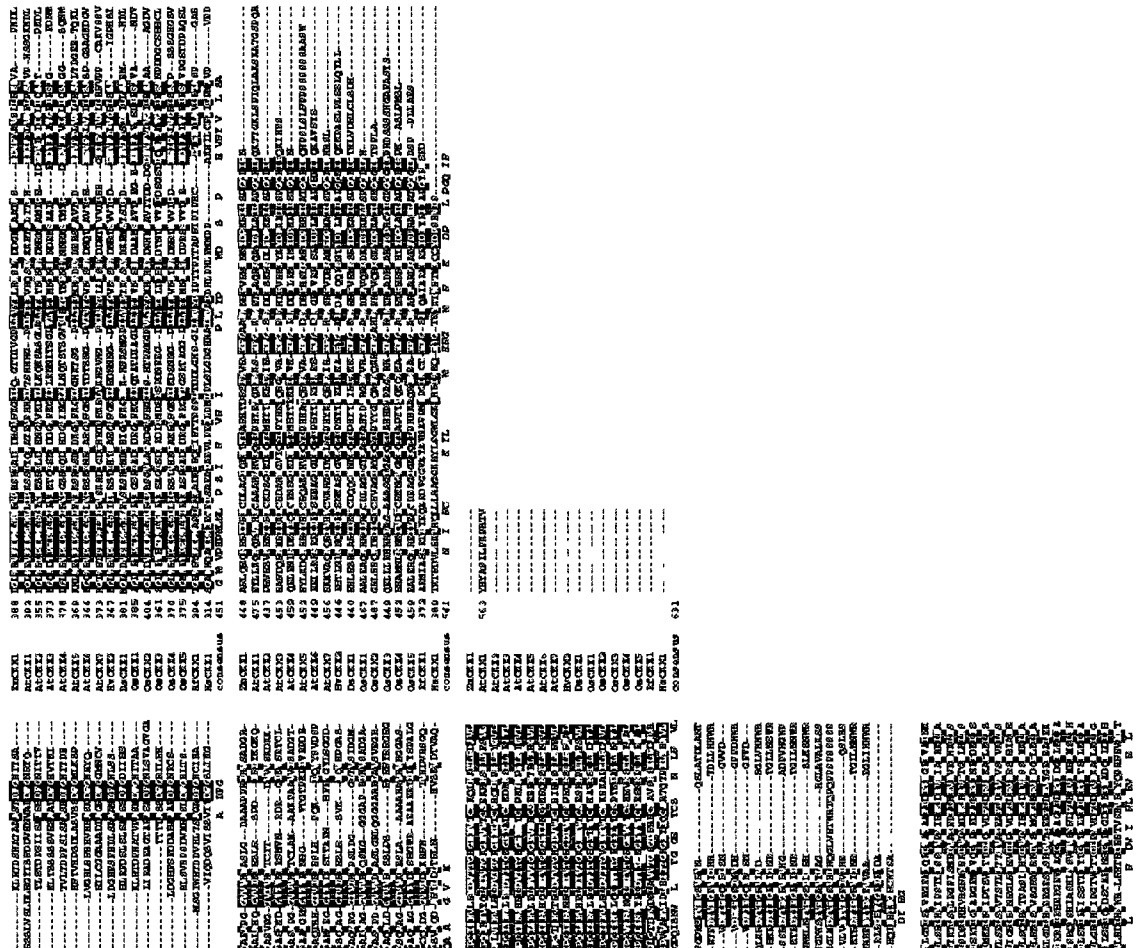

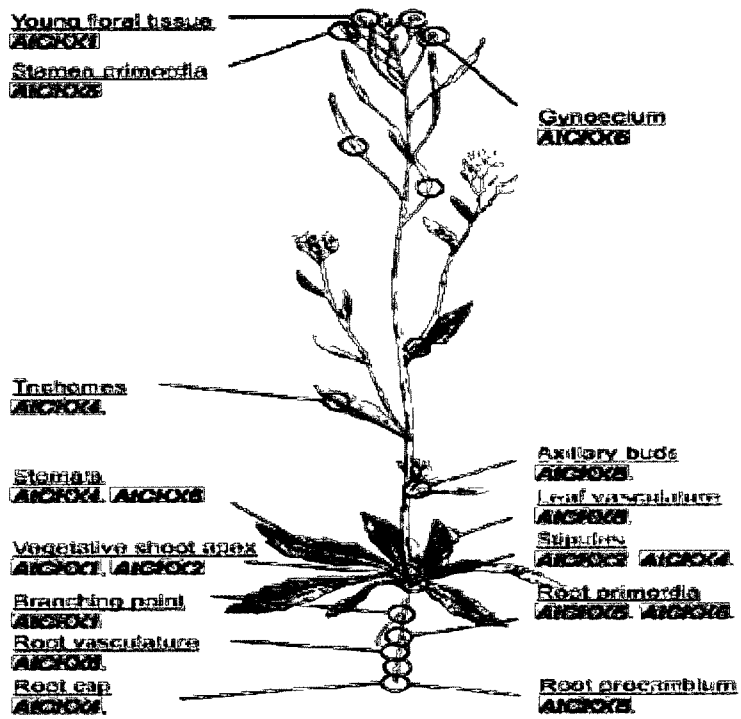

Figure 3.2. *Arabidopsis* CKX gene expression profile in tissues. Six CKX genes (*AtCKX1*, *AtCKX2*, *AtCKX3*, *AtCKX4*, *AtCKX5*, and *AtCKX6* in grey) are expressed in different tissues in *Arabidopsis*. Tissues are underlined *AtCKX7* is not shown here (figure modified from Werner *et al.* 2006)

3.2 Materials and methods

For ease of understanding, all the subsections of the procedures of materials and methods have been ordered in a flow chart (Appendix 2.1). The capital letters on the right of the flow chart refer to the subsections listed below

3.2.1 RNA preparation (A)

RNA samples (extracted by Held *et al.* 2008) from roots and shoots harvested 9 days after planting (DAP) were used to clone *PsCKX2* from wild type and R50, respectively To confirm that the RNA was not degraded, its quality was assessed by gel electrophoresis. RNA samples were mixed with 0 5X formaldehyde loading dye and ethidium bromide The mixture was then incubated on a heat block at 70°C for 15 minutes and loaded into a 1 2% agarose gel buffered with 1X MOPS. Electrophereis was performed at 110 volts for roughly 40 minutes, and the gel was then visualized on a UV transilluminator

RNA concentration was determined using a NanoDrop spectrophotometer (Thermo Scientific) using sterile deionized water (PCR H_2O) as the blank. The absorbance of the sample at 260 nm was measured and its concentration was calculated using the following formula: A260 × 40 × dilution factor = [RNA]µg/ml (Roche Applied Science, Laval, QC).

To remove genomic DNA within the RNA samples, all RNA samples were treated with DNase using the Turbo DNA-free kit (Ambion, 2130 Woodward St., Austin, USA, 2009) All the reagents are listed in Table 3 1 The mixture was incubated at 37°C for 1 hour. To inactivate the DNAse, an inactivating reagent was added and the mixture was incubated at room temperature for 2 min. After centrifuging at 16,000 rpm for 1 min, the supernatant was removed

and placed into a sterile 0.5 ml centrifuge tube.

3.2.2 First-strand cDNA synthesis (B)

The first-strand cDNA template was synthesized using the Superscript II reverse transcriptase kit (Invitrogen, Carlsbad, CA, USA, 2009). To a 12µl solution of reverse transcription reaction, RNA (<5µg), 100µM anchor-T-primer (T20G, T20C, T20A) and 10mM deoxynucleotide triphosphate (dNTP) were added and incubated at 65°C for 5 minutes. After a quick chill on ice, 5X first-strand buffer, 0.1 M dithiothreitol (DTT) and RNaseOUT TM (40 units/µl) were added according to instructions and incubated at 42°C for 2 minutes SuperScript® II Reverse Transcriptase (200 units) was added before incubation at 42°C for 50 minutes The reaction was heat inactivated at 70°C for 15 minutes

To assess whether DNase treatment and the reverse transcription reaction is working, PCR was performed using *PsActin* as primer, and the original RNA, DNase-treated RNA, and first-strand cDNA as the templates (shown in Table 3.2), and followed by gel electrophoresis. All the reagents are listed in Table 3.2.

3.2.3 Gel electrophoresis (C)

Gel electrophoresis was performed using a TAE (40 mM Tris, 20mM acetic acid, 1mM EDTA) 1% (w/v) agarose gel. TAE was also used as the running buffer Ethidium bromide was added directly to the gel to a final concentration of 0 5µg/ml To prepare each sample, 2µl loading dye was added to 8µl PCR product. Gel electrophoresis was performed at 100 volt for about 40 minutes and the gel was visualized using a UV transilluminator.

Table 3.1 Reagents used for DNase treatment

Reagents	volume
Wild type 9-DAP shoot RNA	<10µg
10X TURBO DNase Buffer	1.0µl
DNase	1.0µl
RNase-free water	-
Total	10 0µl

Table 3.2 PCR reaction component to assess DNase treatment

Reagents	Sample 1	Sample 2	Sample 3
PCR Buffer	2.5µl	2.5µl	2.5µl
dNTP (10 mM)	0.5µl	0.5µl	0.5µl
PsActin Forward Primer (10 µM)	0.5µl	0 5µl	0.5µl
PsActin Reverse Primer (10 µM)	0 5µl	0 5µl	0.5µl
Advantage 2 Polymerase	0.5µl	0.5µl	0.5µl
Template	0.5µl (Original RNA)	0.5µl (DNase-treated RNA)	0.5µl (First-strand cDNA)
PCR H_2O*	20 0µl	20 0µl	20.0µl
Total	25 0µl	25.0µl	25 0µl

*PCR H_20 is Milli Q H_2O which has been autoclaved and exposed to UV light.

3.2.4 Polymerase Chain Reaction (D)

3.2.4.1 Gene specific primer design (D.1)

According to Mori's sequence of *PsCKX2* cDNA from the pea cultivar Alaska (personal information), gene-specific primers (Forward: 5'-CCT TCT TCA CCC TTT AAC TAC CAA CCT-3'; Reverse 5'-CTC AGT TGA CTT GAC TCT CCT GCC-3') were designed to amplify *PsCKX2* cDNA from total wild type and R50 cDNA. The fomer primer will bind to the cDNA located before the starting codon, and the latter to that located after the stop codon. Based on Mori's sequence, the expected PCR product was 1700bp.

3.2.4.2 PCR parameters (D.2)

The PCR reaction was performed using the Advantage 2 Polymerase Mix kit (Clontech, 1290 Terra Bella Avenue, Mountain View, CA 94043, USA, 2009), which uses a hot start and proof-reading polymerase Hot Start PCR significantly reduces nonspecific priming, the formation of primer dimers, and often increases product yields All the reagents used in the PCR reaction are listed in Table 3.3, and the reaction conditions are listed in Table 3.4. Positive controls (*PsActin*) and negative controls (without template) were included each time a reaction was run The optimal PCR annealing temperature was determined to be 60.5°C using gradient PCR. PCR was performed using a Mastercycler Gradient Thermocycler Gel electropheresis was performed using 8µl of each PCR product (with 2µl of loading dye). All PCR products were stored at -20°C for future use.

3.2.5 Gel extraction and purification (E)

To purify the PCR product, gel electrophoresis was performed using a 1% TAE agarose gel in TAE buffer run at 80V for approximately 50 min. The expected 1700bp band was excised

and placed in a 1.5 ml sterile centrifuge tube The gel from which the band was excised was visualized again with the transilluminator to confirm that the entire product was removed The PCR products were then purified using illustra™ GFX PCR DNA and a gel band purification kit (GE Healthcare, 500 Morgan Boulevard, Baie d'Urfe Quebec H9X-3V1, Canada, 2009).

3.2.6 Cloning reaction (F)

The concentration of purified PCR products was determined based on absorbance at 260nm using a NanoDrop spectrophotometer (Thermo Scientific) To ligate the PCR product into the pBS/KS vector (Appendix 2.2), a ligation reaction was performed pBS/KS vector confers ampicillin resistance and contains a multiple cloning site within a region encoding β-galactosidase. All the reagents used for the ligation reaction are listed in Table 3.5. The BS/KS vector concentration was 56 ng/μl The ratio between PCR products insert and T-vector ranged from 3:1 to 1·3 and the following PCR product volume was calculated based on the ratios by ligation calculator (http·//www insilico.uni-duesseldorf.de/Lig_Input.html). The ligation reaction was performed in a 1 5 ml sterile centrifuge tube at 4°C overnight

To purify the ligation product, the ligation solution was added to PCR H_2O to a volume of 50μl. After adding 1-butanol (500μl), the mixture was vortexed thoroughly and centrifuged at 13,200 rmp for 15 minutes at room temperature. The supernatant was carefully discarded as to not disturb the pellet Once the pellet was completely air dried, another 8μl PCR H_20 was added to resuspend the pellet. Half of the resuspension was used to do transformation and another half was stored at -20°C for future use.

Table 3.3 PCR reaction component to amplify *PsCKX2* from cDNA

Component	Volume/Reaction	Final concentration
10X PCR Buffer	2.5µl	1X
dNTP (10mM)	0.5µl	200 µM of each dNTP
Specific Forward Primer (10 µM)	0.5µl	0.2µM
Specific Reverse Primer (10 µM)	0 5µl	0 2µM
Advantage 2 Polymerase	0 5µl	1 0 unit/reaction
Template (first-strand cDNA)	0 5µl	Variable
PCR H_20	20.0µl	-
Total	25.0µl	-

These components are from Advantage 2 Polymerase Mix kit from Clontech.

Table 3.4 PCR program used to amplify *PsCKX2* from cDNA

Temperature	Time	Cycle No.
94°C	4 min	1
94°C	30 sec	35
60.5°C	30 sec	35
72 °C	1min	35
72 °C	10 min	1
10 °C	Hold	-

3.2.7 Transformation (G)

Forty µl *E coli* electrocompetent cells and 4µl of the ligation product were mixed together in an ice-chilled electroporation cuvette. The mixture was then quickly electroporated using a BioRad electroporato, 500µl of liquid Luria-Bertani medium (LB 10g bacto-tryptone, 5g yeast extract, 5g NaCl, 15g agar) was added to the cuvette and the mixture was then transferred to a sterile glass tube The bacteria recovered on an orbital shaker at 37°C, 120rpm, for 1 hour

The bacteria were then plated on solid LB medium supplemented with 100 µg/ml ampicillin, 5% X-gal (5-bromo-4-chloro-3-indolyl-beta-D-galactopyranoside), and IPTG (isopropyl-β-D-thiogalactoside) The plates were incubated at 37°C for 18 hours. Selection for transformed bacteria was conferred by ampicilin resistance Selection for transformed bacteria containing the cloned product was conferred by the absence of blue colour, because cloning of the insert into the multiple cloning sites prevents the expression of β-galactosidase, which metabolizes X-gal in the presence of IPTG.

3.2.7.1 Screening (H)

To confirm that white colonies contained the cloned *PsCKX2* cDNA, a PCR screen was performed. Using a T7 vector specific reverse primer sequence and a *PsCKX2* specific forward primer, PCR amplification was performed using extracted plasmid DNA. The reagents required for the reaction are listed in Table 3.6 and the PCR parameters in Table 3.7. The PCR products were visualized on a 1.0% (w/v) agarose gel by gel electrophoresis. The presence of a PCR product of the predicted size indicated successful transformation with the cloned product in the bacterial a colony. The selected colonies were then cultured overnight

with 5 ml LB with 100 μg/ml ampicillin, at 37°C, 120 rmp, for 18 hours

3.2.8 Plasmid extraction (I)

The plasmids containing *PsCKX2* cDNA were extracted using an EZ-10 Spin column plasmid DNA miniprep kit (BIO BASIC INC, 2360 Argentia Road Mississauga, Ontario, 2009). The concentration of plasmids was determined using the NanoDrop spectrophotometer (Thermo Scientific)

3.2.9 Sequence analysis (J)

The final plasmid products were prepared and sent to The Hospital for Sick Children for sequencing (DNA Sequence Facility, Toronto, 2009) Wild type and R50 sequence results were analyzed using the Sequence Alignment Editor software Bioedit 7 0 (http //www mbio ncsu edu/BioEdit/bioedit html) and the DNA Sequencer Chromatogram data software FinchTV 1 4 (http //www.geospiza.com/Products/finchtv.shtml) Nucleotide and deduced amino acid sequences were aligned so that comparison could be made between the wild type and the mutant Alignment with other published CKXs was performed by ClustalW (http://clustalw.genome.jp/). The molecular mass of *PsCKX2* from the wild type was calculated with peptide-mass tool (Wilkins et al 1997); its subcellular localization was estimated with iPSORT (Nakai and Horton 1999), MitProt II program (http //ihg.gsf de/ihg/mitoprot.html), and Predotar program (http //urgi.versailles inra.fr/predotar/predotar.html). Its N-glycosylation sites were predicted with NetNGly (http://www.cbs.dtu.dk/services/NetNGlyc/).

Table 3.5 Ligation reaction of *PsCKX2*

Reagents	Sample
BS/KS vector	1.0μl
10 X T4 ligase Buffer	1.0μl
T4 ligase	1.0μl
PCR products	Variable
PCR H_20	-
Total	10 0μl

Table 3.6 Colony PCR reaction for screening

Reagents	Sample 1
PCR Buffer	2.5μl
dNTP	0.5μl
Specific Forward Primer (10 μM)	0 5μl
T7 Primer (10 μM)	0.5μl
Home-made taq	1.0μl
Cloned template with PCR H_20	5 0μl
PCR H_20	15.0μl
Total	25 0μl

Table 3.7 Colony PCR parameters

Temperature	Time	Cycle No.
94°C	4 min	1
94°C	30 sec	35
55 °C	30 sec	35
72 °C	1min	35
72 °C	10 min	1
10 °C	Hold	-

3.3 Results

All the subsections of the procedures of results have been ordered in a flow chart (Appendix 2.1). The lower-case characters on the left of the flow chart refer to the subsections listed below

3.3.1 RNA quality analysis (a)

RNA was isolated from root (R), shoot (S), nodule (N), flower (FL) of both wild type (wild type) and R50 (R50) at two ages (9 and 17 DAP) by a former student, Mark Held I chose to work with the RNA from wild type root (wild type9R) and from R50 shoot (R509S) obtained from 9 day-old plants. RNA concentrations were measured using the NanoDrop spectrophotometer (Thermo Scientific) Total RNA from those two samples run on a denaturing gel had bands corresponding to those of 28S and 18S rRNA. The 28S rRNA band was approximately twice as intense as that of the 18S rRNA (Fig 3.3) This established that none of the RNA samples were degraded.

3.3.2 Wild type9R PCR reaction (b)

Wild type and R50 were submitted to the same procedures; because their results were similar, I chose to present here only the results for the wild-type to illustrate the procedures

The PCR product amplified using the *PsActin* primer was approximately 560bp (Fig. 3.4 lane 2), which was slightly larger than the product amplified using the cDNA template (Fig. 3 4, lane 4); this indicated that WT9R RNA contained minute amounts of genomic DNA As seen in lane 3 of Fig. 3.4, the DNase treatment of total wild type9R RNA was

successful because no band was obtained. It was determined by gradient PCR (in lanes 6, 7 and 8) that the optimal annealing temperature for the *PsCKX2* primers was between 60.5°C and 63.1°C. The *PsCKX2* fragment was successfully amplified (Fig. 3 4, lanes 7 and 8, top bands), and its size approximated 1700bp, as was expected from Mori's sequence (Personal communication) The lower band (Fig. 3 4, lane 7 and 8) was not taken into account in the following steps because its size did not correspond to the size of Mori's product.

3.3.3 Wild type 9R colony PCR (c)

Eleven colonies potentially containing the *PsCKX2* cDNA clone were screened by colony PCR using a T7 vector specific reverse primer and a gene-specific forward primer. Amplification of a PCR product of the desired size (1700bp) was performed using the DNA template from only one of the 11 colonies (Fig 3.5, lane 7).

3.3.4 Sequencing (d)

3.3.4.1 Sequencing of nucleotides (d.1)

Plasmid DNA of 4 clones from wild type and 3 clones from R50 was sequenced in the forward and reverse directions. BioEdit, FinchTV, and ClustalW (softwares) were used to analyze the original data The full nucleotide sequence and part of the 5' and the 3' UTRs of *PsCKX2* coding region were obtained from the pea cultivar Sparkle. The entire sequence was 1735bp in total length (Fig 3.6) The mutant R50 had a nucleotide sequence identical to that of Sparkle.

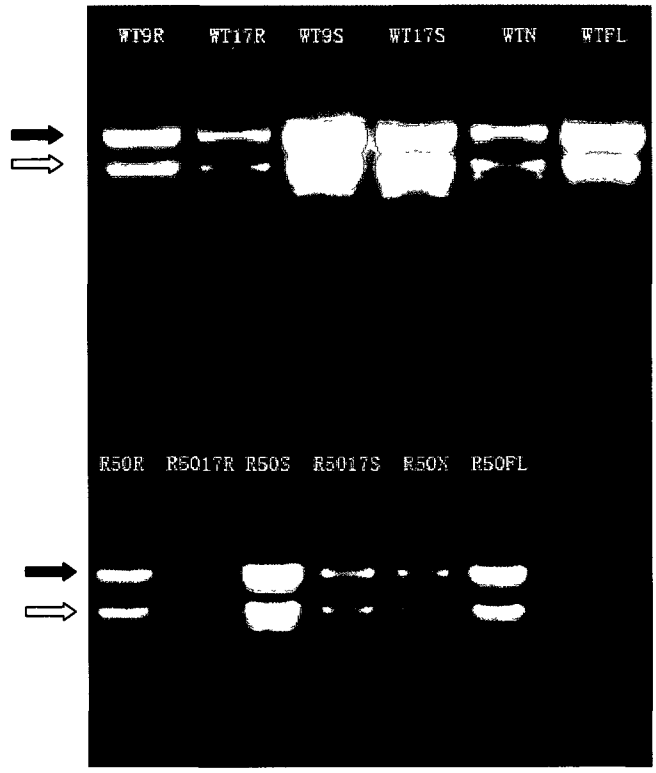

Figure 3.3 Gel electrophoresis of RNA extracts. Samples in the top panel were the RNA from different tissues (R: root; S shoot; N: nodule; FL: flower) and two developmental stages (9, 17 DAP) of wild type (wild type). The lower panel contains RNA samples from different tissues and two developmental (9, 17 DAP) stages of R50 The first top band is 28S (solid arrow), while the bottom band is 18S rRNA (hollow arrow).

Figure 3.4 Gel electrophoresis of wild type 9R RT-PCR reaction. The positive controls using *PsActin* primers are shown in lane 2 (the PCR product was amplified using the wild type 9S RNA as template before DNase treatment), lane 3 (the PCR product was amplified using the wild type 9R RNA as template after DNase treatment) and lane 4 (the PCR product was amplified using the wild type 9R cDNA as template which was synthesized from DNase treated RNA) A gradient PCR was also performed to determine the optimal annealing temperature using the wild type 9R cDNA as templates and *PsCKX2* primers (Lane 6 T=56.6°C, Lane 7 T=60.5°C; Lane 8 T=63 1°C). Negative controls are exhibited in lane 1 (no template with *PsActin* primers) and lane 9 (no template with *PsCKX2* primers). Ladder is GeneRuler 1 kb gene ladder The top arrow indicates the position of the 1500bp band of the gene marker, the middle one indicates the position of the 1000bp band, and the bottom one indicates the position of the 500bp band. Lane 5 was a PCR product amplified by another set of *PsCKX2* primers and it will not be discussed here

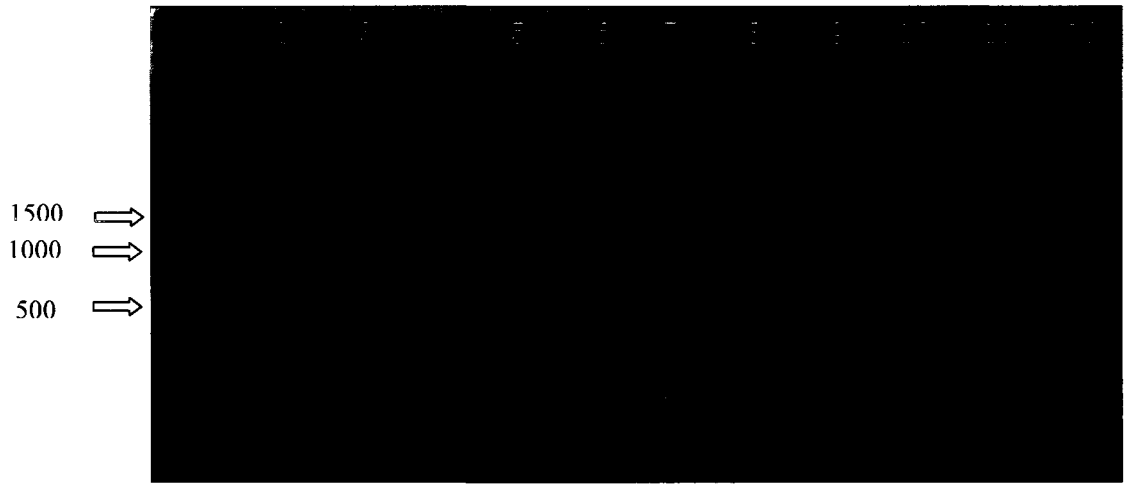

Figure 3.5 Gel electrophoresis of colony PCR reaction of wild type 9R. Lane 1 was the GeneRuler 1 kb DNA ladder The top arrow indicates the size of the 1000bp band, and the bottom one indicates the 500bp band. Lane 2-12 represents 11 selected clones. The band in Lane 7 was 1700bp, as expected.

3.3.4.2 Amino acid sequence and analysis (d.2)

For both wild type and R50, the consensus coding region (1611bp) translated into a 548 amino acid sequence (Fig 3 7). PsCKX2 was predicted to have a mass of 56 71KDa, and to possess 4 N-glycosylation sites These characteristics were consistent with those of known CKXs sequences: CKX sequences vary from 501 to 575 amino acids with a mass from 56.0 to 69 5 KDa, with 1 to 8 N-glycosylation sites. According to iPSORT predictions, PsCKX2 exhibits a mitochondrial targeting sequence. The FAD-binding domain, a GHS motif, is conserved in the N-terminal halves of all CKXs (shown in Fig 3.7), including that of PsCKX2 (amino acid 111-113). All these characteristics support the evidence that the sequence cloned here is one of the CKX genes in pea

3.3.4.3 Alignment (d.3)

PsCKX2 amino acid sequence was compared to that of other CKX proteins using ClustalW The alignment is shown in Fig 3.7. PsCKX2 shares 35-78% homology with other CKX proteins (Table 3 8)

3.3.4.4 Phylogenetic tree (d.4)

A phylogenetic tree (Fig 3.8) was established based on a comparison of all CKX proteins from *Arabidopsis* and pea, homologous proteins from soybean and *Medicago*, yet to be characterized, were also added. AtCKX2 and AtCKX4 are closely related, this relationship is most likely the result of a recent duplication event (Schmülling *et al* 2003) We also see that AtCKX7 shows least homology with the other AtCKXs but that is it highly orthologous to PsCKX1. Neither AtCKX7 nor PsCKX1 have a signal peptide; therefore they are predicted to be cytoplasmic proteins. What is also interesting is that the three proteins (in frame, Fig. 3 8), most closely-related to PsCKX2, share a predicted N-glycosylation site.

```
   1 CCTTCTTCAC CCTTTAACTA CCAACCTATC ATCCATGAAA AAATTGAGAT
  51 ATCCATGTTT CAACCTTGTT AGAGAATACA ACATTTTGTT CATAAAATGC
 101 TTCATGATTT TACTCATAAG CTGTATTACT ATAAGACTTA ATTTCTCTCT
 151 TTCAAGTATC CATTTTTCTT TAAAATCACT TCCTATAGAA GGAAACTTTA
 201 GCTTTGATGA ACTTGACCTT AAAAATGCAG CTAGAGATTT CGGTAACCGG
 251 TACCGATCTC ATCCTATGAC AGTGCTTCAT CCAAAATCAG TTTCTGATAT
 301 TGCAGTTACT GTAAAGCATG TATGGAGTTT AGGTCCTAGC TCGGAGTTAA
 351 CGGTTGCGGC TAGAGGACAT GGTCATTCGC TTCAAGGTCA AGCTCAAGCT
 401 CATGGAGGAA TTGTGATTAA TATGGAATCG CTTAAAGTTG AAGAGATTAA
 451 GGTGTATGGT GGAGAGTTTC CTTATGTGGA TGTTTCAGGA GGTGATTTGT
 501 GGATAAATGT TTTGAATGAG ACATTGAAGT ATGGTTTGGC ACCAAGATCT
 551 TGGACAGATT ATTTGCATTT GACAGTTGGT GGTACTTTGT CGAATGCTGG
 601 TGTTAGTGGT CAGGCTTTTA GACATGGTCC ACAGATCAGT AATGTTCTGA
 651 AAATGGAGAT TGTCACAGGA ACTGGAGAGG TAGTAAACTG TTCTGAAAAG
 701 CAAAATAATG AACTCTTTTA CAGTGTACTT GGAGGCTTAG GACAGTTTGG
 751 CATTATAACA AAAGCAAGAA TCAAGCTAGA GCCAGCACCT GTCATGGTTA
 801 AGTGGATTAG AGTGCTGTAT TCAGATTTCA CAGCATTCAC AAGAGACCAA
 851 GAGCAATTAA TCTTTGCTGA AAAAGCTTTT GATTATATTG AAGGGTTTGT
 901 GATTAAAAAC AGAACTGGTT TGGTAAATAA CTGGAGATTA TCTTTCAATC
 951 CTCAAGATCC AGTTCAAGCT AGCAAGTTCA AATCAGATGG AAGAACTCTT
1001 TTCTGCCTTG AATTGGCCAA ATACTTCAAT TTGGAAGAAT CTTCGGAAGT
1051 AAATCAGGAA GTTGAGAAAC ACTTGTCCCA CTTGAACTAT ATTCAATCAA
1101 CAATTTTTCA AACAGAAGTC ACATATATTG ACTTTTTAGA CAGAGTACAT
1151 ATCTCAGAAG TTAAATTGCG TTCAAAAGGC TTATGGGATG TTCCTCATCC
1201 ATGGCTCAAT CTTTTCATAC CCAAATCCAA AATCCATAAT TTTGCAGATA
1251 CAGTCTTTGG CAATATTGTC AAAGAAACAA GCAATGGTCC TATCCTTATC
1301 TACCCGGTCA ATAAATCAAA GTGGGACGAG AGAACATCGG TTGTTATTCC
1351 GGATGAAGAT ATTTTCTATT TAGTGGCATT TTTAGCATCT GCAATTCCTT
1401 CATCAAATGG AGGAGAAGGG CTTGAACACA TTCTAAGTCA GAACAAAAGA
1451 ATTTTGGAAT ATTGTGAAAG GGAAGATCTT GGAGTAAAGC AATATTTGGC
1501 CCACTATAGT ACACAAGAAG AATGGCAGAC ACATTATGGT CCAAAATGGG
1551 AGATTTTCAA GCAAAGAAAA TCTATTTATG ATCCATTGGC AATACTTGCT
1601 CCTGGCCAAG GAATATTTCA AAAATCAATA GCTTTTTCAT CATGATAATC
1651 AAATTTTATA TTATTTTATT TATATGGAAA AGAATAGGCC TCACAGTATG
1701 TGTGGCACTA AGGCAGGAGA GTCAAGTCAA CTGAG
```

Figure 3.6 The consensus nucleotide sequence of *PsCKX2* cDNA. The start codon (ATG) and stop codon (TGA) are highlighted in red. The designed gene-specific forward and reverse primers are underlined.

Figure 3.7 Amino acid alignment of PsCKX2 with other CKXs. Most homologous CKXs are from *Arabidopsis thaliana* (AtCKX1), *Zea mays* (ZmCKX2), *Oryza sativa* (OsCKX4), *Hordeum vulgare* (HvCKX2), and *Pisum sativum* (PsCKX1). The capital letters in the consensus lane correspond to 100% identity, whereas the small case letters correspond to more than 60% identity Amino acids highlighted in black are more than 80% conserved, those in grey are more than 60% conserved. Single asterisk represents the aspartic acid and the glutamic acid conserved in all isoform found in plants Double asterisks represent the conserved motifs VPHPWLNL and PGQXIF Triple asterisks represent the 4 predicted N-glycosylation sites The FAD-binding motif (GHS) is underlined The predicted mitochondrial targeting sequence is framed.

PsCKX2/1-536 1
ACU22904.1/1-490 1
AtCKX1/1-575 1
ZmCKX2/1-519 1
OsCKX4/1-529 1
HvCKX2/1-526 1
PsCKX1/1-519 1
consensus 1
PsCKX2/1-536 100
ACU22904.1/1-490 116
AtCKX1/1-575 111
ZmCKX2/1-519 86
OsCKX4/1-529 90
HvCKX2/1-526 86
PsCKX1/1-519 69
consensus 131
PsCKX2/1-536 225
ACU22904.1/1-490 242
AtCKX1/1-575 236
ZmCKX2/1-519 208
OsCKX4/1-529 218
HvCKX2/1-526 211
PsCKX1/1-519 196
consensus 261
PsCKX2/1-536 348
ACU22904.1/1-490 365
AtCKX1/1-575 359
ZmCKX2/1-519 331
OsCKX4/1-529 341
HvCKX2/1-526 334
PsCKX1/1-519 324
consensus 391
PsCKX2/1-536 478
ACU22904.1/1-490 491
AtCKX1/1-575 489
ZmCKX2/1-519 460
OsCKX4/1-529 470
HvCKX2/1-526 460
PsCKX1/1-519 453
consensus 521

Table 3.8 Percent mino acid identity of PsCKX1 with other CKX proteins

CKX homolog	Accession No.	Percent identity with *PsCKX2*
PsCKX1	EF030477	40%
ZmCKX1	AF044603	36%
ZmCKX2	NM_001112056	61%
ZmCKX3	AJ606943	59%
AtCKX1	At2g41510	63%
AtCKX2	At2g19500	37%
AtCKX3	At5g56970	42%
AtCKX4	At4g29740	36%
AtCKX5	At1g75450	46%
AtCKX6	At3g63440	61%
AtCKX7	AF303981	41%
HvCKX2	AF540382	60%
HvCKX3	AY209184	59%
OsCKX1	Q0JQ12	36%
OsCKX2	Q4ADV8	35%
OsCKX3	Q8LNV6	40%
OsCKX4	Q5JLP4	60%
OsCKX5	Q5ZAY9	41%
OsCKX6	Q6YW51	37%
OsCKX7	Q6YW50	38%
OsCKX8	A2XVN3	35%
OsCKX9	Q75K78	60%
OsCKX10	Q5Z620	37%
OsCKX11	Q6Z955	37%
Soybean unknown mRNA	BT097654	78%

The first two letters of the names indicate the initials of the species: *Ps-Pisum sativum*; *Zm-Zea mays*, *At-Arabidopsis thaliana*, *Hv-Hordeum vulgare*, *Os-Oryza sativa*.

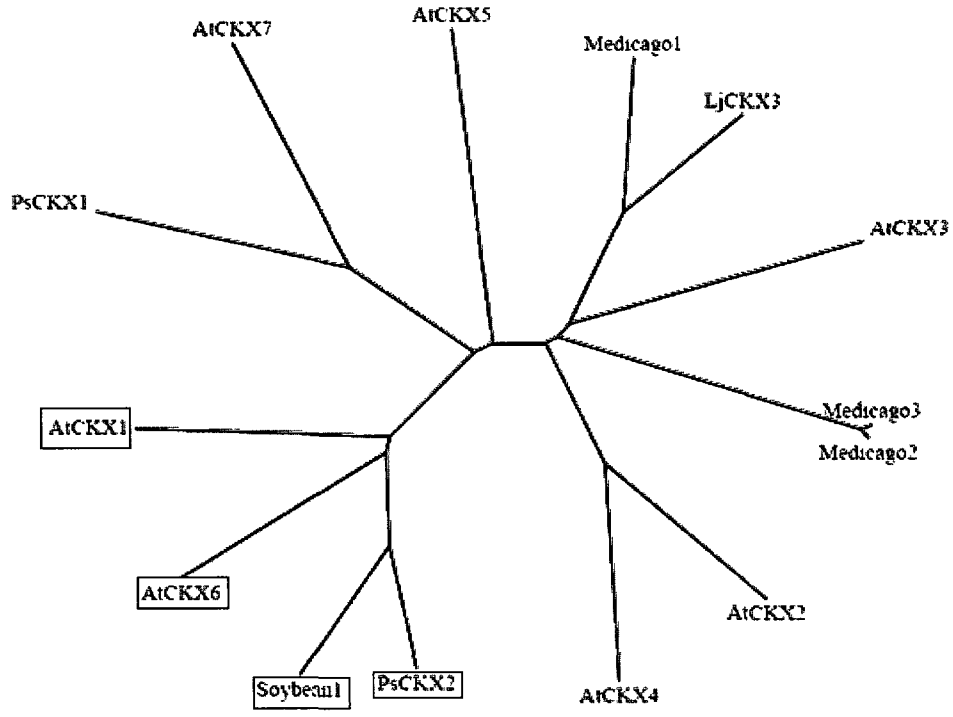

Figure 3.8 Phylogenetic analyses of CKX proteins. Most homologous proteins used to build the tree are listed in Table 3.8 The phylogenetic tree was built based on the full sequence of CKX proteins using the MUSCLE program (http.//www.ebi ac uk/Tools/muscle/index.html). The first two letters of the names indicate the initials of the binomial: Ps-*Pisum sativum*; Lj-*Lotus japonicus*, At-*Arabidopsis thaliana*. The protein named Soybean 1 is an uncharacterized protein from soybean (NCBI database, accession number gil2556448. The proteins named *Medicago* 1, *Medicago* 2 and *Medicago* 3 are uncharacterized proteins from *Medicago truncatula* (NCBI database, accession numbers are ABN05760.1, ABN05767.1, and ABN08744 1, respectively). The proteins the names of which are framed share a similar predicted N-glycosylation site (NRTG). It is worth noting that these four proteins do not share the signal peptide targeting to the mitochondrion.

3.4 Discussion

CKX catalyzes the irreversible degradation of the cytokinins isopentenyladenine (iP) and zeatin (Z) by oxidative side-chain cleavage to produce adenine and 3-methyl-2-butenal (Fig. 1.5; Werner *et al* 2006); the reaction can also occur on nucleosides Because CKX is the only enzyme to degrade cytokinins, it plays a significant role in plant development and physiology Its activity is known to vary during different developmental stages. Thus, in maize, CKX activity increases during the first 10-12 days after pollination, but declines later to reach a stable level about 20-25 days after pollination (Jones *et al.* 1992) In tobacco, mature leaves have a reduced CKX activity compared to young leaves (Singh *et al.* 1992). CKX transcript levels in pea also vary during different developmental stages (Held *et al* 2008) Different *AtCKX*s promoter-*GUS* fusion genes have been placed in transgenic *Arabidopsis* and their transcript levels were assessed (Werner *et al.* 2006) *AtCKX1* is expressed in vegetative shoot apex, young floral tissue and branching points, whereas *AtCKX4* is expressed in trichomes, stomata and root cap. In wild type pea, as shown in Fig 1 9, CKX activity increases but not significantly in mature roots compared to young roots and decreases but not significantly from young shoots to old shoots (Held *et al.* 2008). In the vegetative parts of the pea mutant R50, CKX activity is always lower than in the vegetative parts of wild type Furthermore, it was reduced in mature root, and considerably more in mature shoots (Held *et al.* 2008). Also, R50 exhibits extremely low CKX activity in nodules as compared to wild type (Held *et al.* 2008). This study points to a role played by the CKX enzyme during plant growth and development of pea.

The comparison of the wild type and R50 nucleotide sequence leads to the conclusion

that the two sequences are identical in the gene-coding region. *PsCKX2* is therefore not mutated in R50; in other words, *sym16* is not *PsCKX2* It is possible, however, that other CKX isoforms are candidates for *sym16*.

In higher plants, CKX is encoded by multi-members belonging to a single gene family. For example, there are seven members in *Arabidopsis*, five in maize (*ZmCKX1-ZmCKX5*), and eight in wheat (Schmülling *et al* 2003; Galuszka *et al* 2004) Since the pea genome has not been fully sequenced, it is not known how many members make the CKX gene family in that species, in 2005, only two partial gene sequences were known (Vaseva-Gemisheva *et al* 2005b). The first full-length CKX cDNA named *PsCKX1* was successfully obtained in 2008 (Held *et al* 2008) Here we report that a second member of the family, *PsCKX2*, has been cloned. The knowledge of its sequence will further our understanding of CKX structure and function from a molecular perspective.

The consensus nucleotide sequence of *PsCKX2* is 1735bp long with a coding region of 1611bp, it also includes the partial sequence of the 5' and 3' UTRs *PsCKX2* shares 91% and 81% identity (NCBI BLAST) with one gene from *Medicago truncatula* (accession No. AC119417 17) and one gene from soybean (accession No BT097654.1), respectively, suggesting that these genes are most likely orthologs of *PsCKX2*. Now that the soybean genome has been sequenced (Schmutz *et al.* 2010), it will be worthwhile to identify the CKX genes in this legume, and compare them to the other known CKX genes

The coding region translates into a polypeptide of 548 amino acids, with a predicted molecular weight of 56.71kD; it shares high amino acid homology to those of many CKXs from other plants A GHS motif, common to all CKX proteins and located within the

FAD-binding domain, is found at position 111-113 in PsCKX2. It is found at positions 122-124 in AtCKX1, 97-99 in ZmCKX2, 101-103 in OsCKX4, 97-99 in HvCKX2, and 142-144 in PsCKX1 (Fig. 3.7). The histidine residue within the motif is considered to be the actual binding site of the FAD cofactor (Malito *et al.* 2004). Moreover, two amino acids, an aspartic acid and glutamic acid, are conserved in all isoforms found in plants. They are thought to be key elements in the recognition of the substrate amine group; their location appears to be variable amongst the different isoforms (Malito *et al.* 2004). In PsCKX2, they are found in position 173 and 286 (shown with a single asterisk in Fig 3 7), respectively. Furthermore, some short highly conserved motifs VPHPWLNL (between position 386 to 393 in PsCKX2) and PGQXIF (between positions 523 to 528 in PsCKX2) (shown with a double asterisk in Fig 3 7) are also found in all isoforms (Schmülling *et al* 2003) However, the functions of these motifs are unknown.

Many CKXs are known to have N-glycosylation sites (Schmülling *et al* 2003), *PsCKX2* does not appear to be different as it is predicted to have 4 of them (at position 36-NFSL; 54-NFSF, 292-NRTG; 426-NKSK). In maize, ZmCKX1 has eight predicted glycosylation sites, and five of them are most likely functional sites (Schmülling *et al* 2003) Generally, glycosylated proteins are known to be extracellular It has been reported that some CKX enzymes may not be glycoproteins, such as CKX in tobacco and bean (Kamínek and Armstrong 1990) Moreover, although PsCKX1 is predicted to have 3 glycosylation sites, it is also predicted to be a cytoplasmic protein because it lacks a signal peptide (Held *et al* 2008). Therefore, PsCKX1 is probably not a glycoprotein either (Held *et al.* 2008) The significant difference in pH optima between glycosylated and non-glycosylated forms of

CKX suggest that glycosylation may be correlated to subcellular localization (Kamínek and Armstrong 1990)

Using the iPSORT program, many AtCKXs, OsCKXs and ZmCKXs proteins have been predicted to be targeted to the apoplast because of the presence in their sequence of a N-terminal signal peptide. Because they lack this sequence, AtCKX7 (Schmülling *et al.* 2003) and PsCKX1 (Held *et al.* 2008) are predicted to be cytoplasmic proteins (Fig. 3.1). It should be noted that this predicted cytosolic location for PsCKX1 goes against the presence of N-glycosylation sites (Held *et al* 2008). In this regard, experimental data are more reliable than software prediction to access subcellular compartments Smehilova *et al.* (2009) demonstrated that the ZmCKX1-GFP signal was detected in the apoplast and that of ZmCKX10-GFP in the cytosol. One role of extracellular CKXs could be that of regulating imported cytokinins from source tissues or exported CK from sink tissues (Schmülling *et al.* 2003). Turner *et al.* (1985) proposed that the high CKX activity found in the seed coat of *Phaseolus* fruits is related to limiting the movement of CK to and from developing embryos with low CK levels Individual CKXs, belonging to a multi-gene family, are expressed in different subcellular localizations and therefore may have specific functions.

AtCKX1 and HvCKX3 are predicted to be targeted to mitochondria (Schmülling *et al.* 2003). Apparently, PsCKX2 is also a mitochondrial CKX based on targeting sequences (KLRYPCF NLVREY, using iPOSORT program) and with another version of iPORT program called PORT program (certainty score is 0 8 affirmatively) In MitProt II program, the score of export to mitochondria is 0.0960 and the score is 0.34 in program Predotar program. Because the scores differ so much between software programs, the localization of PsCKX2

in the mitochondrial is questionable Very limited knowledge exists on the role that CKX may play in mitochondria, except that the mitochondrial respiratory complex (*nCI* gene) is regulated by ARR2, a response regulator in cytokinin signal transduction pathway (Lohr-mann *et al.* 2001).

It is well established that cytokinin homeostasis during plant development is regulated by CKX activity (Kaminek *et al.* 1997). Since the CKX enzyme is encoded by a multi-gene family, each isoform may play a role contributing to the total CKX activity (Schmülling *et al* 2003). However, at this point of time, there is no conclusive relationship between cytokinin and CKX genes. It seems plausible that an auto-regulation feedback loop exists between cytokinin and CKX genes Werner *et al* (2003) showed by semiquantitative RT-PCR that cytokinin increased the transcript levels of most *AtCKXs* A relationship between cytokinin and CKX transcription was demonstrated in R50 since this mutant accumulates cytokinin and exhibits high transcript levels of *PsCKX1*. If a positive relationship between CK and CKX exists, then the low transcript levels of *PsCKX2* in cytokinin -accumulating R50 are quite abnormal. Although it has been confirmed that *PsCKX2* is not mutated in R50, the reason of the low transcript level of *PsCKX2* in young shoots and roots (Fig. 1.10, Held *et al* 2008) is still unknown. I propose that the pleiotropic phenotype of R50 would not be directly caused by a mutation of *PsCKX2* but may be the indirect result of the post-transcription of *PsCKX2*.

Chapter 4 Early seedling development and cytokinin homeostasis

4.1 Introduction

4.1.1 Germination and seedling development

Germination is considered complete when the radicle emerges from the seed coat (Bewley, 1997). In pea, it is characterized as being hypogeal, i.e , cotyledons of the germinating seeds remain under the soil, unlike in many other model plants such as *Cucurbita maxima* (pumpkin), *Solanum lycopersicum* (tomato) and *Arabidopsis* where the germination is epigeal, i.e., the cotyledons emerge from the soil, expand, and carry out photosynthesis (Ayele *et al.* 2006). Furthermore, pea seeds are non-endospermic at maturity and their seed coat does not act as a mechanical barrier for radical protrusion when compared to that of the endospermic seeds of *Arabidopsis* and tomato (Ayele *et al* 2006) The cotyledons of pea contain large storage reserves which are mobilized to support the growth of the embryo axis (Ayele *et al* 2006). During seed germination, after the radicle and plumule emerge, and reserves are exhausted, the metabolic mode of the plant changes from heterotrophic to autotrophic. The radicle extends downward into the soil to grow into the root system and the plumule grows into the air to turn into a shoot system. The establishment of these two systems initiates a new growth phase called seedling development, which is terminated by the vegetative phase Seedling development is coordinated with cell division, cell elongation, and cell differentiation (Raghavan 2000). As any other developmental processes, germination is highly regulated by hormones (Finkelstein 2004) Seed germination relies also heavily on external cues, such as temperature, light, or gravity Thus, proper seedling establishment and growth depend on an intricate cross-talk between abiotic cues and metabolic signals, with hormones

undoubtedly at the centre of this communication

4.1.2 Cytokinin, germination, and seedling development

Cytokinins play an important role during seed germination as they promote cellular divisions, thus they contribute directly to the development of the embryonic root and shoot Elevated cytokinin concentrations have been noted in germinating achenes of *Tagetes minuta* (marigold) up to 48 hours after imbibition (Stirk *et al.* 2005) and in germinating pea 5 hours after imbibition (Stirk *et al.* 2008). Earlier work indicates similar results in rice (Saha *et al.* 1984) and *Lupinus albus* (lupin) (Nandi *et al* 1988). The high variations in cytokinin levels and forms (BAP, cZ and ribotides cytokinins) measured in growing pea radicles (Stirk *et al* 2008) are likely another indication of the importance of this hormone in plant early growth and development.

In higher plants, CKs are perceived by a small family of cytokinin receptors (e.g., Frugier *et al.* 2008). The importance of CK perception during seed germination has been highlighted by Riefler et al. (2006), who demonstrated clearly that uncoupling CK signaling through a number of mutations in *Arabidopsis* cytokinin receptors (*AHK*) led to, among other phenotypes, increased seed volume and embryo size, as observed in the *ahk2-5 ahk3-7 cre1-2* triple mutant In addition, cytokinin receptors apparently regulate seed germination as triple mutants unable to perceive cytokinins germinate more rapidly than wild type (Riefler et al. 2006). CRE1/AHK4, specifically, was shown to be involved in germination as PI-55, a known inhibitor to this specific receptor, accelerates seed germination in Arabidopsis (Spíchal et al 2009)

Cytokinin oxidase (CKX), a family of enzymes consisting of many members, is the only enzyme to degrade cytokinins *in planta* [introduced in chapter 1, Schmülling *et al.* (2003)]. CKX transcripts have been well characterized in vegetative and reproductive tissues of all major organs in a number of higher plants such as *Arabidopsis thaliana* (Werner *et al* 2003), barley (Galuszka *et al* 2004), maize (Massonneau *et al.* 2004) and pea (Held *et al* 2008). Nothing is really known about the role of CKX in germination and early development However, for vegetative tissues, cytokinins are known to stimulate the shoot apical meristem (SAM) activity, whereas they play an opposite role in the root apical meristem (RAM) Werner *et al* (2003) overexpressed *AtCKXs* in transgenic *Arabidopsis* plants, the end- result was a decreased cytokinin content, and reduced SAM activity, leaf thickness, and vasculature (Werner *et al* 2003) The CK-deficient roots of these same transgenic plants exhibited increased RAM activity, root diameter and vasculature (Werner *et al* 2003) CKX over-expression positively affects lateral root development, thus, the CKX transgenic *Lotus japonicus* root carrying either *AtCKX3* or *ZmCKX1* had a significantly increased number of lateral roots (Lohar *et al* 2004). Finally, Held *et al.* (2008) found that transcription of *PsCKX1* and *PsCKX2* were up-regulated in the shoots, roots and nodules of R50.

4.1.3 Objectives

In this chapter, I performed a morphological study of the pea seedling development to follow the expression of two CKX members (*PsCKX1* and *PsCKX2*) in wild type and R50 and to study the effects of PI-55 on seed germination and seedling development in pea.

4.2 Materials and Methods

4.2.1 Plant Material

All plants were grown following the protocol and conditions outlined previously. However, in contrast to those used in chapter 2, all seeds (except when mentioned otherwise) were planted in small square pots (9.6cm × 9.6cm), 4 seeds per pot.

4.2.2 Morphology study

4.2.2.1 Embryo and cotyledon weight, and their relative water content (RWC)

The imbibed seeds were harvested. Embryos and cotyledons (n = 24 for each line) were dissected and weighed individually for their fresh and dry weights (72 h at 60°C). Their relative water content (RWC) was determined by subtracting dry weights from fresh weights, and was expressed as a percentage on a fresh weight basis RWC data were transformed (arcsine) before statistical analysis.

4.2.2.2 Young seedling parameters of development

Plants (n=18) were harvested every day from 1 to 8 days after planting (DAP), and their roots washed of vermiculite Various morphological measurements, such as cotyledon fresh weight and dry weight, embryo fresh and dry weights, and the shoot and root fresh and dry weights, were assessed The embryo length, shoot height, and root length were also determined

4.2.2.3 PI-55 effects on radical length in seed germination

Imbibed seeds (n=24 for from wild type and R50) were placed into Petri plates lined with wet Whatman #1 filter paper in darkness Wild type and R50 seeds were treated with DMSO and

1 nM PI-55, respectively They were checked 30 hrs after imbibition for breakage of their coats. Photographs of the germinated seeds were taken and radicle length was measured by Scion image software (Scion Corp., Frederick, MD, USA)

4.2.2.4 PI-55 effects on lateral root number and lateral root primordia in seedlings

Plants were grown in yellow Conetainers™ and treated with PI-55 Wild type and R50 were harvested 7 DAP and 12 DAP; their root systems excised, and cleared according to Pepper *et al.* (2007). Roots were first fixed in a methanol : glacial acetic acid (3.1, v: v) solution for 30 minutes, and then transferred to a solution of 130 mM NaCl, 10mM sodium phosphate (pH 7) and 1% Tween 20 for 5 minutes twice. They were then placed within the clearing solution (0.16g chloral hydrate per milliliter of 20 % glycerol) for 10 min The primordia were counted using the dissecting microscope and the lateral root numbers determined

4.2.2.5 Cotyledon sections

Cotyledons of imbibed seeds and 7 DAP seeds from wild type and R50 were harvested. One piece of cotyledon was ground to powder in a mortar, and 10 ml water was later added. One drop of the mixture was put on a glass slide and visualized under a light microscope (Carl Zeiss Axiostar) Furthermore, sections of cotyledon were hand-made, and visualized under the microscope. Sections were stained with KI (1% iodine, 2% potassium iodine, 97% H_2O) to evaluate the number and size of starch grains

4.2.3 Semi-quantitative RT-PCR for *PsCKX1* and *PsCKX2* of developing seedlings

4.2.3.1 Isolation of RNA

Total RNA was extracted from different plant organs (0 5 g for each) using the TRIZOL

protocol (modified from Roche protocol): from embryos and cotyledons (1DAP) and from cotyledons, shoots and roots (3, 5, and 7 DAP) Each finely-ground tissue powders were transferred to 1 ml TRIZOL reagent (modified from Roche) and incubated for 10 minutes at room temperature. After the addition of 0 2 ml chloroform, the TRIZOL solution and tissue mixture was vortexed for 15 seconds and left incubated for 15 minutes. The mixture was then centrifuged at 13000 rpm for 15 minutes; 0.6 ml of the aqueous supernatant was transferred to a new tube to which was added the same volume of isopropanol. The pellet was re-suspended and washed with 70% ethanol (1 ml ethanol is added and the mixture centrifuged at 10000 rpm for 1 minute). The resulting pellet (extracted total RNA) was dissolved in DEPC water and stored in -80°C for future use In order to remove polysaccharides and proteoglycans from embryos and cotyledons, samples were further purified using an RNeasy Mini kit (Qiagen, Valencia, CA). The DNase treatment (protocol outlined previously in chapter 3) was also applied to all samples

4.2.3.2 Semi-quantitative RT-PCR

Total RNA (5μg) from each tissue was used to synthesize first-strand cDNA with a Super-Script® II Reverse Transcriptase kit (Invitrogen, Carlsbad, CA, USA, 2009). Primers were designed to amplify a β-Actin fragment (accession No X68649, Held *et al* 2008), a 363-bp *PsCKX1* cDNA product [accession No. EF030477, 5'-CAA CTT GTT CCT AGA TCG TGG A-3' (forward) and 5'- CACGTAATCAAAACCGTCACCT -3' (reverse)], and a 331-bp fragment of *PsCKX2* [5'-AAATGGAGGAGAAGGGCTTGAACACAT-3' (forward) and 5'-CTC AGT TGA CTT GAC TCT CCT GCC-3' (reverse)]. The linear range of *PsActin*, *PsCKX1*, *PsCKX2* was determined to be 18-26, 26-34, 26-34 cycles, respectively The PCR

to amplify *PsActin*, *PsCKX1*, and *PsCKX2* products, began with a 4-min denaturation at 94°C, continued 22 cycles for *PsActin*, 30 cycles for *PsCKX1*, and 30 cycles for *PsCKX2* (94°C for 30 seconds, 55°C for 30 seconds, 72°C for 1 min per each cycle), with a final extension of 5 min at 72°C Products were analyzed in ethidium bromide-stained agarose gels using the Alphaimager software (Alpha innotech, Santa Clara, CA)

4.2.4 Statistical analysis

For all experiments, data were analysed for statistical significance with the program Sigma-Stat® version 2 03 software (SPSS Inc , Chicago Illinois) The Student's t-test was applied to determine significant difference ($P \leq 0\ 05$) between wild type and R50, unless mentioned otherwise Each trial was composed of 6 plants for each pea line, and was performed at least in triplicates.

4.3 Results

4.3.1 Embryo and cotyledon weights (fresh and dry) of imbibed seeds

R50 imbibed seeds appeared much larger than wild type seeds (Held *et al* 2008) This difference in size was reflected by a significantly heavier embryo (Fig. 4.1A). As seen in Fig 4.1, R50 exhibited a significant difference for the embryo dry and fresh weights and cotyledon fresh weights from wild type. The embryos of both wild type and R50 took apparently a similar amount of water upon imbibition since their relative water contents (RWC) were close to 58% In contrast, R50 and wild type cotyledonary tissues exhibited significantly different RWC, that of R50 was of 54 20% whereas wild type RWC was equal to 53.32% This likely explains why R50 cotyledon fresh weight was significantly larger than that of wild type, while their dry weights were similar (Fig. 4.1B).

4.3.2 Growth and development of the seedling

For many years, R50 was thought to have a delayed germination (Guinel and Sloetjes 2000), but in this study we learned that the problem with R50 lies in the emergence of its epicotyl (Fig 4.2 A) At 1 DAP, the embryos were difficult to manipulate and we were not able to distinguish in our measurements radicles from epicotyls; therefore we measured the length of the entire embryo and did not calculate statistical significance for that age. However, the wild type seedlings emerged from the soil around day 3, whereas R50 epicotyls were always visible a day or two later. Furthermore, R50 epicotyl was significantly shorter than that of the wild type (Fig

4 2A) R50 radicles were also shorter than those of the wild type upon epicotyl emergence, but 6 DAP the radicles of both lines appeared to be of a similar size (Fig 4.2B) The dry weights (DW) of these organs mirrored most of these differences (Fig 4.3 A&B), with similar weights for the shoot and root until 5 DAP but much heavier weight for the wild type thereafter. This discrepancy [this difference was not seen in the radicle length (Fig. 4.2 B)] may be explained by the fact that at that age, lateral roots of the wild type are at a more advanced stage in their development than those of R50 Seven days after planting, R50 seedlings are different from those of the wild type with shorter epicotyls, fewer lateral roots, and barely open apical hooks (Fig 4 4) Not surprisingly, the FW of the R50 cotyledons were significantly heavier than those of the wild type (Fig. 4.5 A) The cotyledon DW for both lines was expected to decrease as the seedlings would use their reserves when going from heterotrophy to autotrophy However, the DW of R50 cotyledons did not decrease as fast as that of wild type cotyledons (Fig. 4.5 B).

4.3.3 Cotyledon degradation during seedling development

The cotyledons of wild type were never found to become necrotic as they aged (Fig. 4.6 A), in contrast to those of R50 (Fig 4 6 B). In order to find the reason for the necrosis, sections of cotyledons were made by hand. As seen in Fig. 4.7, starch grains (flower-shape) filled the cells of the cotyledons of imbibed seeds. They were much larger in R50 than in wild type; as well, R50 cells were much larger than those of wild type (Fig. 4.7 A&B). Seven days after germination, wild type cells exhibited many small starch grains (black arrow, Fig. 4 8 A), likely resulting from the breaking down of the flower-shaped starch grains seen earlier. In contrast, R50 cells continued to display many flower-shaped starch grains (black and red

arrows, Fig 4.8 B)

4.3.4 PI-55 effects on radicle length in seed germination

Wild type and R50 seeds had all germinated 30 hours after imbibition The radicle length of wild type plants treated either with DMSO- or PI-55 was 2 5 cm, while that of R50 was 2.0 cm. The radicle length of wild type was significantly longer than those of R50 (Fig. 4 9). However, PI-55 had no effect on radicle length either for wild type or for R50 (Fig. 4 9).

4.3.5 PI-55 effects on lateral roots

The results for this experiment are found in Table 4 1. In this table, the control (DMSO) values are shown as a unit (in red) to demonstrate the lateral root growth pattern At 7DAP, lateral root number from wild type was significantly larger than that of R50 (Asterisk in Table 4 1), but the number of lateral root primordia from wild type was smaller, but not significantly so. This could explain why at 12DAP, R50 lateral root number caught up with that of wild type. The difference in lateral root number could also explain why 7DAP wild type seedlings have a primary root length similar to that of R50, but a heavier DW A similar pattern was seen in plants treated with other PI-55 centrations. Lateral roots in R50 were slow to emerge, not to form; these results are in agreement with those of Pepper *et al* (2007). PI-55 appeared to have no effects on lateral roots of wild type plants. This does not match the results I reported in chapter 2 The reason could be that 1) the sample size was too small, and 2) PI-55 acts later in the life of the plants (12 DAP vs 14 DAP) Interestingly, PI-55 stimulated lateral root number and primordia at 12 DAP in R50 (Triangle in Table 4.1) I expect the former. Thus, in R50,

cytokinin perception is likely to play a role in the promotion of lateral root formation, and lateral root development This is in agreement with the negative role that cytokinins are known to have on the root system (Werner *et al.* 2003) PI-55 appears to play an optimal role at 3.5μM. At higher concentration, the number of emerged roots is decreased, and the compound may be toxic Since this is not observed in wild type, this may be because R50 is over-sensitive

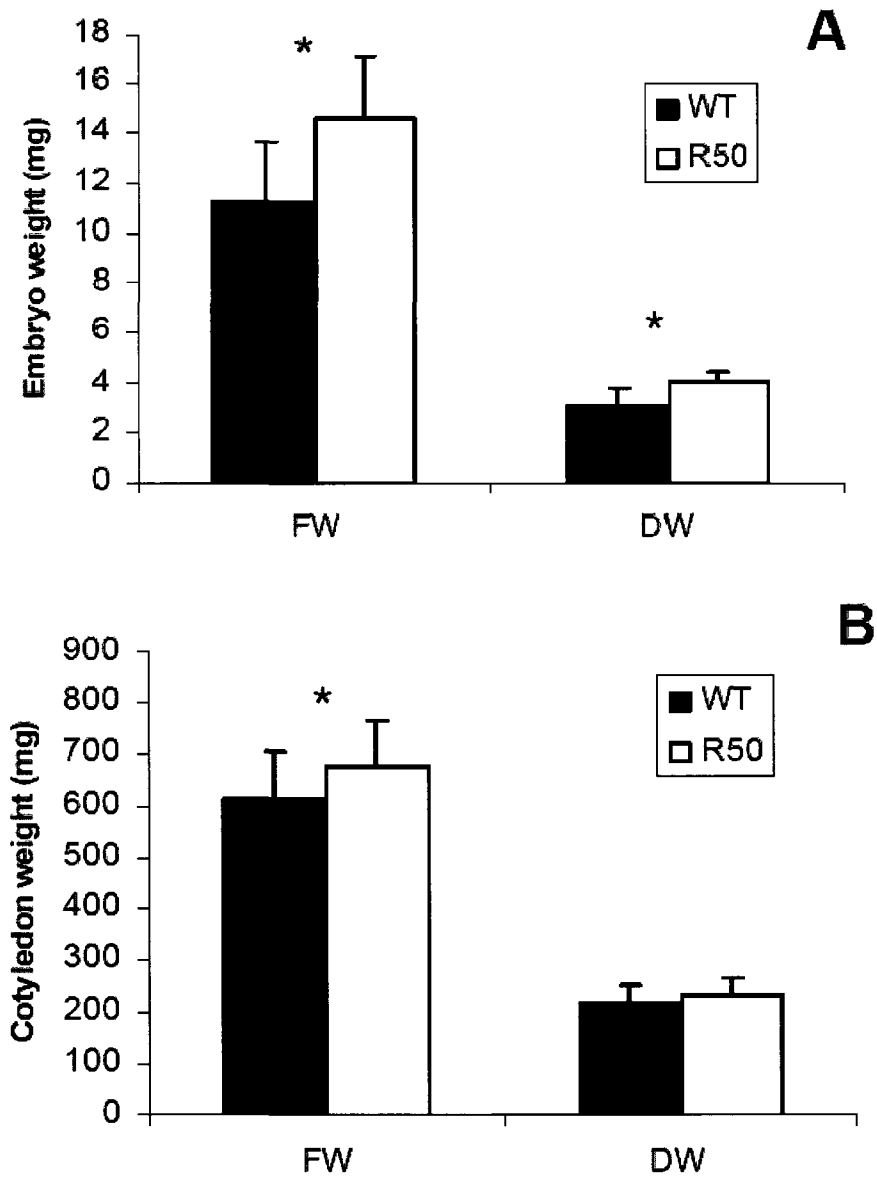

Figure 4.1 FW and DW from embryo and cotyledon. A) Embryo FW (fresh weight) and DW (dry weight) from wild type (WT) and R50 1 DAP B) Cotyledon FW and DW from wild type (WT) and R50 1 DAP Values are means ± SE, data were combined from three trials, n=24. Asterisks represent statistical significance at $P \leq 0.05$. Statistics were determined using t-test comparing the two pea lines

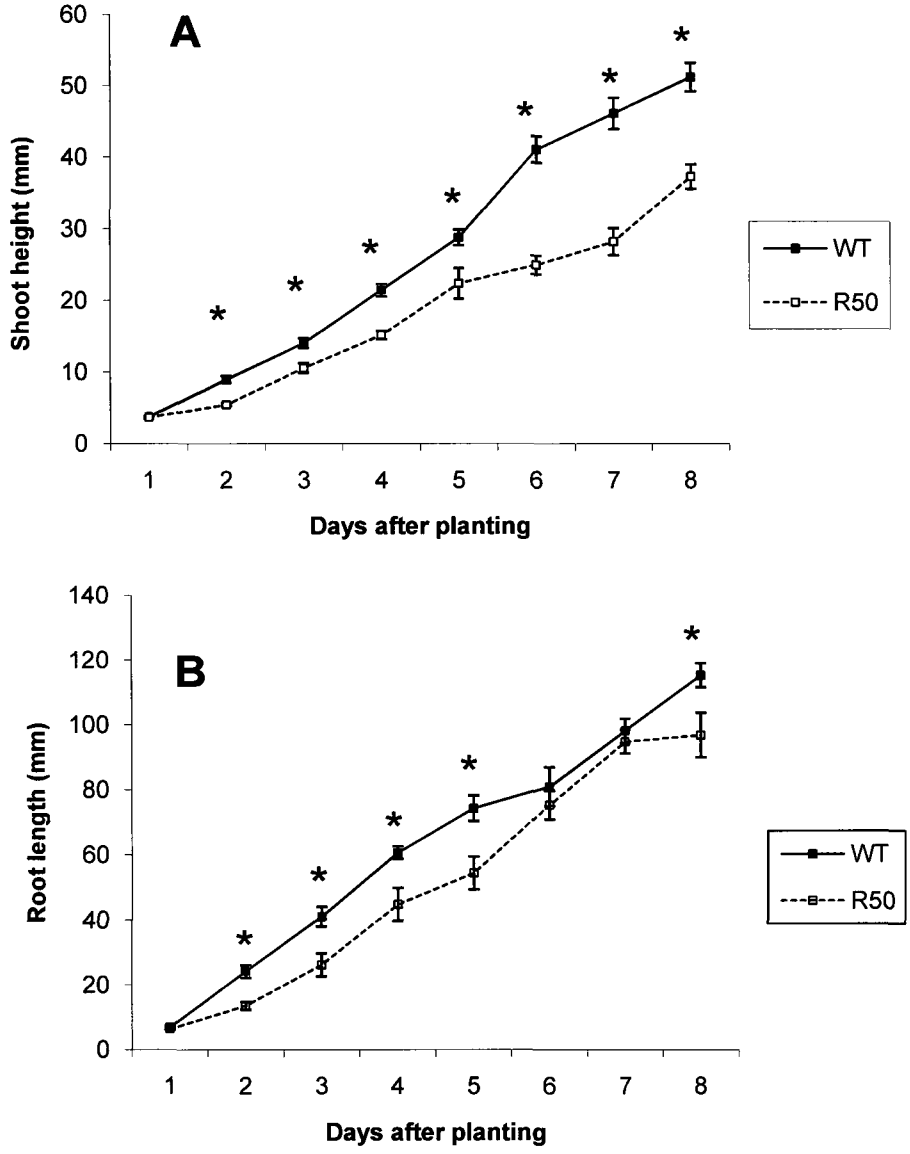

Figure 4.2 Shoot height and root length. A) Shoot height from wild type (WT) and R50 measured from 1 to 8 DAP B) Radicle length from wild type (WT) and R50 measured from 1 to 8 DAP Values are means ± SE, data are combined from three trials, n=18 Asterisks represent statistical significance at $P \leq 0.05$. Statistics were determined using t-test comparing the two pea lines.

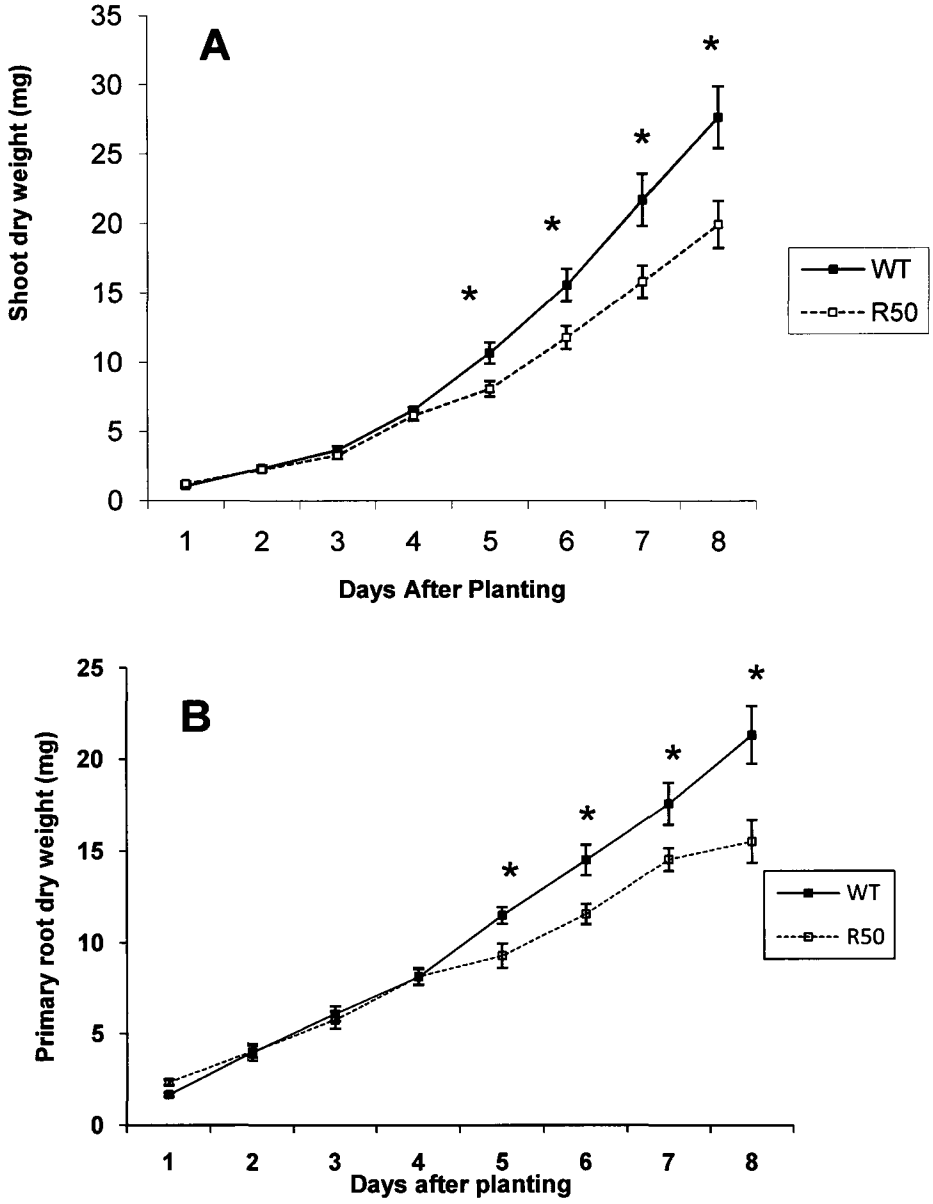

Figure 4.3 Shoot and root dry weight. A) Shoot dry weight from wild type (WT) and R50 measured from 1 to 8 DAP B) Primary root dry weight from wild type (WT) and R50 measured from 1 to 8 DAP. Values are means ± SE; data are combined from three trials, n=18. Asterisks represent statistical significance at $P \leq 0.05$. Statistics were determined using t-test comparing the two pea lines.

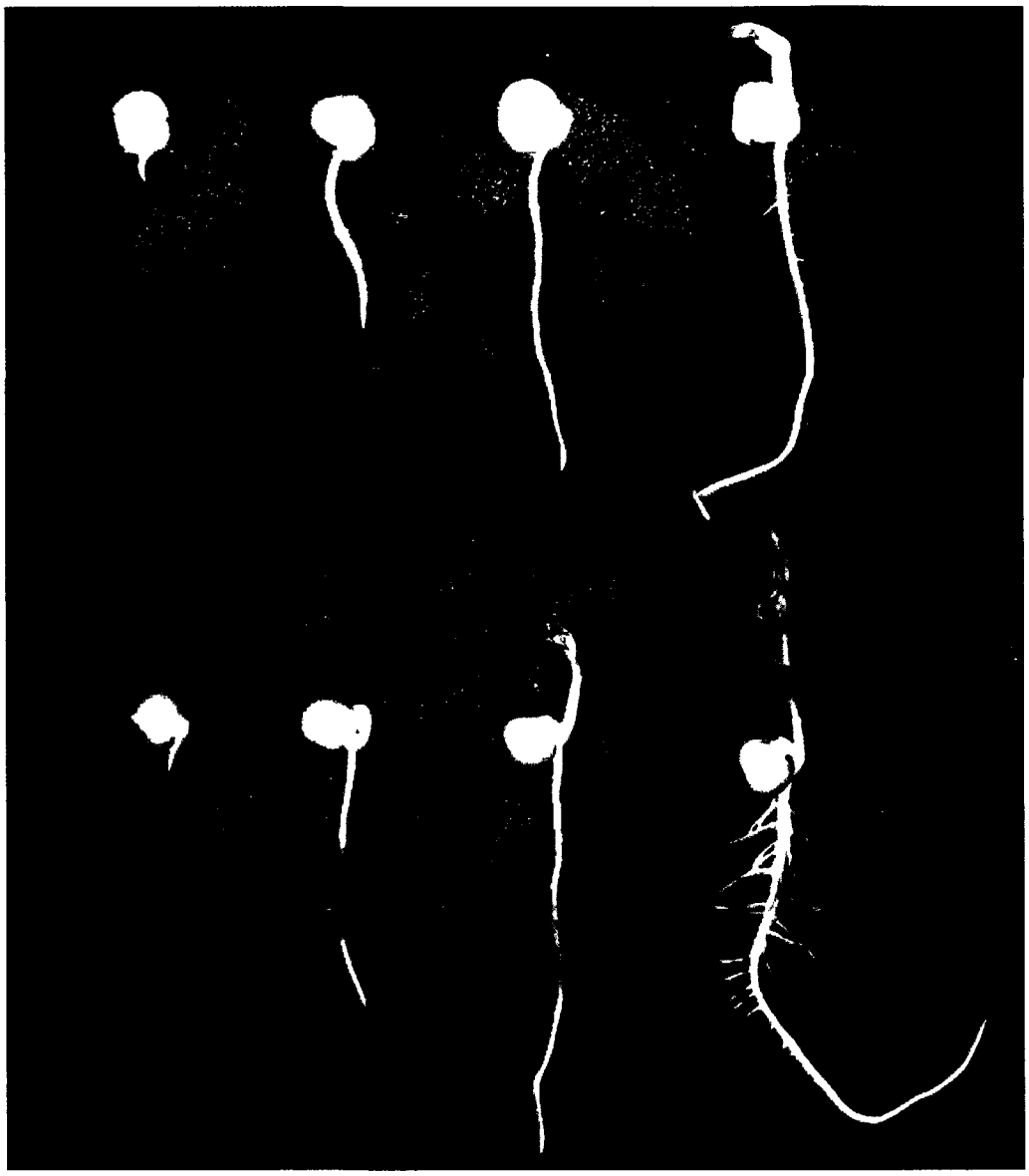

Figure 4.4 Development of Seedlings. R50 seedlings are on top of the image, whereas wild type seedlings are at the bottom From left to right, one can observe seedlings at 1DAP, 3DAP, 5DAP, and 7DAP. Note the differences between the two lines in the epicotyl height and the number of emerged lateral roots.

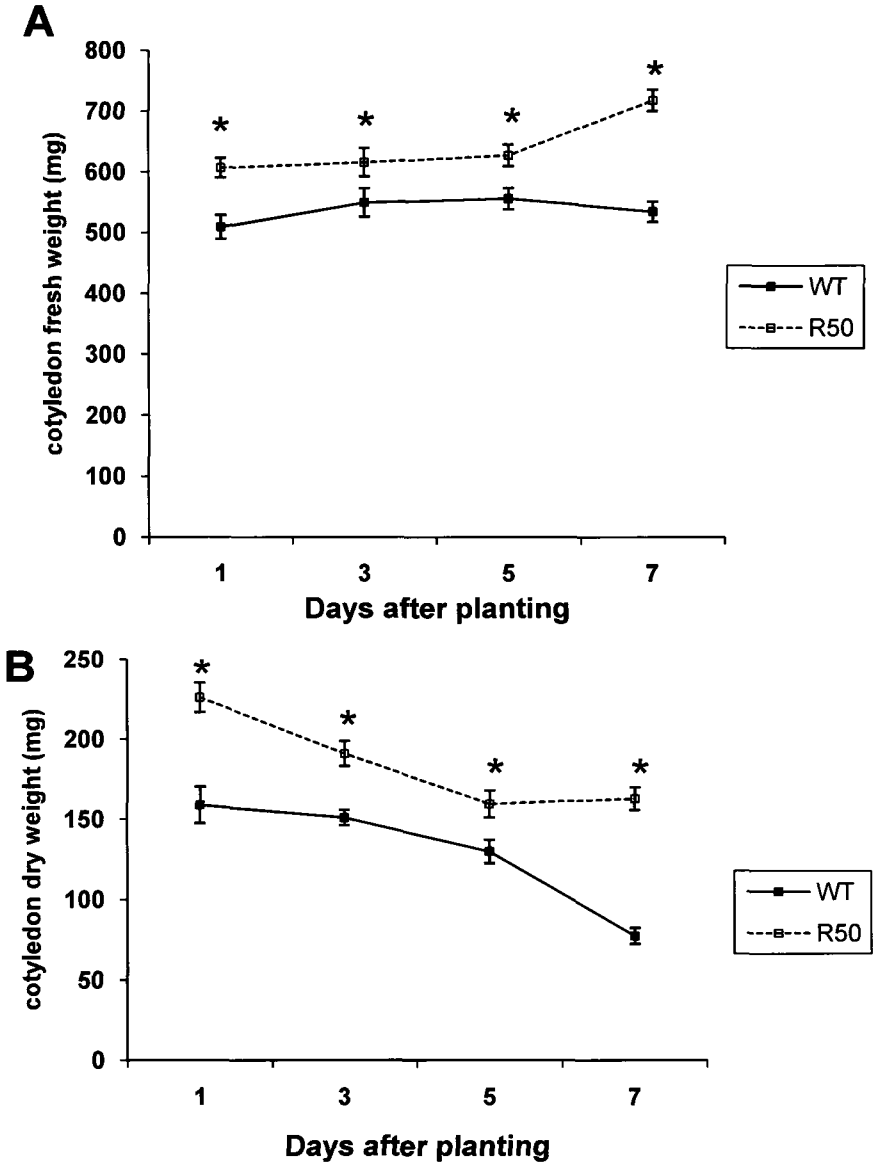

Figure 4.5 Cotyledon fresh and dry weights. A) Cotyledon fresh weight from wild type and R50 measured 1, 3, 5, 7 DAP. B) Cotyledon dry weight from wild type (WT) and R50 measured 1, 3, 5, 7 DAP Values are means ± SE; data are combined from three trials, n=18 Asterisks represent statistical significance at $P \leq 0.05$. Statistics were determined using t-test comparing the two pea lines.

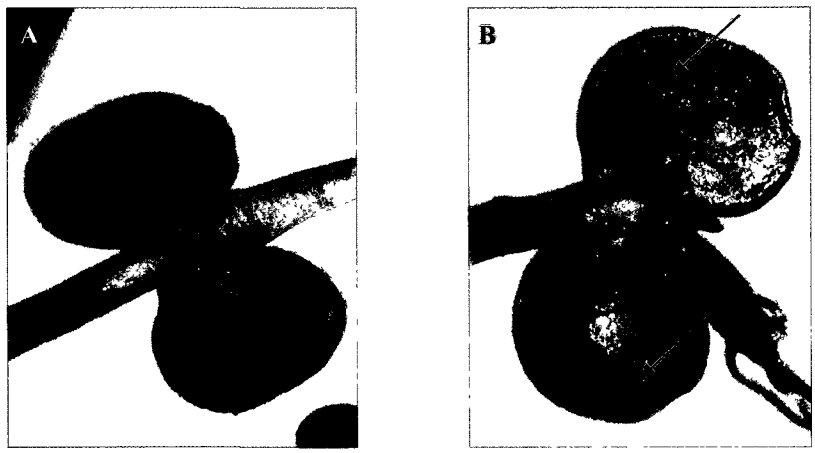

Figure 4.6 Seedling cotyledons at 7DAP. A) Wild type, and B) R50. The arrows point to necrotic area in the R50 cotyledons.

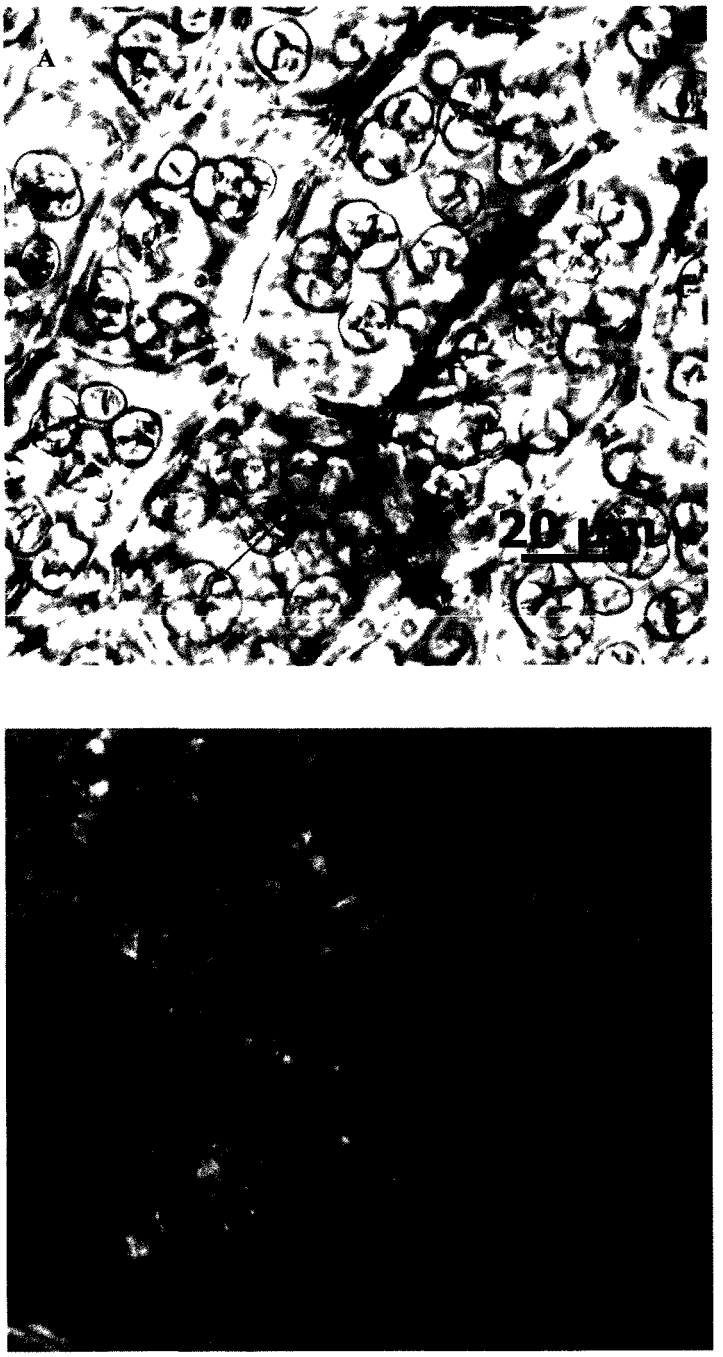

Figure 4.7 Cotyledon of imbibed seeds. A) Wild type cotyledon. B) R50 cotyledon. The arrows point to the starch grains in cells. Picture was taken using microscope (Carl Zeiss Axiostar). Section not stained with KI.

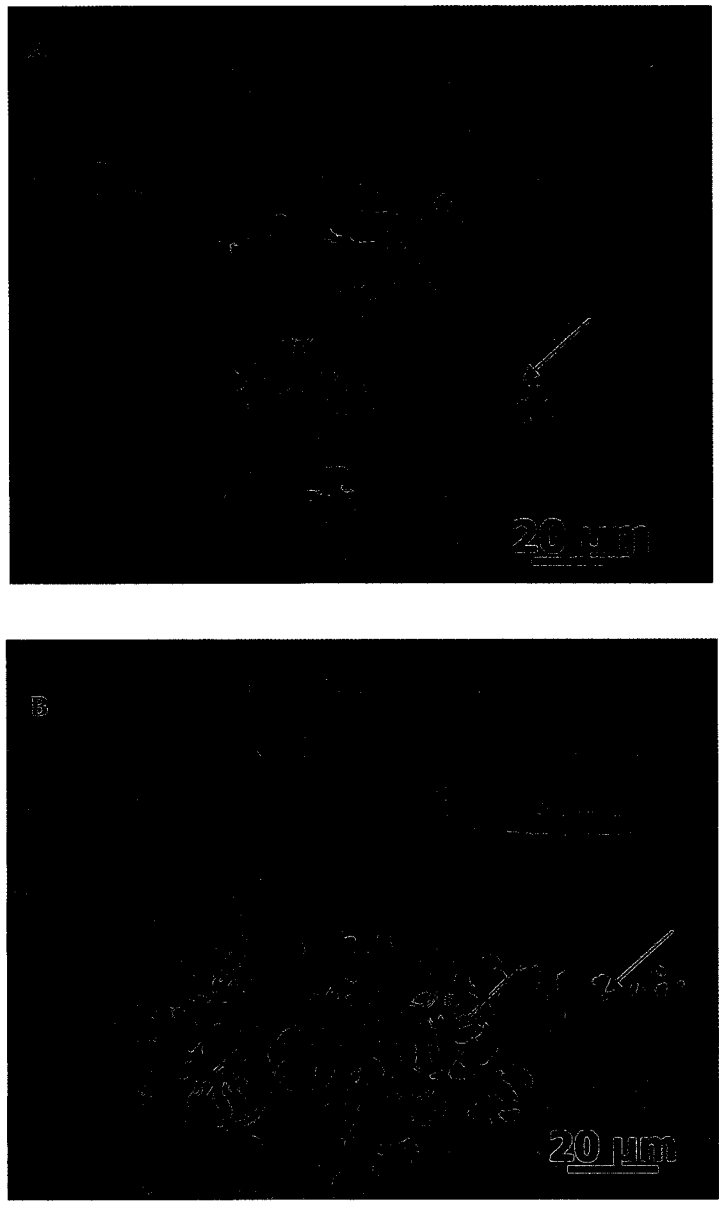

Figure 4.8 Cotyledon of 7DAP seeds. A) Section of a wild type cotyledon. B) Section of a R50 cotyledon. The black arrows point to the small single form of starch grains and the red arrow points to the flower-shaped starch grains. Picture was taken using microscope (Carl Zeiss Axiostar). Section not stained with KI.

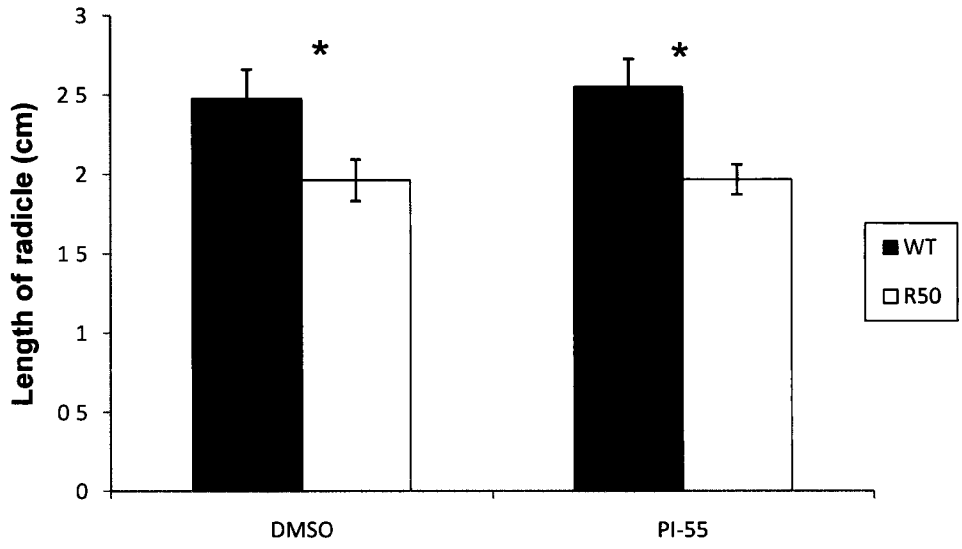

Figure 4.9 PI-55 effects on radical length from wild type (WT) and R50. Values are means ± SE, obtained data combined from three trials, n=24. Asterisks represent statistical significance at $P \leq 0.05$. Statistics were determined using t-test of compare every two groups. The PI-55 concentration is 1nM.

Table 4.1 Lateral root number and lateral root primordia number.

		Lateral root number		Lateral root primordia	
		Wild type	R50	Wild type	R50
DMSO	7 DAP	21 6±3 35	12 8±2 25*	15 66±3 82	18 00±1 46
	12 DAP	34 18±4 49	30 14±4 24	11.27±2.74	7.20±0.80
1μM PI-55	7 DAP	24.5±1 72	8.10±1.30*	12.50±1 55	18.50±1.71
	12 DAP	29.4±2.87	32.8±1.43	14 44±2.36	11 09±1 61
3 5μM PI-55	7 DAP	28.50±1 95	14.75±3.29*	12 66±0 97	20.62±3.14
	12 DAP	37 63±2.57	43 85±0.79$^{\Delta}$	11.09±1 39	14 42±2.05$^{\Delta}$
10μM PI-55	7 DAP	22.28±2.52	8 00±1 52*	14 71±1.89	17 10±0 70
	12 DAP	37.16±2 07	27.3±3.67	14.75±1.95	14.44±2.61

Values are means ± SE, obtained data combined from three trials, n=5-11. Asterisks represent statistical significance compared to wild type at $P \leq 0.05$ Triangle represents statistical significance compared to DMSO at $P \leq 0.05$. Statistics were determined using Student's t-test. The data of 0μM (in red) set up as an example to demonstrate the lateral root growth pattern. Plants treated with the other PI-55 concentrations follow the same pattern as those treated only with DMSO.

4.3.6 Semi-quantitative RT-PCR

4.3.6.1 RNA quality analysis

RNA was isolated from embryo (E), cotyledon (C), root (R) and shoot (S), of both wild type and R50 at four ages (1, 3, 5, and 7 DAP). RNA concentrations were measured using the NanoDrop spectrophotometer (Thermo Scientific). Total RNA from those two pea lines run on a denaturing gel had bands corresponding to those of 28S and 18S rRNA (Fig. 4 10). The 28S rRNA band was approximately twice as intense as that of the 18S rRNA. That presence of the bands corresponding to 28S and 18S rRNA established that the RNA samples were not degraded.

4.3.6.2 Semi-quantitative RT-PCR to confirm *PsActin*, *PsCKX1* and *PsCKX2* fragments.

Semi-quantitative RT-PCR was used to quantify the transcript levels of *PsCKX1* and *PsCKX2* mRNA in different tissues Using a 544 bp *PsActin* fragment (Fig. 4 11, lane 2) as an internal control allowed me to quantify the target gene fragments. *PsCKX1* is likely to be 363 bp and *PsCKX2* to be 331 bp (Fig. 4 11 in lanes 3 and 4, respectively).

4.3.6.3 Linear range for *PsActin*, *PsCKX1* and *PsCKX2* fragments.

To determine the linear range of the PCR reaction for *PsActin*, *PsCKX1*, and *PsCKX2*, the cDNA from wild type 5 DAP root was synthesized. The *PsActin*, *PsCKX1* and *PsCKX2* products were loaded on a 1% agarose gel stained with ethidium bromide (Figs. 4 12 A, 4.13 A, and 4 14 A) and quantified by intensity-based conversion (Figs. 4.12 B, 4.13 B, and 4.14 B). The intensity-based conversion was calculated using the DNA marker λHind III as the standard unit, converting each sample into the standard unit by intensity, and then converting the obtained data to LOG. The linear range summary is shown in Table 4.2.

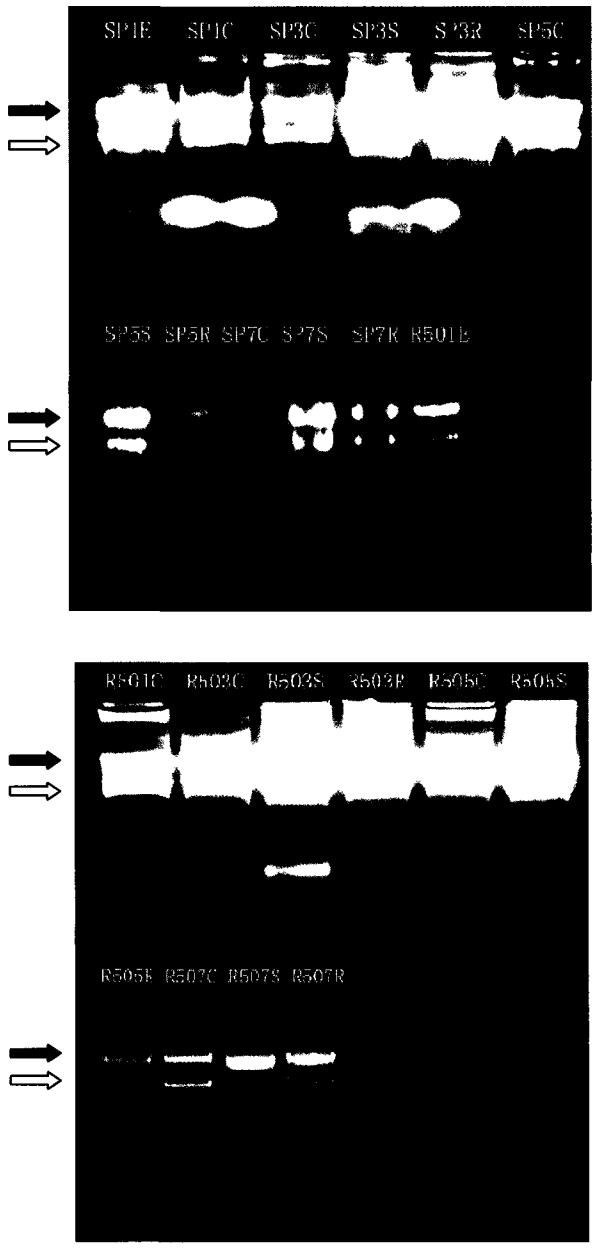

Figure 4.10 Gel electrophoresis for RNA samples. Samples were the RNA from different tissues (E: embryo; C: cotyledon; R: root; S: shoot) and different developmental stages (1, 3, 5, 7 DAP) of wild type and R50. For example, SP1E is short for Sparkle 1DAP in embryo. The first top band is 28S rRNA (solid arrow), while the bottom band is 18S rRNA (white arrow).

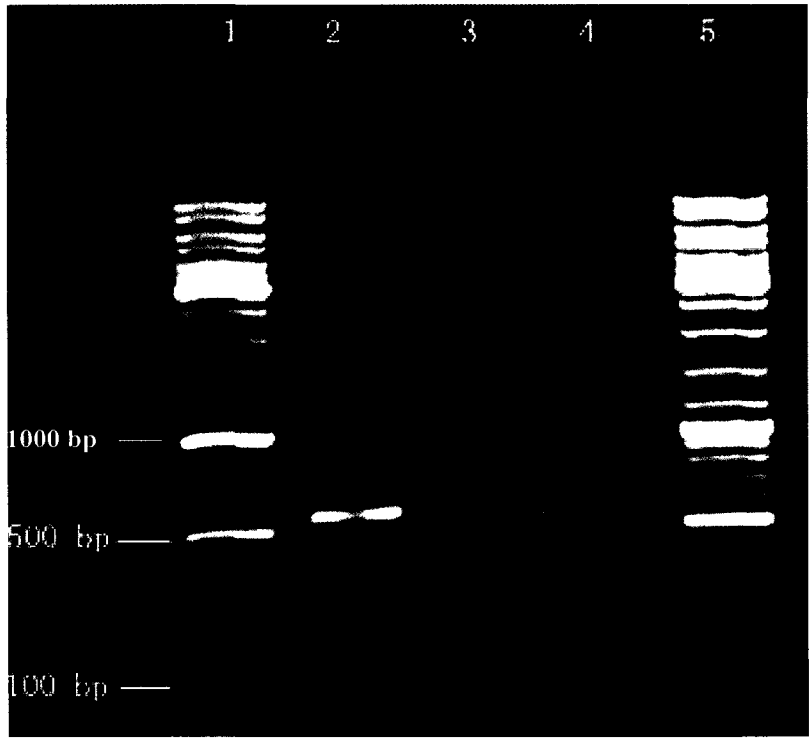

Figure 4.11 PCR amplification of *PsActin*, *PsCKX1* and *PsCKX2* fragments from cDNA. These fragments were used for semi-quantitative RT-PCR. The 544 bp fragment (lane 2) is used as an internal control for the quantification of the target gene fragments *PsCKX1* and *PsCKX2*. The 363 bp *PsCKX1* and 331 bp *PsCKX2* products are shown in lanes 3 and 4, respectively. Lanes 1 and 5 are 1 kb gene ladder. This figure was obtained with cDNA from wild type roots, but is representative of data obtained from both pea lines and from all tissues

A)

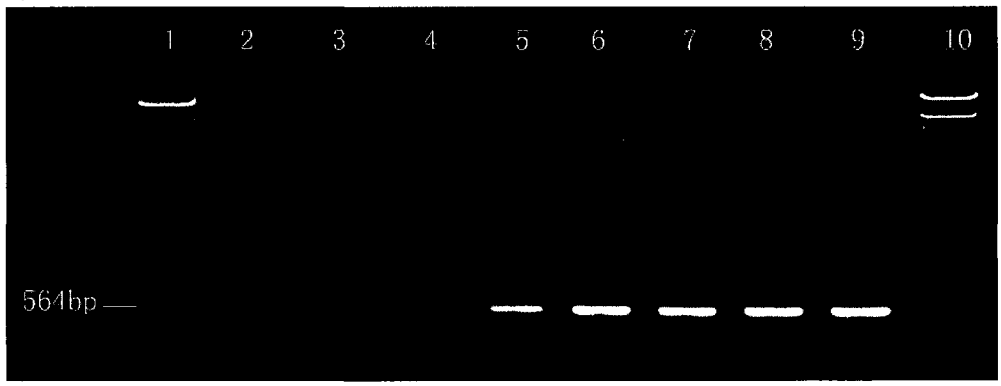

B)

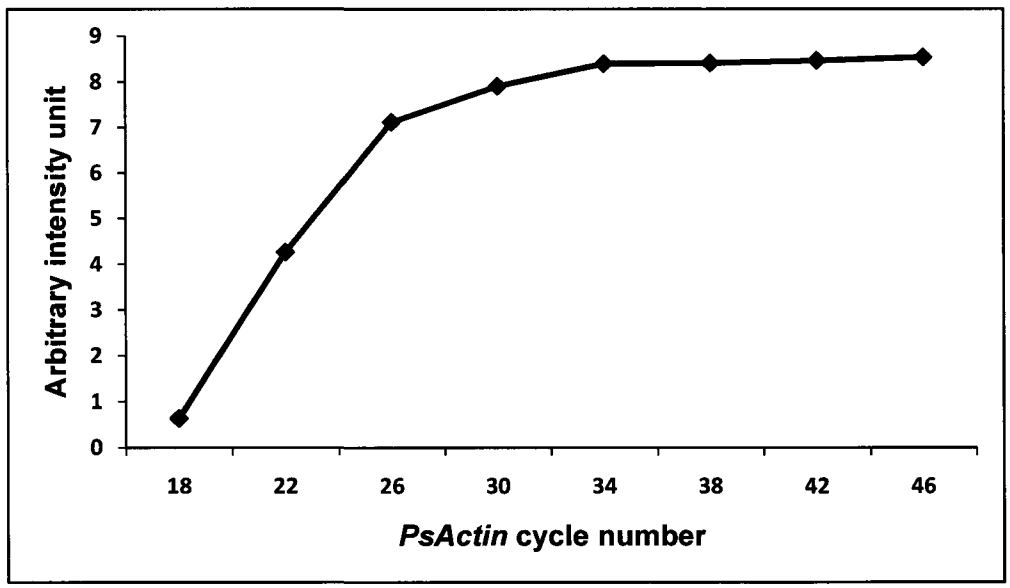

Figure 4.12 PCR amplification of *PsActin*. A) Electrophoresis of *PsActin* PCR reaction. Lanes 1 and 10 contain DNA marker λHind III (3µl and 6µl, respectively). Lanes 2-9 correspond to the amplification of the *PsActin* product after 18, 22, 26, 30, 34, 38, 42, and 46 cycles Aliquots (8µl) of the total reaction volume were loaded in each lane. B) Quantification of product intensity (arbitrary unit) after LOG conversion over the range of *PsActin* PCR cycles.

A)

B)

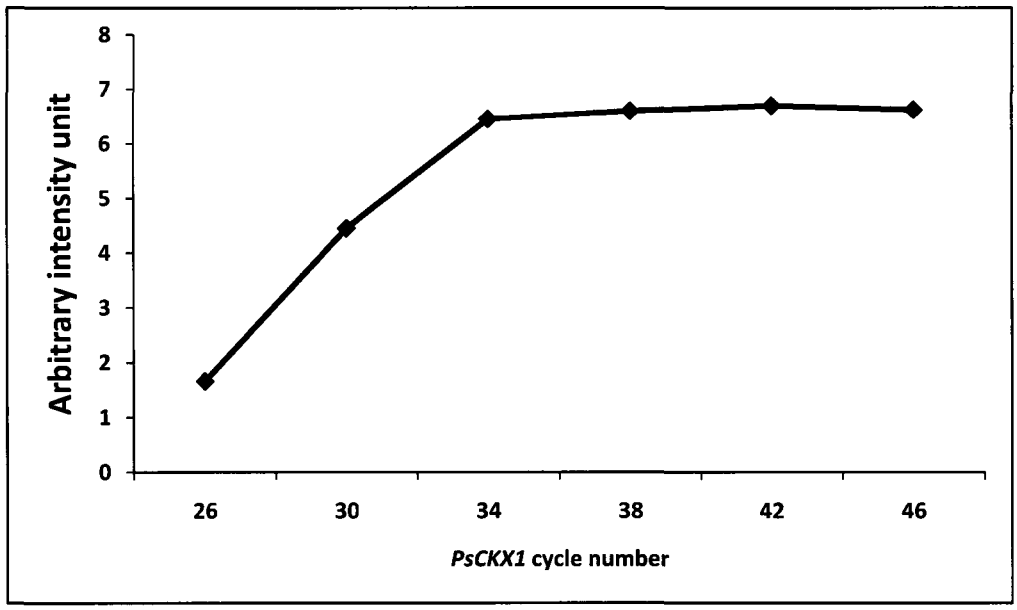

Figure 4.13 PCR amplification of *PsCKX1*. A). Electrophoresis of *PsCKX1* PCR reaction. Lanes 1 and 10 contain DNA marker λHind III (3µl and 6µl, respectively) Lanes 2-9 correspond to the amplification of the *PsCKX1* product after 18, 22, 26, 30, 34, 38, 42, and 46 cycles Aliquots (8µl) of the total reaction volume were loaded in each lane B) Quantification of product intensity (arbitrary unit) after LOG conversion over the range of *PsCKX1* PCR cycles.

A)

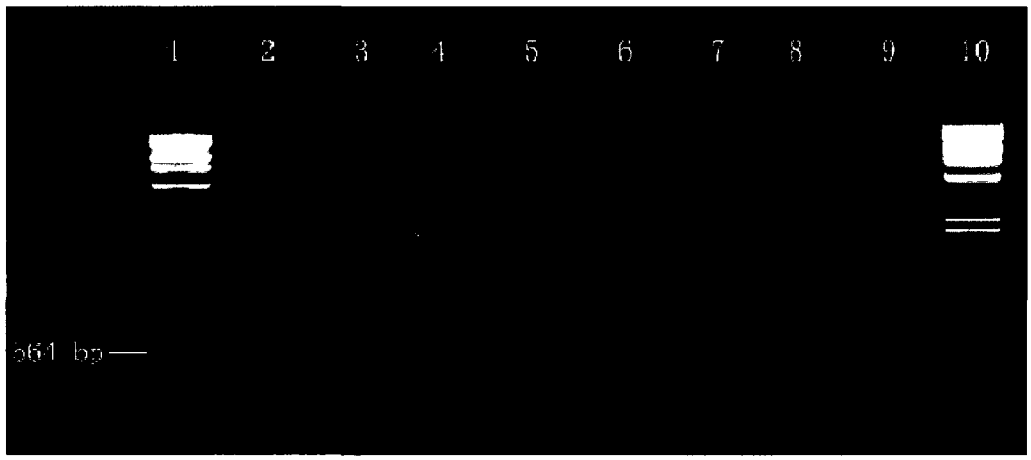

B)

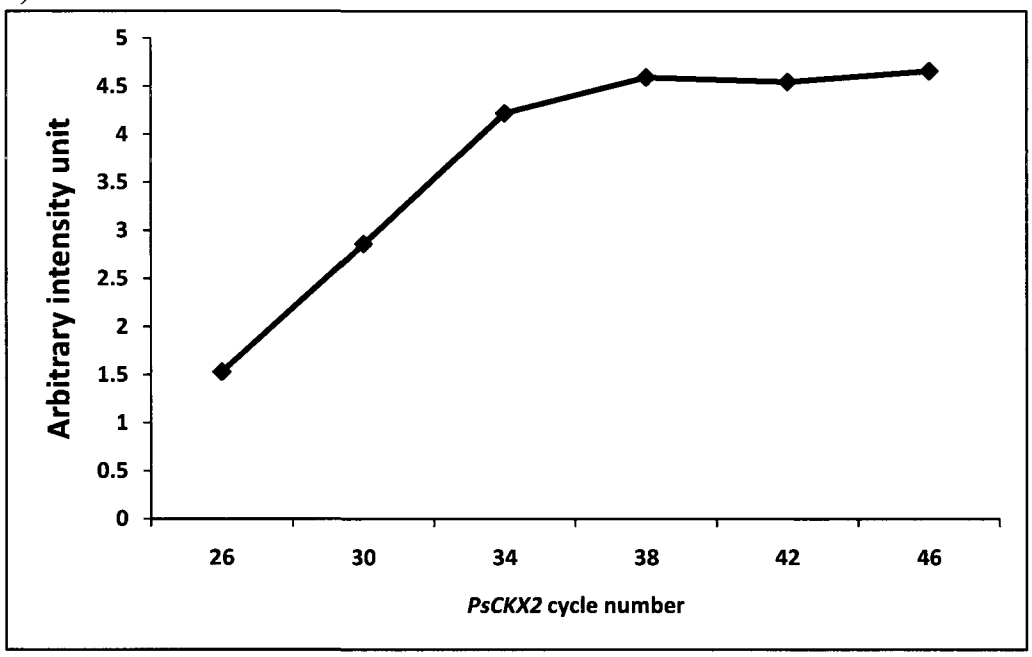

Figure 4.14 PCR amplification of *PsCKX2*. A). Electrophoresis of *PsCKX2* PCR reaction Lanes 1 and 10 contain DNA marker λHind III (3µl and 6µl, respectively) Lanes 2-9 correspond to the amplification of the *PsCKX2* product after 18, 22, 26, 30, 34, 38, 42, and 46 cycles Aliquots (8µl) of the total reaction volume were loaded in each lane. B). Quantification of product intensity (arbitrary unit) after LOG conversion over the range of *PsCKX2* PCR cycles.

Table 4.2 Linear range determination summary.

	PsActin	*PsCKX1*	*PsCKX2*
Tissue	SP5R*	SP5R*	SP5R*
First observation	18	26	26
Saturation	26	34	34
Linear range	18-26	26-34	26-34

*SP5R is short for wild type 5 DAP root

4.3.6.4 Profiles of *PsCKX1* and *PsCKX2* expression

PsCKX1 transcript level of R50 cotyledons seemed to be lower but not significantly so than that of wild type at 1DAP, but it was significantly higher (1 9 fold more) at 3 DAP (Fig 4.15) At other ages, no significant differences were found between the two pea lines (Fig. 4.15). The *PsCKX1* expression pattern in wild type was a parabolic curve, but the *PsCKX1* expression of R50 did not follow this pattern because of the significantly high *PsCKX1* expression at 3 DAP (Fig. 4.15) No *PsCKX2* transcript levels were detected in cotyledons of either wild type or R50 at all ages studied. In shoots, there were no differences between wild type and R50 in the transcript levels of *PsCKX1* (Fig. 4.16A). The *PsCKX1* expression increased with age for both pea lines to reach a plateau at around 5 DAP (Fig. 4.16A). *PsCKX2* transcript levels displayed an exponential growth curve in wild type, although not significant, differences were noted between the two pea lines with *PsCKX1* expression in R50 reaching a plateau at 5 DAP (Fig. 4 16B) In roots, the *PsCKX1* transcript levels displayed no difference between wild type and R50, as both increased with age (Fig 4.17A); the levels exhibitd also an exponential growth (Fig. 4.17A). *PsCKX2* expression followed a similar pattern in both wild type and R50 (Fig. 4.17B). However, *PsCKX2* transcript levels were significantly higher (by 2.5 fold) in R50 than in wild type at 7DAP (Fig. 4 17B).

Comparing the transcript levels of both *PsCKX* members, in embryos and shoots, of the two pea lines, *PsCKX1* transcript levels were more abundant than those of *PsCKX2* at all ages studied (Figs 4 16A & 4.16B). In roots, at the early stages (1DAP and 3 DAP), *PsCKX1* transcript levels were more abundant than those of *PsCKX2* (Fig. 4.17A & 4.17B).

Comparing the different tissues, *PsCKX1* was expressed weakly in embryos (Fig. 4.17A).

PsCKX1 transcript levels were more abundant in shoots than in cotyledons and roots (Fig. 4.15, 4 16A and 4 17A). Surprisingly, the highest *PsCKX1* transcript levels were found in 7DAP cotyledons (Fig. 4 15) Similarly, *PsCKX2* was expressed weakly in embryos (Fig. 4 17B). *PsCKX2* expression seemed similar in shoots and roots (Fig. 4 16B&4.17B), except for R50 7DAP root in which the transcript levels were extremely high (Fig. 4.17B)

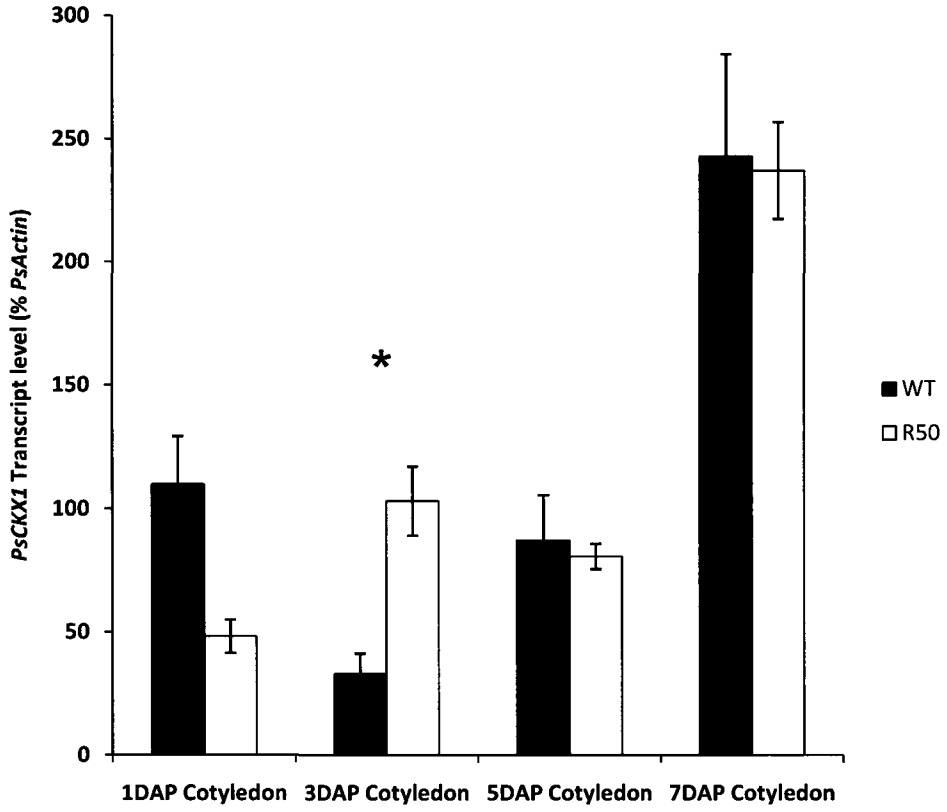

Figure 4.15 *PsCKX1* expression profiles in cotyledons. Quantification of *PsCKX1* product intensity (% *PsActin* control) for wild type (WT, black bars) and R50 (white bars). Values are means ± SE, n=3. Asterisks represent statistical significance from the control at $P \leq 0.05$ Statistics were determined using t-test comparing the two pea lines.

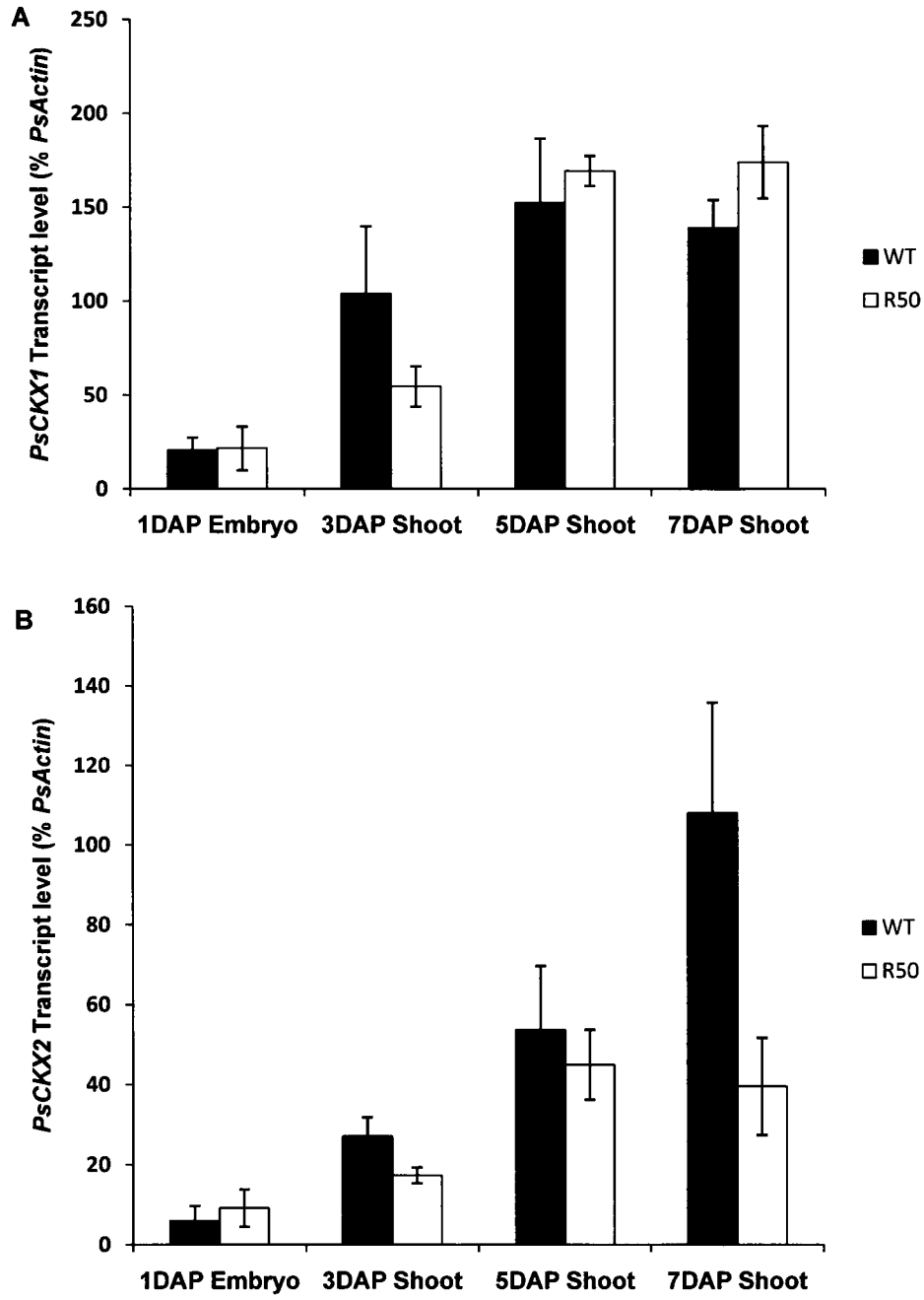

Figure 4.16 *PsCKXs* expression profiles in embryo and shoots. A) PsCKX1 expression profiles. B) PsCKX2 expression profiles Quantification of PsCKX1 product intensity (% PsActin control) for wild type (WT, black bars) and R50 (white bars) in embryo (1DAP) and shoot (3, 5, 7 DAP). Values are means ± SE, n=3. Statistics were determined using t-test comparing the two pea lines.

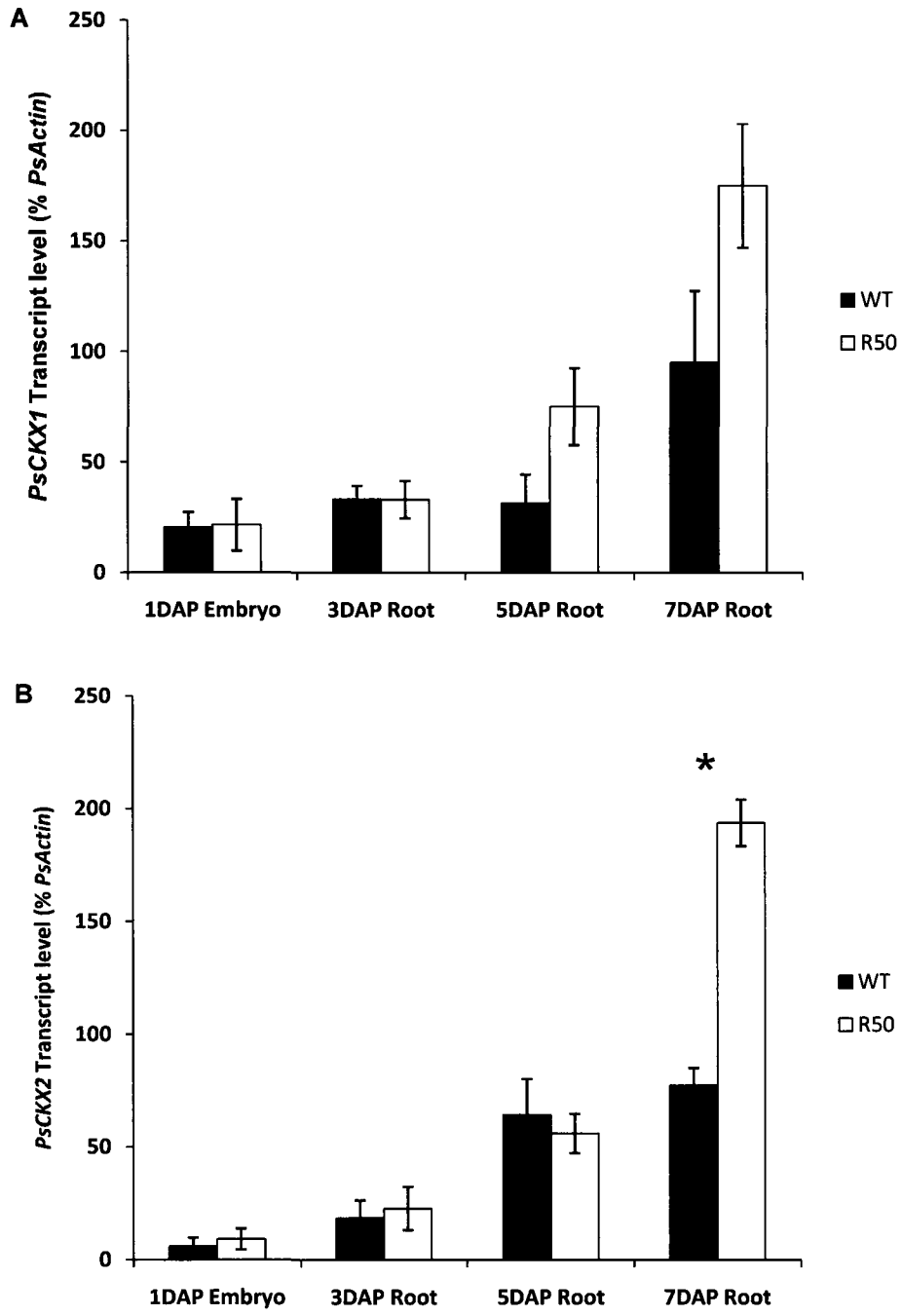

Figure 4.17 *PsCKXs* expression profiles in embryo and roots. A) PsCKX1 expression profiles. B) PsCKX2 expression profiles.Quantification of PsCKX1 product intensity (% PsActin control) for wild type (WT, black bars) and R50 (white bars) in embryo (1DAP) and shoot (3, 5, 7 DAP) Values are means ± SE, n=3. Asterisks represent statistical significance from the control at $P \leq 0.05$. Statistics were determined using t-test comparing the two pea lines

4.4 Discussion

Cytokinins maintain their homeostasis by synthesis, perception and degradation. Here, I assessed the role of a cytokinin receptor, CRE1/AHK4, in germination and lateral root development by applying the antagonist PI-55 I found that it has no effect on germination or total radicle length either in wild type or R50 Jaroslav Nisler (personal communication) also studied the effects on PI-55 on germination (sample size 60 seeds), his results are in agreement with those reported here. However, he noticed that the radicle length of germinated seeds treated with PI-55 is longer than that of control plants Therefore, he separated the germinated seeds into 5 groups (<0.5cm, 0 5-1 0cm, 1.0-1 5cm, 1.5-2 0cm, and >2.0cm) according to the length of their radicle He found that seeds treated with high levels of PI-55 (100nM) had longer radicle than the control seeds (Appendix 4.1). In this regard, PI-55 promoted radicle growth.

I also evaluated the potential role played by CKX by studying the expression of two *PsCKX* members over the time of seedling development I focused on seedling development because it is an important stage in life as the organism moves from a heterotrophic to an autotrophic state (Raghavan 2000). During this transition, many biological processes occur, such as the use of reserves in cotyledons, the development of new organs, high metabolism, and the transcription of many photosynthetic genes (Raghavan 2000). My results indicate that the two *PsCKX* family members I studied play different roles during early development. *PsCKX2* is not detected in the cotyledons and is expressed weakly in the embryo, suggesting that its product may act in the embryo but not in the cotyledons. On the contrary, *PsCKX1* appears to play an essential role during seedling establishment and what follows is a synopsis of my interpretation of this event. We proposed that *PsCKX1* is important during the transition phase between seed

and seedling. At 1DAP, *PsCKX1* transcripts in the wild type cotyledons are relatively high suggesting that the cytokinin levels are low. At 3DAP, this has changed with lower levels of *PsCKX1* transcripts with a likely high content of cytokinin. It is possible that the cytokinins available in the cotyledons play a significant role in the molecular switch occurring during the transition from heterotrophy to autotrophy, i e., in the degradation of starch. The depression of CKX levels seen in the wild type at 3DAP may be important for proper seedling establishment; that depression is not seen in R50. In R50, *PsCKX1* at 3DAP are high, suggesting that cytokinins are low, in fact as low as the cytokinins in wild type at 1DAP; this low cytokinin may explain the abnormal behavior of R50 cotyledons. Of interest and likely linked with the abnormal *PsCKX1* transcript levels in R50 cotyledons is the abnormal fate of the starch grains in R50 Large starch grains (flower-shaped) filled the cells of the cotyledons of imbibed wild type and R50 seeds. Seven days after germination, few single small starch grains but no flower-shaped starch grains were visible in wild type, while both of those forms were still observed in R50 These results indicate that R50 starch grains are likely not digested as fast as those of wild type. This would explain that at 7DAP the DW of R50 cotyledons has not decreased as much as that of wild type cotyledons However, it is difficult to understand why the cotyledons continued to gain weight when their content should be degrading.

PsCKX transcripts in the wild type embryo, shoots, and roots increase with age, likely regulating tightly the cytokinins involved in the early development of the organs as it is known that cytokinins are promoting D-type cyclins, important proteins controlling the cell cycle of meristematic cells (Roitsch *et al* 2000). In wild type, the pattern of *PsCKX1* and *PsCKX2* expression over time was similar; transcripts of genes increased in shoots and roots as seedlings

developed but at different levels and rates In R50, the profile of *PsCKX1* and *PsCKX2* expression followed the same pattern as that in wild type shoots and roots. However, 7DAP, in R50 roots, *PsCKX2* was expressed significantly higher than in those of wild type. These high transcript levels may explain the generation of lateral root primordia at 7DAP, not observed in my study but mentioned in Pepper *et al* (2007) who had a larger sample size than me. An inhibitory role of cytokinin towards lateral root formation has been proposed by Mathesius (2008). If high *PsCKX2* transcription results in decreased cytokinin levels, this may stimulate the activity of the progenitor cells of the lateral roots.

PsCKX1 and *PsCKX2* are differentially expressed in various tissues (roots and shoots) at various developmental stages (seedling and vegetative) in wild type and R50 (this study and Held *et al* 2008, respectively). Few studies have reported on CKX expression with respect to the spatial and temporal development of plants Galuszka *et al.* (2004), using RT-PCR, reported the expression of three CKX genes from barley (*HvCKX1*, *HvCKX2*, and *HvCKX3*). In roots, whereas *HvCKX1* is expressed strongly at 7-day, *HvCKX2* is not. Furthermore, the *HvCKX3* cannot be detected in this tissue. As for *ZmCKX1* and *ZmCKX2* during maize development, Massonneau *et al* (2004) revealed that both are expressed weakly in young root (1 week old seedling) and highly in old roots (40-day old plants) As for the shoot system, Galuszka *et al.* (2004) reported that *HvCKX1* and *HvCKX2* are expressed equally in both young leaves (7 days) and old leaves (14 days). However, the *HvCKX3* is detected only in young leaves. Massonneau *et al.* (2004) found that young leaves and old leaves have similar *ZmCKX1* transcript levels and that *ZmCKX3* is present only in old leaves. As for *ZmCKX2*, its expression is weak in young leaves and high in old leaves. Growth oc-

curs with age. I observe an increase in the transcript levels of both *PsCKX1* and *PsCKX2* and for both roots and shoots. It is known that cytokinins are important during growth as they stimulate cell divisions. However, for this to occur correctly, cytokinins must be tightly regulated. Not enough cytokinins may slow down growth but too high levels may inhibit growth. The expression and activities of CKX members will be important in maintaining optimal levels for growth. In pea, as in other species, the transcription of the members of the family is under developmental regulation.

Massonneau *et al.* (2004), comparing the location of transcripts of different CKX members, found that there were variations In maize, they reported that *ZmCKX1* is mainly expressed in kernel, but its expression is weak in roots, *ZmCKX2* is expressed in mature tassels, *ZmCKX2* and *ZmCKX3* are expressed in old leaves, *ZmCKX4* is expressed in immature tassels; and *ZmCKX5* is expressed in immature ears Similarly, the CKX genes of barley exhibited different profiles of gene expression (Gulaszka *et al* 2004). I made similar observations in pea. These results likely indicate that different genes have distinct functions within the plant and throughout development. Furthermore, the same gene may be expressed in two or more organs. For example, *PsCKX1* and *PsCKX2* both are expressed in shoots and roots, indicating redundancy of gene expression Interestingly, different genes can be detected in different organs For example, *ZmCKX3* cannot be detected in roots and leaves (Massonneau *et al* 2004) *HvCKX3* cannot be detected in roots (Gulaszka *et al* 2004) Similarly, *PsCKX2* cannot be detected in cotyledons, indicating that *PsCKX2* may not play a role in cotyledon degradation.

This is the first study on *PsCKX* transcription in pea seedlings. This study fills the gap

left by previous studies of *PsCKX* transcription in seeds (Long *et al* unpublished) and vegetative plants (Held *et al.* 2008) This is also the first study reporting the CKX expression levels in the embryo and cotyledon of pea.

Chapter 5 Concluding Remarks

The role played by cytokinin in nodulation, that of R50 in particular, is very complicated. Many students from our lab have tried to elucidate this mystery Lorteau et al (2001) confirmed a crosstalk among ethylene, cytokinin and nodulation, when they demonstrated that synthetic cytokinin BAP stimulated ethylene production and induced a dose-dependent effect on nodulation. Based on Lorteau's results, Ferguson et al. (2005) hypothesized that the low nodulation of R50 was caused by too high levels of cytokinin, they demonstrated that R50 in fact accumulated cytokinin in its shoots and roots. High levels of a compound can be caused either by increased production or decreased degradation. Held et al (2008) according to the principle of parsimony studied the degradation of cytokinin by cytokinin oxidase (CKX). In doing so, they found that the elevated cytokinin content in R50 was linked to a low CKX activity However, the levels of *PsCKX* transcripts were higher in R50 than in Sparkle in young roots and shoots.

When I began working on R50, many researchers performing molecular studies had illustrated that cytokinins play a significant role in nodulation (e.g Lohar *et al.* 2004, Frugier *et al.* 2008). I used a different approach My report offers the first cytokinin antagonist study relating cytokinin perception to nodulation (chapter 2). I concluded that pea nodulation is regulated by a cytokinin transduction pathway, especially that initiated by CRE1/AHK4. It was also the first time that the effect of the cytokinin oxidase inhibitor INCYDE was studied. The application of INCYDE did not inhibit nodule number but on the contrary promoted nodulation (chapter 2). Pea nodulation is therefore regulated by cytokinin oxidase. Further studies should be undertaken For example, LGR-911 would be a good tool to test whether AHK3 is also involved in pea nodulation because it is a cytokinin receptor antagonist which binds primarily

to AHK3 (Nisler *et al.* 2010). Furthermore, high concentrations of INCYDE should be tested on nodulation to assess whether or not we could obtain a complete mimic of R50 nodulation phenotype. Neither cytokinin antagonist nor CKX inhibitor can fully alter the wild type phenotype to mimic all R50 traits; they do so only partially, indicating that the R50 phenotype may be caused only partially by a defective cytokinin signal transduction pathway or a defective cytokinin degradation (chapter 2)

In conclusion, *sym16* must play a role in R50 nodulation phenotype but whether it is a direct or indirect one has yet to be determined. It maybe a direct one if its action is located in the Nod factor transduction pathway or an indirect one if it acts only once the cytokinin has been perceived. Although I did not identify which gene is *sym16*, my results indicate that *sym16* is likely not *PsCKX2* (chapter 3) It is still worth identifying other isoforms in the *PsCKX* family since higher plants usually have more than two members. Furthermore, examining the post-transcriptional process of *PsCKX1* and *PsCKX2* would be worthwhile in view of Scott Clemow's proposal (MSc thesis, Wilfrid Laurier University, 2010) of alternative splicing for *PsCKX1*.

This study fills the gap left by previous studies of *PsCKX* expression in seeds (Long *et al.* unpublished) and vegetative plants (Held *et al.* 2008) (chapter 4) I studied the expression of *PsCKX1* and PsCKX2 during seedling development (chapter 4). Unfortunately, the corresponding cytokinin content and total CKX activities have not been measured. One of the most interesting results of this study is that starch grains in R50 cotyledons are not digested as fast as those of wild type. We designed a working model to explain how the R50 phenotype may be related to an abnormal relationship between cytokinin and starch synthesis (Fig. 5 1) and starch

degradation (Fig. 5 2)

First I will describe the processes of starch synthesis within the wild type (Fig 5 1) Generally, sucrose is generated by the maternal plant and it must move apoplastically to the seed. It is catalyzed by a cell wall invertase which converts it into glucose and fructose, thus contributing to the hexose pool (Buchanan *et al.* 2000). High concentration of hexoses can induce D-type cyclin expression, subsequently the mitotic activity of the developing cotyledon is stimulated (Roitsch *et al.* 2000).The hexoses can also be utilized to synthesize starch which will be used later as a reserve for the developing seedling. Starch synthesis requires three enzymes: ADP-glucose pyrophosphorylase, soluble starch synthase, and granule-bound starch synthase (Buchanan *et al* 2000). Throughout these biological processes, cytokinin plays a significant role. It stimulates cell wall invertase, D-type cyclin, and mitotic activity (Roitsch *et al.* 2000); it also promotes the action of the three enzymes involved in starch synthesis (Miyazawa *et al* 1999) This is likely why cytokinins transiently accumulate in the seeds, and especially in their coats (Emery *et al.* 2000). In R50, where cytokinins are known to be higher in the dry seeds (Long *et al* unpublished), it is likely that all the reactions described above will be exacerbated If one assumes that R50 seed coat contains cytokinin in great quantity (Emery *et al* 2000), its cell wall invertase (Roitsch and Gonzàlez 2004) and the enzymes required for starch synthesis (Miyazawa *et al.* 1999) may be highly stimulated compared to the wild type because of the higher cytokinin content This would trigger a cascade effect resulting in a large hexose pool and in a high accumulation of starch. Both types of sugar would explain the large seed of R50.

Now looking at starch degradation (Fig. 5.2) in the wild type, four enzymes are needed

(Buchanan *et al* 2000) One of them, α-amylase, is negatively regulated by cytokinin. For example, according to Juliano and Varner (1969), exogenously-applied BAP retards growth and slows down starch degradation In R50, the dry seeds of which contain high levels of cytokinins (Long *et al.* unpublished), α-amylase expression as well as starch degradation would be inhibited; however, this is apparently contradictory to the high transcript level of *PsCKX1* found in 3DAP cotyledons Nonetheless, we propose that the seedlings of R50 would be deprived of available sugar because of this inhibition, resulting in its slower epicotyl growth

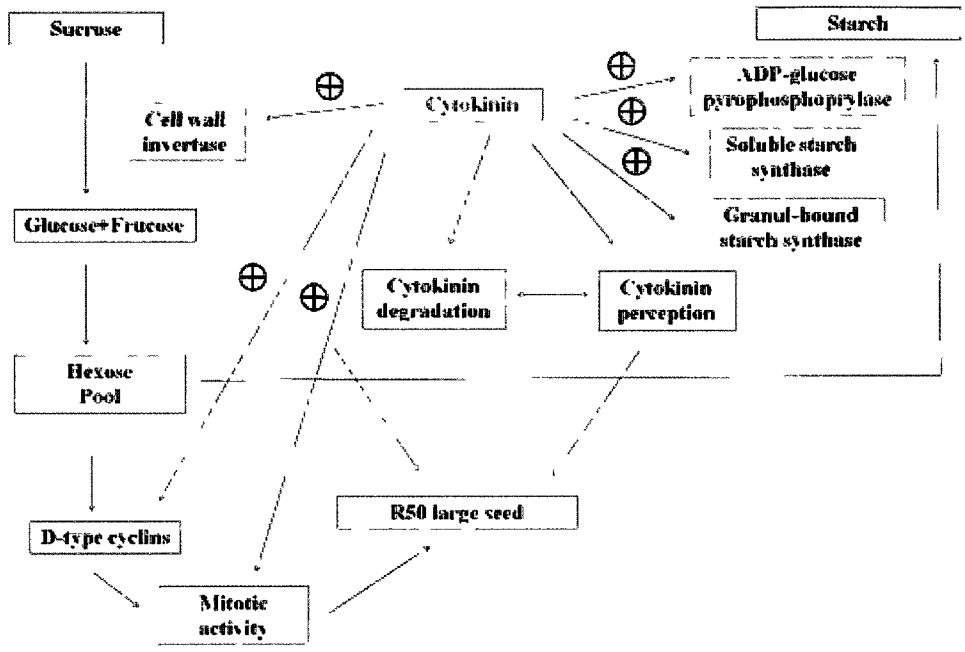

Figure 5.1 Starch synthesis, cytokinin, and R50. This study contributes to the understanding of the R50 large seeds correlating its abnormal cytokinin homeostasis and starch synthesis before germination. Reference to the literature needed for this model is found within the text The model begins by sucrose in the maternal tissue and results in the abnormal size of R50 seed All the enzymes are framed in red Cytokinin (in red), the most important factor in regulating all metabolites, is in the center. The plus symbols represent stimulatory effects.

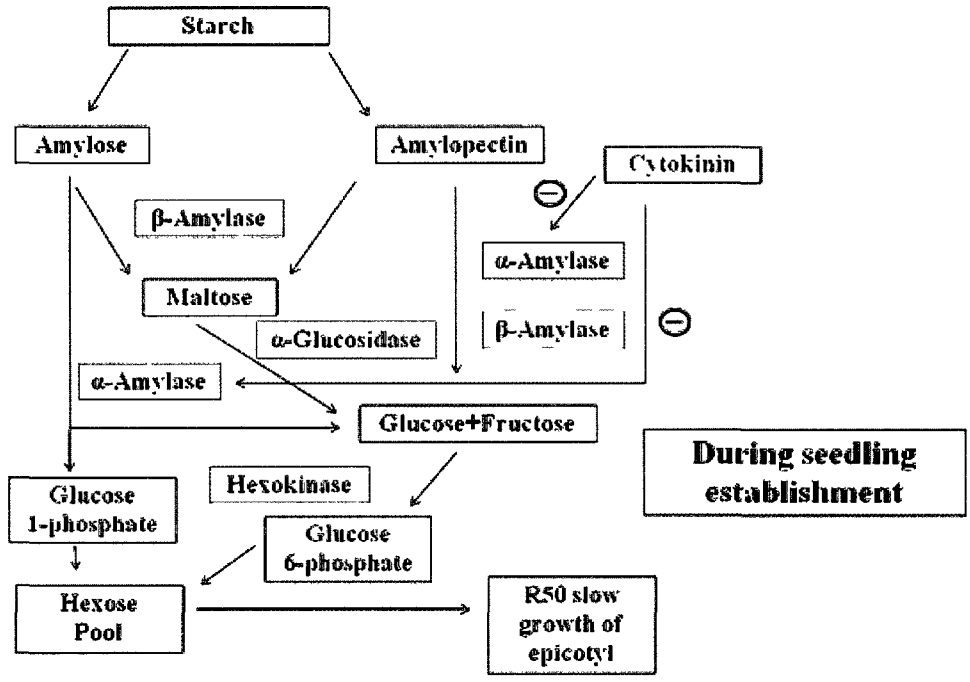

Figure 5.2 Starch degradation, cytokinin, and R50. This study contributes to the understanding of the slow epicotyl growth of R50 correlating its abnormal cytokinin homeostasis and starch degradation during seedling establishment. Reference to the literature needed for this model is found within the text. The model begins by starch in the cotyledons and results in the abnormal growth of R50. All the enzymes are framed in red Cytokinin (in red), the most important factor in regulating all metabolites, is in the right. The minus symbols represent inhibitory effects.

References

Ainscough, E W , Brodie, A.M., and Wallace, A.L. 1992. Ethylene-an unusual plant hormone. *J Chem Educ* 69, 315-318

Akiyoshi DE, Klee H, Amasino RM, Nester EW, Gordon MP 1984. T-DNA of *Agrobacterium tumefaciens* encodes an enzyme of cytokinin biosynthesis. *Proc Natl Acad Sci USA* 81, 5994-5998.

Amasino, R 2005 1955: Kinetin arrives The 50th anniversary of a new plant hormone. *Plant Physiol* 138, 1177-1184.

Arora, N., Skoog, F , and Allen, O.N. 1959. Kinetin-induced pseudonodules on tobacco roots. *Am J Bot* 46, 610-613

Ayele, B.T , Ozga, J A , Kurepin, L V., and Reinecke, D.M 2006. Developmental and embryo axis regulation of gibberellin biosynthesis during germination and young seedling growth of pea. *Plant Physiol* 142, 1267-1281

Barciszewski, J , Siboskr, G E , Petersen, B O , Clark, B F C , and Rattan, S I.S 1996 Evidence for the presence of kinetin in DNA and cell extracts *FEBS Letters* 393, 197-200

Barry, G.F., Rogers, S G., Fraley, R.T., Brand, L. 1984. Identification of a cloned cytokinin biosynthetic gene. *Proc Natl Acad Sci USA* 81, 4776-4780

Bauer, P., Ratet, P , Crespi, M.D , Schultze, M , and Kondorosi, A 1996 Nod factors and cytokinins induce similar cortical cell division, amyloplast deposition and *MsEnod12A* expression patterns in alfalfa roots *Plant J* 10, 91-105

Bewley, J.D. 1997 Seed germination and dormancy *Plant Cell* 9, 1055-1066

Bijay-Singh, Yadvinder-Singh, G S., Sekhon. 1995. Fertilizer-N use efficiency and nitrate pollution of groundwater in developing countries *J Contam Hydrol* 20, 167-184

Bodelier, P L E., Roslev, P , Henckel, T , and Frenzel, P 2000 Stimulation by ammonium based fertilizers of methane oxidation of soil around rice roots *Nature* 403,421–424

Bright, L J., Liang, Y., Mitchell, D.M , and Harris, J.M 2005. The LATD gene of *Medicago truncatula* is required for both nodule and root development. *MPMI* 18, 521-532.

Brelles-Marino, G., and Ané, J M. 2008. Nod factors and the molecular dialogue in the rhizobia-legume interaction. In: Couto GN, editor Nitrogen fixation research progress Hauppauge, NY: Nova Science Publishers, Inc.

Brownlee, B.G , Hall, R H , and Whitty, C.D 1975. 3-Methyl-2-butenal: An enzymatic degradation product of the cytokinin, N^6- isopentenyladenine. *Can J Biochem* 53, 37-41.

Buchanan, B.B., Gruissem, W., and Jones, R L 2000. Cytokinins In: Biochemistry and molecular biology of plants. PP 873-884.

Caplin, S M., and Steward, F.C. 1948. Effect of coconut milk on the growlh of explanls from carrot root. *Science* 108, 655.

Chen., C-M, Kristopeit , S.M. 1981a. Metabolism of cytokinin. dephosphorylation of cytokinin ribonucleotide by 5'-nucleotidases from wheat germ cytosol *Plant Physiol* 67, 494–498

Chen., C-M, Kristopeit SM. 1981b. Metabolism of cytokinin: deribosylation of cytokinin ribonucleoside by adenosine nucleosidase from wheat germ *Plant Physiol* 68, 1020–1023

Cooper, J B , and Long, S R 1994. Morphogenetic rescue of *Rhizobium melilotl* nodulation mutants by trans-zeatin secretion *Plant Cell* 6, 215-225.

Das, N K , Patau, K , Skoog, F 1956. Initiation of mitosis and cell division by kinetin and indoleacetic acid in excised tobacco pitb tissue *Physiol Plantarum* 9, 64

de Billy, F., Grosjean, C., May, S., Bennett, M., and Cullimore, J.V. 2001. Expression studies on *AUX1*-like gens in *Medicago truncatula* suggest that auxin is required at two steps in early nodule development. *MPMI* 14, 267-277.

Ellis, T.H.N., and Poyser, S.J. 2002. An integrated and comparative view of pea genetic and cytogenetic map *New Phytol* 153, 17-25

Emery, R.J.N , Ma, Q., Atkins, C A , 2000. The forms and sources of cytokinins in developing white lupine seeds and fruits *Plant Physiol* 123, 1593–1604.

Fang, Y , and Hirsch, A.M 1998 Studying early nodulin gene ENOD40 expression and induction by nodulation factor and cytokinin in transgenic alfalfa *Plant Physiol* 116, 53-58.

Ferguson, B.J.,Mathesius, U. 2003 Signaling interactions during nodule development. *J Plant Growth Regul* 22, 47–72.

Ferguson, B J., Wiebe, E.M , Emery, R.J.N , and Guinel, F.C. 2005 Cytokinin accumulation and an altered ethylene response mediate the pleiotropic phenotype of the pea nodulation mutant R50 (*sym16*). *Can J Bot* 83, 989-1000

Ferreira, F J., and Kieber, J.J 2005. Cytokinin signaling. *Curr Opin Plant Biol* 8, 518-525.

Finkelstein, R.R. 2004. The role of hormones during seed development and germination. In Plant hormones· Biosynthesis, Signal transduction, Action' Davies P.J ed. Dordrecht, Netherlands. Kluwer Academic Publishers, PP. 513-537.

Frébort, I., Galuszka, P., Šebela, M., Strnad, M., and Pec˘ P. 1999 Cytokinin oxidase (or cytokinin dehydrogenase?) from wheat purification, characterization and evidence for dehydrogenation mechanism of the enzyme reaction *Biol Plant* 42, S119.

Frugier, F., Kosuta, S., Murray, J.D., Crespi, M., and Szczyglowski, K. 2008. Cytokinin: secret agent of symbiosis. *TIPS* 13, 115-120.

Galuszka, P., Frébortová, J., Werner, T., Yamada, M., Strnad, M , Schmülling, T , and Frébort, I 2004. Cytokinin oxidase/dehydrogenase genes in barley and wheat: cloning and heterologous expression. *Eur J Biochem* 271, 3990-4002.

Gerhauser, D and Bopp, M 1990. Cytokinin oxidases in mosses 2. Metabolism of of kinetin and benzyladenine in vitro *J Plant Physiol* 135, 714-718

Gonzalez-Rizzo, S , Crespi, M., and Frugier, F. 2006 The Medicago truncatula CRE1 cytokinin receptor regulates lateral root development and early symbiotic interaction with *Sinorhizobium meliloti Plant Cell* 18, 2680-2693.

Goodlass, G , and Smith, K.A. 1979. Effects of ethylene on root extension and nodulation of pea (*pisum sativum* L.) and white clover (*Trifolium ripens* L). *Plant and Soil* 51, 387-395

Grefen, C , and Harter, K. 2004 Plant two-component systems principles, functions, complexity and cross talk. *Planta* 219, 733-742.

Grobbelaar, N., Clarke, B , and Hough, M.C. 1971. The nodulation and nitrogen fixation of isolated roots of *Phaseolus vulgaris* L. *Plant and soil (Special Volume),* 215-223.

Guinel, F.C 2009. Getting around the legume nodule: I. The structure of the peripheral zone in four nodule types *Botany* 87, 1117-1138.

Guinel, F C , and LaRue, T.A. 1991. Light microscopy study of nodule initiation in *Pisum sativum* L.cv Sparkle and its low-nodulation to pea mutant E2 (*sym 5*) *Plant Physiol* 97, 1206-1211.

Guinel, F.C , and LaRue, T.A 1992 Ethylene inhibitors partly restore nodulation to pea mutant E107 (*brz*). *Plant Physiol* 99, 515-518.

Guinel, F C., and Sloetjes, L.L. 2000. Ethylene is involved in the nodulation phenotype of *Pisum sativum* R50 (*sym16*), a pleiotropic mutant that nodulates poorly and has pale green leaves *J Exp Bot* 51, 885-894

Haberer, G , and Kieber, J.J 2002. Cytokinins New Insights into a Classic Phytohormone. *Plant Physiol.* 128, 354-362.

Hare, P.D., and van Staden, J. 1994 Cytokinin oxidase Biochemical features and physiological significance. *Plant Physiol* 91, 128-136

Held, M., Pepper, A.N , Bozdarov, J., Smith, M.D., Emery, R.J.N., and Guinel, F.C 2008. The pea nodulation mutant R50 (*sym16*) display altered activity and expression profiles for cytokinin dehydrogenase. *J Plant Growth Regul* 27, 170-180.

Heyl, A., and Schmülling, T 2003 Cytokinin signal perception and transduction. *Curr Opin Plant Biol.* 6, 480-488

Hirose, N , Takei, K , Kuroha, T., Kamada-Nobusada, T., Hayashi, H., and Sakakibara, H 2008 Regulation of cytokinin biosynthesis, compartmentalization and translocation. *J Exp Bot* 59, 75-83

Hirsch, A M , Bhuvanrswari, T.V , Torrey, J.G , and Bisseling, T. 1989 Early nodulin genes are induced in alfalfa root outgrowths elicited by auxin transport inhibitors *Proc Natl Acad Sci USA* 86, 1244-1248

Houba-Hérin, N , Pethe, C., d'Alayer, J., and Laloue, M. 1999 Cytokinin oxidase from *Zea mays*: purification, cDNA cloning and expression in moss protoplasts. *Plant J* 17, 615-626

Hymowitz, T , and Singh, R.J. 1987 Taxonomy and speciation In JR Wilcox, ed, Soybeans. Improvement, Production and Uses Agronomy Monograph 16 American Society of Agronomy, Madison, WI, PP 23–48.

Inoue, T., Higuchi, M., Hashimoto, Y., Seki, M., Kobayashi, M., Kato, T., Tabata, S., Shinozaki, K., and Kakimoto, T 2001 Identification of CRE1 as a cytokinin receptor from Arabidopsis *Nature* 409, 1060-1063.

Jones RJ, Schreiber BM , Brenner ML and Foxon G. 1992. Cytokinin levels and oxidase activity during maize kernel development. In: Kamínek M., Zaz´ímalová E. and Mok D.W.S. (eds), Physiology and Biochemistry of Cytokinins in Plants. SPB Academic Publishing, The Hague, The Netherlands, PP 235–239

Juliano, B.O., and Varner, J.E. 1969. Enzymic degradation of starch granules in cotyledons of germinating peas *Plant Physiol.* 44, 886-892

Kakimoto, T. 1996. CK11, a histidine kinase homolog implicated in cytokinin signal transduction. *Science* 274, 982-985

Kakimoto, T. 2001. Identification of plant cytokinin biosynthetic enzymes as dimethylallyl diphosphate: ATP/ADP isopentenyltransferases. *Plant Cell Physiol* 42, 677-685

Kamínek, M., Armstrong, D J 1990. Genotypic variation in cytokinin oxidase from *Phaseolus* callus cultures. *Plant Physiol* 93, 1530–1538

Kamínek, M., Motyka, V., Vaková, R. 1997. Regulation of cytokinin content in plant cells. *Physiol Plant* 101, 689–700

Kaplan, L., and Lynch, T F 1999. Phaseolus (Fabaceae) in archeology: AMS radiocarbon dates and their significance in pre-Colombian agriculture *Econ Bot.* 53, 261-272

Karlowski, W.M., and Hirsch, A.M. 2003. The overexpression of an alfalfa *RING-H2* gene induces pleiotropic effects on plant growth and development. *Plant Mol Biol.* 52, 121-133

Kasahara H, Takei K, Ueda N, Hishiyama S, Yamaya T. 2004. Distinct isoprenoid origins of *cis*- and *trans*-zeatin biosyntheses in *Arabidopsis J Biol Chem* 279:14049–54

Kevei, Z , Lougnon, G , Mergaert, P., Horváth, G.V., Kereszt, A., Jayaraman, D., Zaman, N., Marcel, F , Regulski, K , Kiss, G.B , Kondorosi, A , Endre, G , Kondorosi, E., and Ané, J 2007 3-hydroxy-3-methylglutaryl coenzyme a reductase1 interacts with NORK and is crucial for nodulation in *Medicago truncatula Plant Cell* 19, 3974-3989

Kneen, B.E. and LaRue, T.A 1988. Induced symbiosis mutants of pea (*Pisum sativum*) and sweet clover (*Melilotus alba annua*) *Plant Sci* 58, 177-182

Kneen, B.E , Weeden, N.F., and LaRue, T.A. 1994 Non-nodulating mutants of *Pisum sativum* (L.) cv Sparkle. *J Hered.* 85, 129-133.

Kudo, T , Kiba, T , and Sakakibara, H 2010 Metabolism and Long-distance Translocation of Cytokinins *J Integr Plant Biol* 52 (1), 53-60

Kurakawa, T., Ueda, N., Maekawa, M., Kobayashi, K., Kojima, M., Nagato, Y., Sakakibara, H , and Kyozuka, J. 2007. Direct control of shoot meristem activity by a cytokinin-activating enzyme *Nature* 445, 652-655.

Laloue, M. and Fox, J.E. 1989 Cytokinin oxidase from wheat. *Plant Physiol* 90, 899-906

Lee, K H and LaRue, T.A. 1992a Pleiotropic effects of *sym17 Plant Physiol* 100, 1326-1333

Lee, K.H. and LaRue, T A 1992b Exogenous Ethylene Inhibits Nodulation of *Pisum sativum* L. cv Sparkle. *Plant Physiol* 100, 1759-1763.

Libbenga, K R., van Iren, F , Bogers, R.J , and Schraag-Lamers, M.F. 1973. The role of hor-

mones and gradients in the initiation of cortex proliferation and nodule formation in *Pisum sativum* L. *Planta* 114, 29-39

Lohar, D.P, Schaff, J.E., Laskey, J.G., Kieber, J J., Bilyeu, K D , and Bird, D.M 2004. Cytokinin play opposite roles in lateral root formation, and nematode and Rhizobial symbioses. *Plant J* 38, 203-214.

Lohrmann, J., Sweere, U., Zabaleta, E., Bäuerle, I., Keitel, C., Kozma- Bognar, L., Brennicke, A., Kudla, J , Schäfer, E., Harter, K. 2001. The response regulator ARR2 a pollen-specific transcription factor involved in the expression of nuclear-encoded mitochondrial complex I genes *Mol Gen Genomics* 265, 2–13.

Lorteau, M.A., Ferguson, B J., and Guinel, F.C. 2001. Effects of cytokinin on ethylene production and nodulation in pea (*Pisum sativum*) cv. Sparkle. *Physiol Plant* 112, 421-428

Mähönen, A.P , Bonke, M., Kauppinen, L., Riikonen, M , Benfey, P.N., and Helariutta, Y. 2000 A novel two-component hybrid molecule regulates vascular morphogenesis of the *Arabidopsis* root. *Genes Dev* 14, 2938-2934

Malito, E , Coda, A , Bilyeu, K D., Fraaije, M.W , and Mattevi, A 2004 Structure of Michaelis and product complexes of plant cytokinin dehydrogenase implications for flavoenzyme catalysis *J Mol Biol* 341, 1237-1249.

Massonneau, A., Houba-Hérin, N , Pethe, C., Madzak, C., Falque, M., Mercy, M., Kopecny, D., Majira, A., Rogowsky, P , and Laloue, M 2004. Maize cytokinin oxidase genes: differential expression and cloning of two new cDNAs *J Exp Bot* 55, 2549-2557.

Mathesius, U 2008 Auxin at the root of nodule development? *Funct Plant Biol* 35, 651-668.

Mathesius, U., Schlaman, H.R.M , Spaink, H.P., Sautter, C., Rolfe, B.G , and Djordjevic, M.A. 1998 Auxin transport inhibition precedes nodule formation in white clover roots and is regulated by flavonoids and derivatives of chitin oligosaccharides. *Plant J* 14, 23-34.

McGaw, B A , Horgan, R. and Heald, J.K. 1985. Cytokinin metabolism and the modulation of cytokinin activity in radish *Phytochem* 24, 9-13.

Miller, C.O., Skoog, F., Okuniuru, F.S., von Saltza, F.M , and Strong, F M 1956.. Isolation, structure and synthesis of kinetin, a substance promoting cell division *J Am Chem Soc* 78, 1375

Miller, C.O., Skoog, F., Saltza, M H., and von Strong, F.M. 1955 Kinetin, a cell division factor from deoxyribonucleic acid. *J Am Chem Soc* 77, 1329-1334

Miyazawa, Y., Sakai, A , Miyagishima, S , Takano, H., Kawano, S., and Kuroiwa, T. 1999.

Auxin and cytokinin have opposite effects on amyloplast development and the expression of starch synthesis genes in cultured Bright Yellow-2 tobacco cells. *Plant Physiol.* 121, 461-470

Mok, D.W.S., and Mok, M.C. 1994. Cytokinin, Chemistry, Activity and Function *Boca Raton, FL CRC Press* 1994, 81-86.

Mok, D.W., and Mok, M.C. 2001 Cytokinin metabolism and action. *Annu Rev Plant Physiol Plant Mol Biol* 52, PP 89-118.

Morris, R.O., Bilyeu, K.D., Laskey, J.G., and Cheikh, N.N. 1999. Isolation of a gene encoding a glycosylated cytokinin oxidase from maize. Biochem. Biophys. *Res Commun* 255, 328-333

Murray, J.D., Karas, B J., Sato, S., Tabata, S , Amyot, L., and Szczyglowski, K 2007. A cytokinin perception mutant colonized by rhizobium in the absence of nodule organogenesis. *Science* 312, 101-104

Nakai, K , Horton, P 1999. PSORT a program for detecting sorting signals in proteins and predicting their subcellular localization *Trends Biochem Sci* 24, 34–36

Nandi, S K , Paini, L.M.S., Letham, D S , and Knypl, J S. 1988 The biosynthesis of cytokinins in germinating lupin seeds *J Exp Bot* 30, 1649-1665

Nisler, J., Zatloukal, M., Popa, I., Dolež˘al, K , Strnad, M., and Spíchal, L. 2010. Cytokinin receptor antagonists derived from 6-benzylaminopurine. *Phytochem* 71, 823-830

Nutman, P.S 1948 Physiological studies on nodule formation. I. The relation between nodulation and lateral root formation in red clover. *Ann Bot (Lond)* 12 (2), 81-96.

Pačes, V, Werstiuk, E. and Hall, R H 1971. Conversion of N^6-isopentenyladenosine to adenosine by enzyme activity in tobacco tissue *Plant Physiol* 48, 775-778.

Pepper, A.N., Morse, A.P., and Guinel, F.C. 2007. Abnormal root and nodule vasculature in R50 (*sym16*), a pea nodulation mutant which accumulates cytokinins *Ann Bot* 99, 765-776.

Polhill, R.M., Raven, P.H., Stirton, C.H. 1981 Evolution and systematics of the *Leguminosae* In Polhill RM, Rave PH n, eds, Advances in Legume Systematics Part 1 Royal Botanic Gardens, Kew, UK, PP 1–26.

Raghavan V (2000) Developmental of biology of flowering plants. New York Springer-Verlag.

Ridge, R.W., Bender, G L., and Rolfe, B G 1992 Nodule-like structures induced on roots of wheat seedling by addition of the synthetic auxin 2.4-dichlorophenoxyacetic acid and the effects of omicroorganisms. *Aust J Plant Physiol.* 19, 481-492

Riefler, M., Novak, O., Strnad, M., and Schmülling, T 2006. *Arabidopsis* cytokinin receptor mutants reveal functions in shoot growth, leaf senescence, seed size, germination, root development, and cytokinin metabolism *Plant Cell* 18, 40-54.

Roitsch, T. 2000. Regulation of source/sink relations by cytokinins, *Plant Growth Regul.* 32, 359-367

Roitsch, T., González, M.C. 2004. Function and regulation of plant invertases: Sweet sensations *Trends Plant Sci* 9, 606–613

Saha, S., Nagar, P K , and Sircar, P.K 1984 Changes in cytokinin activity during seed germination in rice (*Oryza sativa* L.). *Ann Bot* 54, 1-5

Saha, S. 1992. Cytokinin activity during seed germination in pea (*Pisum sativum* L.). *Indian J Plant Physiol* 35, 278-280

Sakakibara, H 2004 Cytokinin biosynthesis and metabolism. In:Plant Hormones Biosynthesis, signal transduction, Action! (3rd Ed.), Davies PJ (ed), Kluwer Academic Publishers, Dordrecht, Netherlands. 95-114

Sakakibara, H 2006. Cytokinin Activity, Biosynthesis, and Translocation *Ann Rev Plant Biol* 57, PP 431-439.

Schmülling, T , Werner, T , Riefler, M., Krupkova, E , and Manns, Y B 2003. Structure and function of cytokinin oxidase/dehydrogenase genes of maize, rice, *Arabidopsis*, and other species. *J Plant Res* 116, 241-252

Schmutz, J , Cannon, S B , Schlueter, J., et al 2010 Genome sequence of the palaeopolyploid soybean *Nature* 463,178–183.

Singh, S., Palni, L M.S , and Letham, D S 1992 Cytokinin biochemistry in relation to leaf senescence. V. Endogeneous cytokinin levels and metabolism of zeatin riboside in leaf discs from green and senescent tobacco (*Nicotiana rustica*) leaves *J Plant Physiol* 139, 279-283

Skoog, F., Hamzi, H.Q., Szweykowska, M., Leonard, N J , Carraway, K L., Fugji, T., Helgelson, J.P., and Leoppky, R.W. 1967. Cytokinin· structure/activity relationships *Phytochem* 6, 1169-1192.

Šmehilová, M , Galuszka, P , Bilyeu, K.D , Jaworek, P., Kowalska, M , Šebela, M., Sedlá r˘ová, M., English, J.T. and Fre´ bort, I. 2009. Subcellular localization and biochemical comparison of cytosolic and secreted cytokinin dehydrogenase enzymes from maize. *J Exp Bot* 60, 2701–2712.

Smil, V. 1999. Nitrogen in crop production *Global Biogeochem Cy* 13, 647-662.

Specht. R.L , Connor, D.J , and LiffordI, H.T. 1977. The heath-savannah problem· the effect of fertilizer on sand-heath vegetation of North Stradbroke Island, Queensland. *Aust J Ecol* 2, 179-186.

Spíchal, L., Rakova, N.Y., Riefler, M., Mizuno, T , Romanov, G.A , Strnad, M., and Schmülling, T 2004. Two cytokinin receptors of *Arabidopsis thaliana*, CRE1/AHK4 and AHK3, differ in their ligand specificity in a bacterial assay *Plant Cell Physiol.* 49, 1299-1305.

Spíchal, L., Werner, T., Popa, I., Riefler, M., Schmülling, T., and Strnad. M. 2009a. The purine derivative PI-55 blocks cytokinin action via receptor inhibition *FEBS J* 276, 244-53

Spíchal, L , Werner, T., Galuszka, P., Zatloukal, M., Kopecny, D., Schmülling, T., Strnad, M. 2009b. Characterization and biological activity of novel purine-derived inhibitor of cytokinin oxidase/dehudrogenase INCYDE and its potential use for in vivo studies ACPD 2009 book of abstracts 06-2

Stirk, W.A , Gold, J.D., Novak, O., Strnad, M., and van Staden, J. 2005 Changes in endogenous cytokinins during germination and seedling establishment of *Tagetes minuta* L. *J Plant Growth Regul* 47, 1-7

Stirk, W A , Novák, O , Václavíková, K , Tarkowski, P., Strnad, M , and van Staden, J 2008. Spatial and temporal changes in endogenous cytokinins in developing pea roots *Planta* 227, 1279-1289

Strnad, M 1997. The aromatic cytokinins *Physiol Plant* 101, 674-688

Suzuki, T , Sakurai, K., and Imamura, A. 2001. The *Arabidopsis* sensor His-Kinase, AHK4, can response to cytokinins. *Plant Cell Physiol* 42, 107-113.

Takei, K., Yamaya, T., and Sakakibara, H 2004 Arabidopsis *CYP735A1* and *CYP735A2* encode cytokinin hydroxylases that catalyze the biosynthesis of trans-zeatin. *J Biol Chem* 279, 41866-41872

Timmers, A.C.J., Auriac, M. and Truchet, G 1999. Refined analysis of early symbiotic steps of the *Rhizobium-Medicago* interaction in relationship with microtubular cytoskeleton rearrangement. *Development.* 126, 3617-3628

Tirichine, L., Sandal, N , Madsen, L.H , Radutoiu, S., Albrektsen, A S , Sato, S., Asamizu, E., Tabata, S., and Stougaard, J. 2007 A gain- of-function mutant in a cytokinin receptor triggers spontaneous root nodule organogenesis. *Science* 315, 104-107.

To, J P C., and Kieber, J.J. 2008. Cytokinin signaling two-components and more *TIPS* 13, 85-92.

Turner, J.E., Mok, M.C., Mok, D W S 1985 Zeatin metabolism in fruits of *Phaseolus* comparison between embryos, seed coat and pod tissues *Plant Physiol* 79,321–322

Ueguchi, C., Sato, S., Kato, T., and Tabata, S 2001 The AHK4 gene involved in the cytokinin-signaling pathway as a direct receptor molecule in *Arabidopsis thaliana. Plant Cell Phys.* 42, 751-755.

Vaseva-Gemisheva, I., Sergiev, I , Todorova, D., Alexieva, V , Stanoeva, E., Lachkova, V., and Karanov, E 2005a. Antagonistic effects of triazolo 4,5-d pyrimidine and pyridylurea derivatives on cytokinin-induced cytokinin oxidase/dehydrogenase activity in young pea plants *Plant Growth Regul.* 46, 193-197.

Vaseva-Gemisheva, I , Lee, D., and Karanov, E. 2005b. Response of *Pisum sativum* cytokinin oxidase/dehydrohenase expression and specific activity to drought stress and herbicide treatments. *Plant Growth Regul.* 46, 199-208.

Veereshlingam, H , Haynes, J G , Penmetsa, R V , Cook, D R., Sherrier, D.J., and Dickstein, R 2004 *nip*, a symbiotic *Medicago truncatula* mutant that forms root nodules with aberrant infection threads and plant defense-like response *Plant Physiol* 136, 3692-3702.

Vogel, J.P., Woeste, K.E., Theologis, A., and Kieber, J J 1998 Recessive and dominant mutations in the ethylene biosynthetic gene *ACS5* of Arabidopsis confer cytokinin insensitivity and ethylene overproduction, respectively *Proc Natl Acad Sci USA* 95, 4766-4771.

Wahab, A.M.A., Zahran, H H and Abd-alla, M.H. 1996. Root-Hair infection and nodulation of four grain legumes as affected by the form and the application time of nitrogen fertilizer *Folia Microbiol* 41, 303-308.

Werner, T , Motyka, V., Laucou, V., Smets, R , Onckelen, H.V , and Schmulling, T. 2003 Cytokinin-deficient transgenic *Arabidopsis* plants show multiple development alterations indicating opposite function of cytokinins in the regulation of shoot and root meristem activity. *The Plant Cell.* 15, 2532-2550.

Werner, T., Kollmer, I., Bartrina, I., Holst, K., and Schmülling, T 2006 New insights into the biology of cytokinin degradation. *Plant Biol* 8, 371-381

Wilkins, M.R., Lindskog, I , Gasteiger, E., Bairoch, A., Sanchez, J.C., Hochstrasser, D F., Appel, R.D 1997. Detailed peptide characterization using PEPTIDEMASS: a World-Wide Web accessible tool. *Electrophoresis* 18, 403–408.

Wopereis, J., Pajuelo, E., Dazzo, F B., Jiang, Q., Gresshoff, P.M., De Bruijn, F.J., Stougaard, J.,

and Szczyglowski, K 2000 Short root mutant of *Lotus japonicus* with a dramatically altered symbiotic phenotype *Plant J* 23, 97-14

Yamada, H , Suzuki, T., Terada, K., Takei, K., Ishikawa, K., Miwa, K., Yamashino, T., and Mizuno, T 2001. The *Arabidopsis* AHK4 histidine kinase is a cytokinin-binding receptor that transduces cytokinin signals across the membrane. *Plant Cell Physiol* 42, 1017-1023.

Appendix

Appendix 2.1 Flow chart of material and method and result.

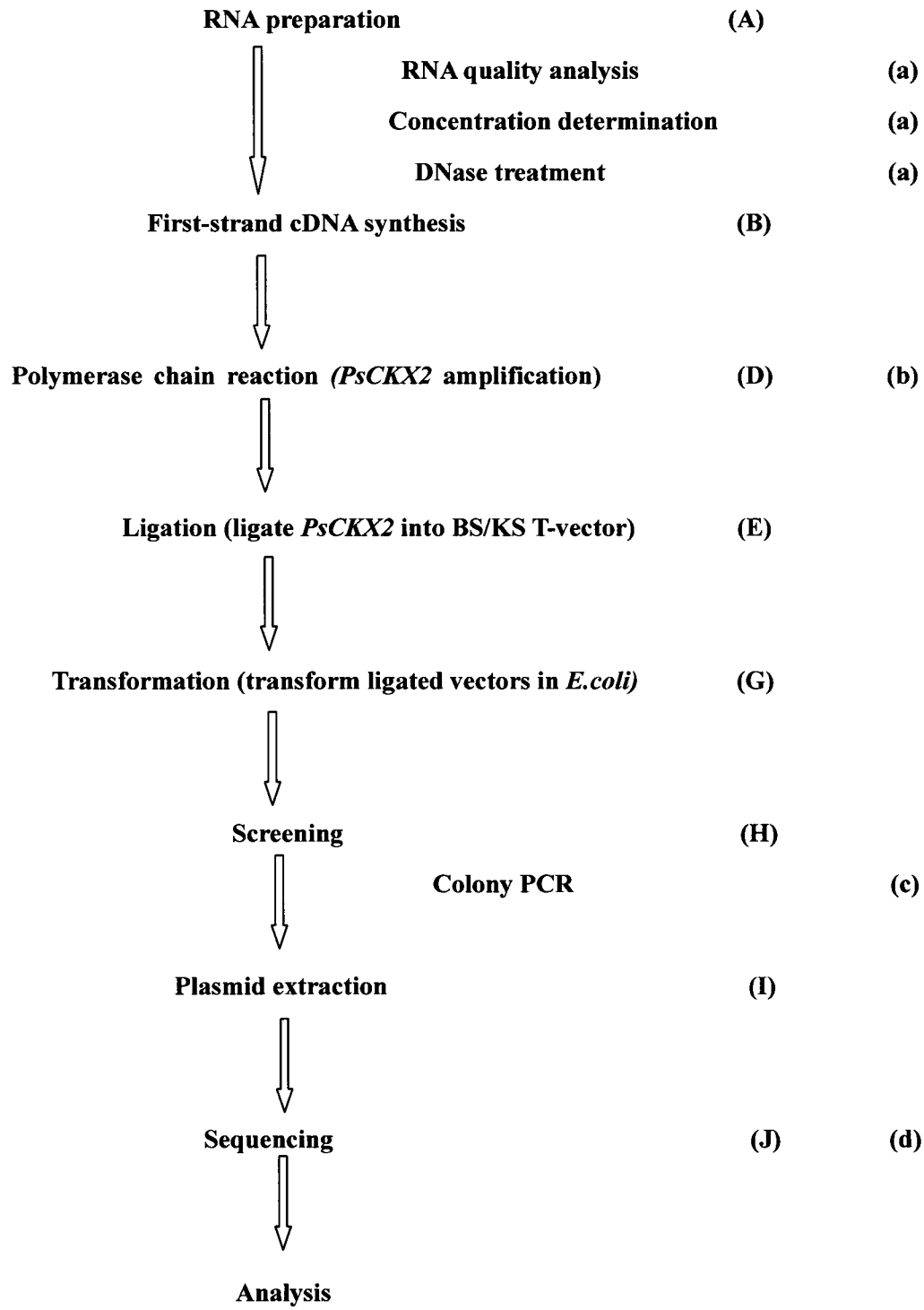

Appendix 2.2 BS/KS vector structure

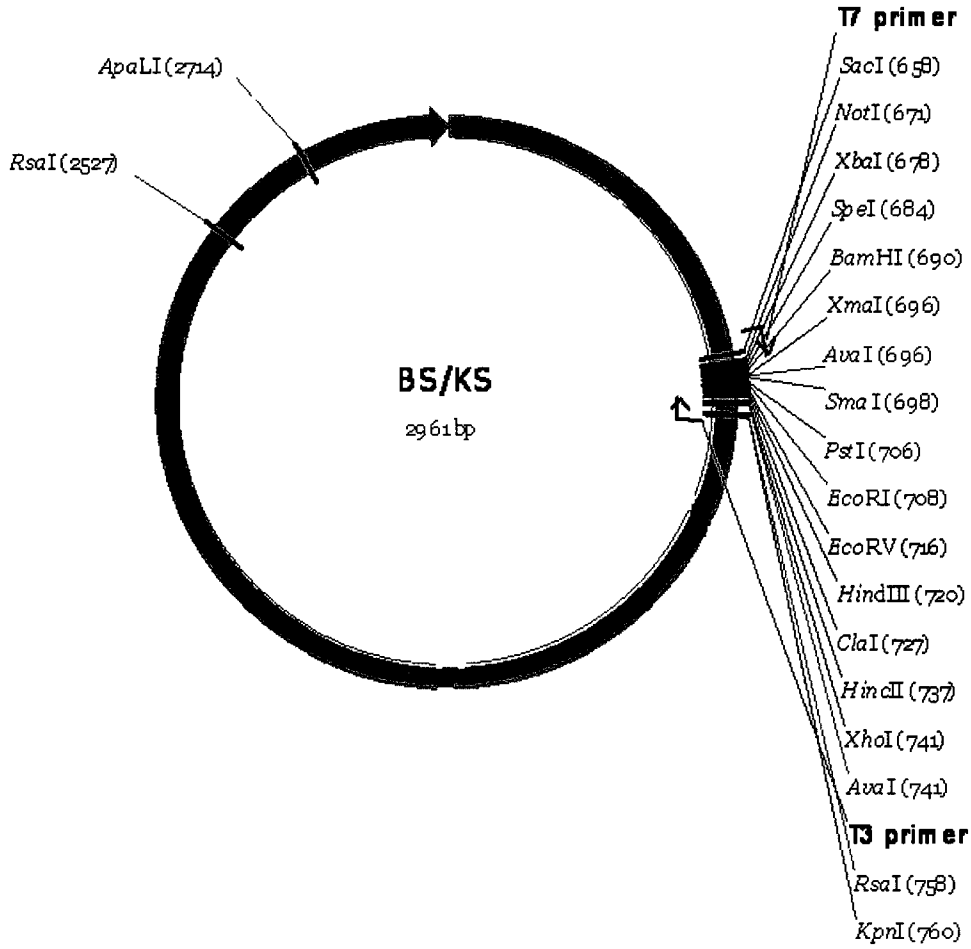

The vector was obtained from Dr Moffatt lab.

Appendix 4.1 PI-55 effects on radicle length in germinated seeds